THE EFFECT OF DNA METHYLATION ON DNA STRUCTURE AND DNA-SMALL MOLECULE INTERACTIONS

A THESIS SUBMITTED TO
THE GRADUATE SCHOOL OF NATURAL AND APPLIED SCIENCES
OF
MIDDLE EAST TECHNICAL UNIVERSITY

BY

GÖZDEM ÇAVDAR

IN PARTIAL FULFILLMENT OF THE REQUIREMENTS
FOR
THE DEGREE OF MASTER OF SCIENCE
IN
BIOTECHNOLOGY

JULY 2020

Approval of the thesis:

THE EFFECT OF DNA METHYLATION ON DNA STRUCTURE AND DNA-SMALL MOLECULE INTERACTIONS

submitted by **GÖZDEM ÇAVDAR** in partial fulfillment of the requirements for the degree of **Master of Science** i**n Biotechnology, Middle East Technical University** by,

Prof. Dr. Halil Kalıpçılar
Dean, Graduate School of **Natural and Applied Sciences** _____

Assoc. Prof. Dr. Can Özen
Head of the Department, **Biotechnology** _____

Assoc. Prof. Dr. Özgül Persil Çetinkol
Supervisor, **Chemistry, METU** _____

Examining Committee Members:

Assoc. Prof. Dr. Can Özen
Biotechnology, METU _____

Assoc. Prof. Dr. Özgül Persil Çetinkol
Chemistry, METU _____

Assist. Prof. Dr. Antoine Marion
Chemistry, METU _____

Assist. Prof. Dr. Müslüm İlgü
Biology, METU _____

Assist. Prof. Dr. Halil İbrahim Okur
Chemistry, Bilkent University _____

Date: 22.07.2020

I hereby declare that all information in this document has been obtained and presented in accordance with academic rules and ethical conduct. I also declare that, as required by these rules and conduct, I have fully cited and referenced all material and results that are not original to this work.

Name, Last name : Gözdem Çavdar

Signature :

ABSTRACT

THE EFFECT OF DNA METHYLATION ON DNA STRUCTURE AND DNA-SMALL MOLECULE INTERACTIONS

Çavdar, Gözdem
Master of Science, Biotechnology
Supervisor: Assoc. Prof. Dr. Özgül Persil Çetinkol

July 2020, 101 pages

Epigenetics is the field of science which investigates the heritable changes in DNA conformation, gene expression, and phenotype that are not related to DNA sequence. Epigenetic modifications are known to be associated with many different diseases including cancer. One of these modifications is the methylation of DNA at the 5^{th} carbon of cytosine. Among different cancer types, the methylation level differs but the mechanism of this difference is not well-known. The increased stability of DNA, accompanied by the decreased flexibility is thought to be one of the contributing factors to this difference by affecting the gene expression.

In this study, the effect of deoxy-5-methylcytosine (*d5mC*) on stability and secondary structure of double helical Dickerson dodecamer DNA (DDD) was examined systematically using UV-Vis and CD spectrophotometry. Within the context, DDDs with different number of *d5mC*s at different positions were compared. Our results revealed that while the location of *d5mC* does not affect the structure and stability of DDD, the increased number of *d5mC* substitutions changed the DNA conformation slightly and increased the stability. Moreover, the effect of DNA methylation on DNA-small molecule interactions was also

investigated using DDD and DDD8, which has no and 8 *d5mC*s, respectively, as model systems. All the molecules, especially intercalators (although having lower binding affinities compared to groove binders), change the structure of DDD more than DDD8 but have effect on the stability of both DDD and DDD8. The gained stability of DNA in the presence of *d5mC* does not allow the structural alteration upon small molecule binding. This thesis opens a door to design new drug candidates targeting specific DNA methylation regions.

Keywords: Epigenetics, DNA methylation, Deoxy-5-methylcytosine, Dickerson dodecamer, DNA-small molecule interactions

ÖZ

DNA METİLASYONUNUN DNA YAPISI VE DNA-KÜÇÜK MOLEKÜL ETKİLEŞİMİ ÜZERİNDEKİ ETKİLERİ

Çavdar, Gözdem
Yüksek Lisans, Biyoteknoloji
Tez Yöneticisi: Doç. Dr. Özgül Persil Çetinkol

Temmuz 2020, 101 sayfa

Epigenetik, DNA yapısı, gen ifadesi ve fenotipte görülen, DNA diziniyle ilişkili olmayan, kalıtsal değişiklikleri konu alan bir bilim dalıdır. Epigenetik modifikasyonların kanser dahil olmak üzere pek çok hastalıkla ilişkili olduğu bilinmektedir. Bu modifikasyonlardan biri, sitozinlerin 5. karbonunda görülen DNA metilasyonudur. Farklı kanser tiplerinde farklı metilasyon seviyeleri gözlenmektedir; ancak bu farklılığa yol açan mekanizma henüz tam anlamıyla anlaşılamamıştır. DNA'nın esnekliğinin azalmasına sebep olan stabilitedeki artışın bu farklılığa sebep olan nedenlerden biri olduğu ve gen ifadesini etkilediği düşünülmektedir.

Bu çalışmada deoksi-5-metilsitozinin (*d5mC*) çift zincirli Dickerson dodecamer (DDD)'in stabilitesi ve ikincil yapısı üzerine olan etkileri UV-Vis ve CD spektrofotometri kullanılarak sistematik olarak incelenmiştir. Bu amaçla, farklı sayıda ve pozisyonda *d5mC* içeren DDD dizinleri karşılaştırılmıştır. Elde ettiğimiz sonuçlar, *d5mC* pozisyonunun DDD stabilitesi ve yapısına herhangi bir etkisi olmadığını, *d5mC* miktarının artışının ise DNA yapısını bir nebze değiştirdiğini ve stabiliteyi artırdığını göstermiştir. Buna ek olarak, DNA metilasyonunun DNA-küçük molekül etkileşimi üzerindeki etkileri de *d5mC* içermeyen DDD ve 8 adet

d5mC içeren DDD8 dizinleri model olarak kullanılarak belirlenmiştir. Tüm moleküller, özellikle interkalatörler (oluklara bağlanan moleküllere göre daha düşük bağlanma sabitine sahip olsalar da), DDD'nin yapısını DDD8'e göre daha fazla değiştirmiş; ancak hem DDD hem DDD8'in stabilitesi üzerinde etkili olmuşlardır. *d5mC* varlığında DNA'nın stabilite kazanması, küçük moleküllerin bağlanmasından kaynaklanan yapısal değişiklikleri engellemiştir. Bu tez, spesifik DNA metilasyon bölgelerini hedefleyen yeni ilaç adaylarının tasarlanması için bir kapı açmıştır.

Anahtar Kelimeler: Epigenetik, DNA metilasyonu, Deoksi-5-metilsitozin, Dickerson dodecamer, DNA-küçük molekül etkileşimleri

To everything and everyone that causes me to be who I am…

ACKNOWLEDGEMENTS

I would like to start by expressing my deepest gratitude and sincerest appreciation to my supervisor Assoc. Prof. Özgül Persil Çetinkol for the precious mentorship, criticism, and kind heart. She has taught me the value of a smile and cared for me as a sister.

I would like to thank my labmates. Fahriye Nur Kırmacı, Sercan Güloğlu, Aynur Özel, Aybüke Gülkaya, Ecenaz Bilgen, Kübra Doğan, and Müge Usta are the best friends who make our laboratory more enjoyable. For his gentleness and kind helps, I especially thank Dr. Mehrdad Forough. I am indebted to Serra Tütüncü who is a sincere friend and a nice teacher, who makes me laugh and makes my life better.

I am very grateful to Hakan Özcan for being a friend who wants the best for me. For his valuable encouragement and faith that I will be successful, I would like to pay my special regards to Hikmet Taner Teker.

Prof. Hüseyin Vural deserves special thanks. I have learned from him the value of good intention. İLKYAR has given me chances to touch many people's life with kindness. I will never forget the days I spent with numerous children and books. ☺

I would like to acknowledge all members of my dear family, Fatih Çavdar, Özlem Çavdar, Erdem Çavdar, and Nurten Palabıyık. Their understanding, patience, support, and endless love are undeniable. I whole-heartedly appreciate my beloved grandfather, Mehmet Palabıyık who I will always remember with great respect.

For their help and support, I would like to express my appreciation to the members of my workplace at the Biotechnology department at Niğde Ömer Halisdemir University.

I gratefully thank The Scientific and Technological Research Council of Turkey (TUBITAK) for the financial support under the grant number 118Z339.

TABLE OF CONTENTS

LIST OF TABLES

TABLES

LIST OF FIGURES

FIGURES

LIST OF ABBREVIATIONS

ABBREVIATIONS

3D	3-dimensional
A	Adenine
Å	Angstrom
K_a	Association constant
B.C.	Before Christ
BPDE	Benzo(a)pyrene diol epoxide
bp	Base pair
BPES	Buffered phosphate EDTA
cm	Centimeter
CD	Circular dichroism
CTCL	Cutaneous T-cell lymphoma
C	Cytosine
˚C	Degree celcius
d5mC	Deoxy-5-methylcytosine
DNA	Deoxyribonucleic acid
DNMT	DNA methyltransferase
Dox	Doxorubicin
EGCG	(-)-epigallocatechin-3-gallate
EtBr	Ethidium bromide

FDA	Food and Drug Administration
G	Guanine
H	Hydrogen
HAT	Histone acetyltransferase
HDAC	Histone deacetylase
Hoe	Hoechst 33258
TP53	Human tumor protein 53
LINE	Long interspersed nuclear elements
T_m	Melting temperature
MBDP	Methyl-binding domain proteins
MBP	Methyl-CpG-binding proteins
μ	Micro
miRNA	MicroRNA
mdeg	Millidegree
min	Minute
M	Molar
nm	Nanometer
Net	Netropsin
N	Nitrogen
O	Oxygen
Π	Pi
RNA	Ribonucleic acid

SINE	Short interspersed nuclear elements
T	Thymine
UV-Vis	Ultraviolet-visible
WBC	White blood cell

CHAPTER 1

INTRODUCTION

1.1 DNA Structure and History

Nucleic acids are biopolymers which take roles in cell division, growth, and transfer of heritable characters, and thus are one of the most important constituents of the cell (Pauling & Corey, 1953).

In 1869, Friedrich Miescher, a physiological chemist, noticed a molecule, with high phosphorous content and resistance to protein digestion, in white blood cells (WBCs) and named it 'nuclein' (Years after, it will be called 'deoxyribonucleic acid'.) (Dahm, 2008). Then, another chemist, Phoebus Levene set up a 'polynucleotide model' to show that nucleic acids were the molecules composed of a series of monomers called 'nucleotides', which have a common structure: one of four nitrogen-including bases, a pentose (a five-carbon including sugar molecule), and a phosphate group. According to his model, the nucleotides were bound always in the same order (i.e. G-C-T-A-G-C-T-A-…) (Levene, 1919; Pray, 2008). Nowadays, the bases are divided into two categories: the purines (adenine and guanine) and the pyrimidines (cytosine, thymine, and uracil). It is also accepted that there are two kinds of nucleic acids: Deoxyribonucleic acid (DNA) and ribonucleic acid (RNA) which have differences in the sugar (deoxyribose in DNA and ribose in RNA) and the organic bases (DNA includes thymine, not uracil, while RNA includes uracil, not thymine.). The findings of other scientists revealed that the polynucleotide model of Levene was precise in many respects (Pray, 2008).

Years later, Erwin Chargaff mentioned that the nucleotides in DNA were not linked always in the same order and the composition differed among species. He set out 'Chargaff's rule' which showed that the total amount of purines equals to the number of pyrimidines in the DNA of a given organism (Chargaff, 1950). The explanations of Chargaff became very critical for the research in the following years. With the help of X-ray crystallography studies of Rosalind Franklin and Maurice Wilkins, the biologist James Watson and the physicist Francis Crick presented the three-dimensional, double helical model of DNA. Only months prior to this, a biochemist Linus Pauling and Robert B. Corey submitted a triple helical model but the Watson-Crick model proved that it was inappropriate (Pray, 2008).

According to the Watson-Crick model, DNA is made up of two, right-handed, helical chains run in opposite directions. The bases are located in the inside of the helix and the phosphates are on the outside while the sugar is perpendicular to the base (Watson & Crick, 1953). This double helix has an anti-parallel structure and there is a systematic base-pairing between two strands: The purine bases in one strand make hydrogen bonding with the pyrimidine bases in the complementary strand (Lodish et al., 2000; Pray, 2008). There is a 0.34 nm distance between bases along the helix which twists in every 3.4 nm, resulting in 10 pairs per turn (Lodish et al., 2000).

The reasons for the helicity of DNA can be mentioned as the hydrogen bonding, hydrophobic and van der Waals interactions between base pairs (bp) (Lodish, 2000). Moreover, the structure of nucleic acids alters with respect to their environment. Under different humidity, salt, ionic strength, and solvent conditions, in the presence of proteins which interact with DNA, and sometimes because of the base sequence, the structure of DNA might differ (Bloomfield et al., 2000; Pierce, 2005).

The structure of DNA defined by Watson and Crick is called 'B-form' of DNA, which is the most stable configuration under physiological conditions (when there is enough water surrounding the molecule and no odd base sequence). In an

environment with less water content, ‘A-form’ of DNA which is a shorter and wider version of B-form structure can be observed. The bases are bent away from the center of the molecule in the A-form. ‘Z-form’ of DNA produces a left-handed helix under physiological conditions if the molecule includes alternating base sequences, especially guanines and cytosines. The sugar-phosphate backbone crisscrosses back and forth in the Z-form DNA structure (Bloomfield et al., 2000; Pierce, 2005).

The gaps between the strands produce two helical grooves which have altered widths named ‘major groove’ and ‘minor groove’ (Lodish et al., 2000). Each groove is covered by potential hydrogen-bond donor and acceptor atoms which allow particular interactions with proteins. In the minor groove, the 3rd nitrogen of adenine or guanine and the 2nd oxygen of thymine or cytosine can perform as hydrogen acceptors, and the amino group of the 2nd carbon of guanine can behave as a hydrogen donor. In the major groove, the 7th nitrogen of adenine or guanine, the 4th oxygen of thymine, and the 6th oxygen of guanine can serve as hydrogen acceptors while the amino groups of the 6th carbon of adenine and the 4th carbon of cytosine might be hydrogen donors (Berg et al., 2002).

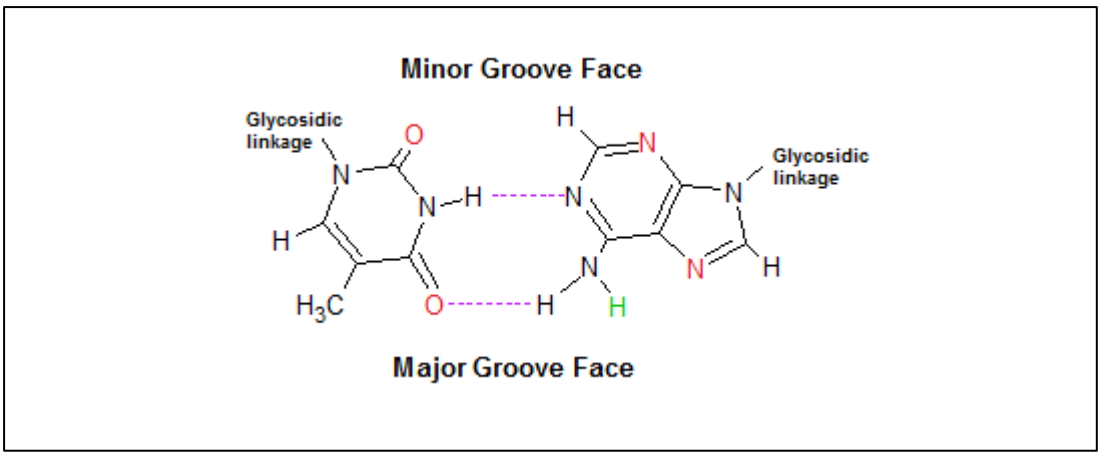

Figure 1. Major and minor groove sides for thymine-adenine

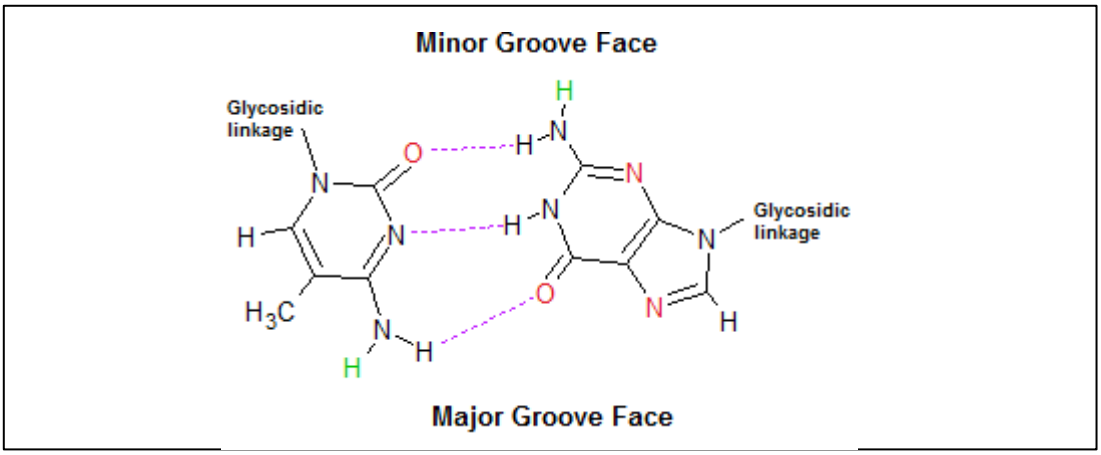

Figure 2. Major and minor groove sides for cytosine-guanine

As can be seen in Figure 1 and 2, the major groove has more specifications which can differentiate one bp from another than does the minor groove. And, although the wider major groove is available for higher number of interactions with proteins which bind particular DNA sequences than the minor groove, both of them are used by various classes of DNA-binding proteins, including the ones which have important roles in replication and gene expression (Berg et al., 2002; Pray, 2008). As indicated before, DNA-protein interactions alter the structure of DNA and bend the axis of the helix because of the absence of hydrogen bonds between successive residues in a DNA strand (Lodish, 2000).

Although the studies of Watson and Crick proved that the DNA structure model of Pauling was unsatisfactory, with the advances in following years it was accepted that specified DNA sequences favorably produce also multi-stranded, non-B-form structures under physiological conditions. These structures are known as DNA triplexes and DNA quadruplexes (Van Dyke, 2005). In a triplex DNA, a single-stranded oligonucleotide makes hydrogen bonding with the bases in the major groove of a duplex. This hydrogen bonding between the bases of the 3rd strand and duplex is named 'Hoogsteen-like hydrogen bonds'. Quadruplex structures are formed by the planar assembly of four identical bases. For example, G-quadruplex structures, which are formed by the assembly of four guanine bases, are generally noticed in human telomeric repeats (Rosu et al., 2002).

1.2 Chromatin Structure

In the cell, genomic DNA is organized in a packaged form called chromatin by interactions with histone proteins. A 146 bp of DNA is enveloped around a histone octamer including two copies of each histone, H2A, H2B, H3, and H4, to form a nucleosome core. Many nucleosome cores congregate and are stabilized by a linker histone, H1, to produce nucleosomes, which arrange into chromatin fibers upon high-order looping and folding (Cheung & Lau, 2005). This stable organization plays a role in the regulation of replication, transcription, and repair by controlling the approach of nuclear factors to DNA. Besides, posttranslational modifications in histone proteins such as acetylation, methylation, phosphorylation, and ubiquitination are also effective ways of regulations (Ngo et al., 2016; Cheung & Lau, 2005) which produce euchromatin and heterochromatin forms, including transcriptionally active and inactive regions, respectively (Bannister & Kouzarides, 2011).

1.3 Epigenetics

Epigenetics was firstly mentioned in 350 B. C. by Aristotle. He explained a ‘vital cause’ for the development of an adult from embryo through some steps called ‘epigenesis’. This argument was against ‘preformation’ which supports the idea of complete predevelopment of zygotes. After the observation of embryos and enhanced knowledge of genetics, Thomas Hunt Morgan clarified the contribution of both heredity and modifications throughout development for characteristic features. Genetics provides the information for gene expression while interpretation of this information is needed for the regulation (Hurd, 2010). Conrad Hal Waddington was the first person who used the term ‘epigenetic’ while the description of embryonic development. He stated that the development occurs with the help of preformed components of a fertilized egg which permit only a limited number of reactions. The interactions of these components between each other and

with the external environment result with the formation of tissues and organs different from the original ones. The production of an organ or tissue should be regarded as both a genetic and an 'epigenetic' event (Waddington, 1939). On this basis, in the later years, he explained epigenetics as an area of biology trying to investigate the interactions between the genes and proteins which generate a phenotype (Goldberg et al., 2007). Afterwards, David Ledbetter Nanney described an epigenetic system as a supportive mechanism that decides which specificities will be selected for expression in any specific cell (Nanney, 1958). Even though most common clarification for epigenetics term comes from Arthur Riggs, 'the study of mitotically and/or meiotically heritable changes in gene function that cannot be explained by changes in DNA sequence' (Russo et al., 1996), Adrian Bird gave a more recent explanation that the structural modification of chromosomal regions in order to express, stimulate or continue the changed activity states (Bird, 2007).

Adaptation to environmental alterations and cell specialization in multi-cellular life forms need complicated coordination of the transcription. Each cell, from the simplest prokaryote to the most complex human neuron, can remember past events, such as variations in the exterior environment or developmental signals (Bonasio et al., 2010). Cells take the information from their ancestors and transfer to their descendants through cell division. The greater part of this 'memory' is stored in the sequence of the genome. Nucleic acids offer high stability and precise heritability essential for keeping the memory throughout evolution. For a shorter time, cells may also receive and transfer the information not kept as alterations in the genomic sequence. With the help of this 'epigenetic' memory, cells might position into one of at least two different regulatory states and in multicellular organisms, cells including the same zygotic genomes might have diverse functions in the same environments (Dodd et al., 2007). The differentiation signal is responsible for making subgroups of progeny cells which take part in different programs of gene expression, i.e. their genes are expressed in different times and different places (Bonasio et al., 2010; Güler & Peynircioglu, 2016). Consequently,

their developmental route and functions vary. Although this signal comes only once throughout gestation, the uniqueness of each cell type remains for a lifetime (Bonasio et al., 2010).

Epigenetic regulation of gene expression is indispensable for normal cell development and function (Lim & Maher, 2010). Epigenetic mechanisms enable to suppress the expression of particular genes while stimulating the activity of others (Güler & Peynircioglu, 2016). They are potentially reversible alterations affecting both the modified gene and the neighbor genes and might be altered by the environment with a higher frequency compared to genomic changes (Feinberg, 2004). Any disorder in an epigenetic mechanism might result in enhanced activation or repression of gene expression and result in diseases such as cancer (Lim & Maher, 2010; Güler & Peynircioglu, 2016).

The most common epigenetic modifications might be sorted into three categories: DNA methylation, histone modifications, and non-coding RNAs (Sawan et al, 2008).

1.3.1. DNA Methylation

In eukaryotic organisms, a post-synthetic modification, called DNA methylation, is noticed at cytosine residues (Suzuki & Bird, 2008). In mammalian DNA, methylation occurs by a transfer of methyl group from S-Adenosyl methionine (SAM) to the 5^{th} carbon of a cytosine to produce deoxy-5-methylcytosine (*d5mC*), with the catalysis of DNA methyltransferases (DNMTs) (Moore et al., 2013).

The stably packed organization of DNA in nucleosome controls the replication, transcription, and repair. Large methyl groups in cytosine residues provide a partial widening in the major groove and, as a result, a partial narrowing in the minor groove. The close distance of the methyl group to the phosphodiester backbone in major groove is thought to result with steric hindrance, consequently,

limitation of the conformational variations and weak attachment of DNA to the histone proteins which makes nucleosome unpacking easier. Therefore, DNA can be highly accessible (Ngo et al., 2016; Machado et al., 2014). In addition, cytosine methylation may change the 3D structure of the DNA recognition spot after hydration of cytosine residues through C–H···O interactions. This alteration is also thought to affect the recognition of cytosines by polar groups in DNA-binding proteins (Machado et al., 2014; Taqi et al., 2012).

The DNA methylation mostly takes place on CpG islands which are DNA sections approximately 1000 bp long including more CpG dinucleotides than the other regions of the genome (Moore et al., 2013). CpG islands usually appear on the promoters, the regions where the transcription starts. In the human genome, the dinucleotides in CpG islands, particularly the ones related to promoters, are generally unmethylated. Only a little of CpGs turn out to be methylated throughout the embryonic development for transcriptional silencing of the related gene. This exception may have many consequences including X-chromosome inactivation and genomic imprinting, which indicate the significance of methylation on gene expression (Herman & Baylin, 2003; Suzuki & Bird, 2008). In addition, the non-coding regions of the genome consist of repeat elements, introduced viral sequences, and transposons are generally methylated due to the fact that transcription of these components may be detrimental for the cell (Herman & Baylin, 2003).

Methylation of CpG dinucleotides on a promoter region suppresses the transcription directly, by inhibiting the binding of particular transcription factors to their binding regions in promoters, and indirectly, by bringing transcriptional repressors, methyl-CpG-binding proteins (MBPs), and changing the chromatin structure into an inactive form. On the other hand, methylation of CpG dinucleotides in gene bodies might stimulate the transcription by restricting useless transcription start in the transcribed sections (Wang et al., 2013).

The reason behind such gene regulation via DNA methylation is thought to be the alterations in structure, dynamics, and thermal stability of DNA (Římal et al., 2015).

In addition to the regulation of gene expression, DNA methylation has also a role in the maintenance of genomic integrity. In the mammalian genome, most of the CpG dinucleotides outside the CpG islands are methylated. The majority of these methylated dinucleotides are placed in repetitive sequences called retrotransposons. DNA methylation limits the expression of retrotransposons in order to prevent the incorporation of repetitive sequences in transcriptional regions to DNA. A high level of methylation in chromatin regions is thought to block irregular recombination and keep chromosomal structure (Kosova et al., 2011).

According to usually acknowledged information, the methylation in cytosine stabilizes the double stranded DNA. The thermal denaturation experiments with long DNA sequences including one methylated cytosine demonstrate an increase in the annealing temperature compared to non-methylated DNA. However, the experiments with shorter DNA sequences could not verify the temperature increase observed with the longer sequences (Římal et al., 2015).

1.3.2. Histone Modifications

Epigenetic modifications might also occur in histone proteins, especially in lysine and arginine amino acids. These reversible modifications consist of phosphorylation, acetylation, and methylation (Gros et al., 2012); by the formation of loose or tightly packed chromatin construction, they regulate the accessibility of transcription factors and enhance or suppress gene expression (Gros et al., 2012; Bhatla et al., 2012). For instance, histone acetyltransferases (HATs) give acetyl group and negative charge to histone amino acids and then obstruct their binding to DNA with the same charge. As a consequence, transcription factors can reach DNA easily to stimulate gene expression. This modification and its effects go backward by the activity of histone deacetylases (HDAC) (Kim & Bae, 2011).

As mentioned above, methyl groups included in CpG regions near the promoter sequences are responsible for gene suppression. Methyl-binding domain proteins (MBDP) attach the sequences nearby the promoter, hence occupy the region where RNA polymerase II normally binds and blocks the gene expression with the help of HDAC which forms a packed chromatin structure in regulatory parts. HDAC 1, 2 and 6 expressions are reported to be increased in a number of tumors. Also, abnormal histone modifications are known to suppress the genes and play a role in cancer progression (Sarkar et al., 2013).

1.3.3. Non-coding RNAs

A big part of the human genome was considered as non-functional until it was revealed that almost every gene in the genome has a function. Only 2% of the whole genome is known to encode for proteins, where the rest is known to be non-coding or coding for non-coding RNAs which take part in the control of gene expression (Lardenoije et al., 2015).

1.4 Epigenetics and Cancer

Epigenetic changes play role in various human diseases, including cancer. Two main epigenetic reasons for cancer are defined as total DNA hypomethylation and site-specific promoter hypermethylation (Gonzalo, 2010). The genomes of cancer cells are highly hypomethylated compared to normal cells except for hypermethylation at genes included in cell cycle control, tumor cell attack, DNA repair and silencing promotes metastasis (Phillips, 2008).

Hypomethylation generally occurs at repetitive genomic regions consist of satellite DNA and retrotransposons (such as Long Interspersed Nuclear Elements (LINE) and Short Interspersed Nuclear Elements (SINE)) (Kaneda & Tsukada, 2017). These sequences are generally methylated and not expressed in normal cells because of their ability to destabilize DNA or be harmful to the cell (Khan &

Hilliker, 2014). The hypomethylation and transcriptional activation of repeat-rich regions may lead to mutations, chromosomal reorganizations, and genomic instability through enhanced mitotic recombination outcomes (Khan & Hilliker, 2014; Phillips, 2008). For example, the highly methylated nature of pericentromeric heterochromatin is known as protecting chromosomal conformation and preventing aberrant recombination by blocking recombination initiation sites or suppressing homologous recombination. Hypomethylation of centromeric heterochromatin results with chromosomal abnormalities such as isochromosomes, translocations, and deletions (Kosova et al., 2011). In addition, hypomethylation might lead to oncogenic cell growth by activating the transcription of proto-oncogenes (Lim & Maher, 2010). Gene-specific hypomethylation might help tumor cells to familiarize with the environment and stimulate metastasis (Robertson, 2005).

Hypermethylation is noticed in many cancer cells, especially in the CpG islands in promoter regions of tumor suppressor genes (Lim & Maher, 2010). Epigenetic alterations may occasionally cause cancer because of the mutagenic nature of *d5mC* which goes through spontaneous hydrolytic deamination to trigger C→T modifications (Jones & Baylin, 2002). This unstable nature of *d5mC*s might lead to the inactivation of tumor suppressor genes (Lim & Maher, 2010). For example, almost 50% of point mutations in an exon of human tumor protein 53 (TP53) gene, which is a tumor suppressor gene, are seen at *d5mC*s in CpG islands. The methyl groups in these particular regions of TP53 gene enhances the rate of mutations stimulated by Ultraviolet (UV) light. This enhancement supports the proliferation of skin cancers. Furthermore, in mammalian cells, methylated CpG dinucleotides are targeted by benzo(a)pyrene diol epoxide (BPDE) presents in tobacco to generate G→T modifications (Jones & Baylin, 2002).

1.5 Therapeutic Strategies which Target Epigenetic Modifications

In recent years, it has been discovered that many human diseases have an epigenetic basis. This knowledge enhanced drug research & development studies to interfere with epigenetic modifications (Bora & Yurter, 2007). The difference between epigenetic modifications and genetic change is the reversibility of the former (Sawan et al., 2008). Because of conditional and environmental changes, epigenetic alterations can occur in forward or reverse direction and they can even be entirely eliminated (Heerboth et al., 2014). Hence, abnormal levels and distributions of epigenetic modifications might be preferable targets to stimulate silenced tumor-suppressor and DNA repair genes for cancer therapy (Sawan et al., 2008). Many candidate drugs which can change DNA methylation and histone modification profiles have been designed; preclinical and clinical tests were performed for some of them (Sawan et al., 2008; Bora & Yurter, 2007). Among those, the most promising ones are known as DNMT inhibitors and HDAC inhibitors (Bora & Yurter, 2007).

DNMT inhibitors can be divided into two categories: nucleoside analogs and non-nucleoside analogs (Bora & Yurter, 2007). Nucleoside analogs are the oldest type of methylation inhibitors (Heerboth et al., 2014); with the help of their structure similar to DNA base, they can be added into a newly synthesized DNA strand. A covalent bond between inhibitors and DNMTs prevents the activity of the enzyme and makes the strand hypomethylated (Bora & Yurter, 2007). For instance, 5-azacytidine is a cytidine analog which has a nitrogen atom instead of the 5^{th} carbon. Only its cytotoxicity for cancer cells was known before the discovery of its mechanism in recent years. After its phosphorylation in the cell and integration into DNA throughout replication, it is recognized by DNMT1 and the methyl group is transferred. Nevertheless, the nitrogen atom in the 5^{th} position triggers the formation of a bond between it and DNMT1. As a result, the enzyme loses its activity and results in an extensive decrease in methylation (Heerboth et al., 2014). After this discovery of its action mechanism, 5-azacytidine has become the

preferred drug for many different purposes such as the reactivation of various genes silenced in-vitro, chromatin decondensation, and cellular differentiation (Kosova et al., 2011). The integration of 5-azacytidine into DNA occurs throughout replication makes fast dividing cancer cells more vulnerable to its impacts (Heerboth et al., 2014).

The usage of 5-azacytidine in the treatment of myelodysplastic syndrome has been approved by Food and Drug Administration (FDA) (Bora & Yurter, 2007) but further improvement is needed because of its instability in physiological media, severe toxicity, and infeasibility for oral administration. In addition, nucleoside analogs have low bioavailability, low effect on solid tumors, and large nonspecific alterations to epigenome (Heerboth et al., 2014; Tollefsbol, 2018). Because of these limitations, the development of new specific inhibitors is ongoing (Tollefsbol, 2018). Zebularine, a more stable and less toxic cytidine analog (Tollefsbol, 2018), is one of these inhibitors and with the same mechanism with 5-azacytidine (Heerboth et al., 2014).

Non-nucleoside analog DNMT inhibitors have also been designed after the realization of limitations in the application of nucleoside analogs. For instance, RG108 and EGCG [(-)-epigallocatechin-3-gallate] bind to the active region of DNMT and inhibit enzyme activity (Bora & Yurter, 2007). Because RG108 does not need to trap the enzyme, it has low toxicity. Furthermore, it can enhance the stability of hypomethylated chromatin. The treatment of RG108 into human cancer cell lines reduced the speed of cell growth after a considerable level of demethylation and stimulation of the transcription of the p16 tumor suppressor gene (Heerboth et al., 2014). Also, EGCG, which is the main polyphenol in green tea, reduced DNA methylation in cancer cells. Procaine and procainamide are antiarrhythmic drugs; they attach to CG-rich target sequences and restimulate hypermethylated tumor suppressor genes (Bora & Yurter, 2007).

Beside analogs, certain oligonucleotides are designed to inhibit the transcription of DNMTs and called epi-miRNAs. They are constructed as

complementary to the untranslated region in 3' of the DNMT1 mRNA in order to inhibit the transcription of the DNMT1 gene. For example, MG98 administration gave rise to DNMT inactivity, restimulation of tumor suppressor genes, and decrease of tumor growth in pre-clinical experiments. Although it was not successful in clinical trials because of toxicity and inefficiency (Castillo-Aguilera et al., 2017), the administration of MG98 together with a common drug used in chemotherapy, Roferon-A, reduced the amount of DNMT1 and decelerated tumor development with slight toxicity (Heerboth et al., 2014).

On the other side, HDAC inhibitors increase histone acetylation by counteracting HDACs, produce an accessible chromatin structure, thus trigger the gene expression (Bhatla et al., 2012). They regulate the expression of the genes involved in cell cycle checkpoint, apoptosis, cellular variation, and stalling growth, as DNMT inhibitors do (Luszczek et al., 2010). Furthermore, they increase the acetylation of non-histone proteins such as transcription factors and tumor suppressor proteins (Bora & Yurter, 2007). Vorinostat is the 1st drug accepted by the FDA as an HDAC inhibitor and is used in the treatment of cutaneous T-cell lymphoma (CTCL) (Kim & Bae, 2011).

DNMT and HDAC inhibitors can be preferred to be used alone, together with each other, or combined with various cytotoxic drugs in clinics. Epigenetic mistakes are considered as more easily treatable than genetic faults. However, the agents which might be helpful for epigenetic disorders have some limitations such as their short-term effects and non-specificity which may cause global hyperacetylation, deacetylation, and demethylation (Bora & Yurter, 2007).

Besides the administration of agents which are able to alter methylation profiles, chemotherapeutic drugs which damage malignant tumor cells by inhibiting their division are still in use in clinics. Nevertheless, they do not differentiate normal and tumor cells, and therefore are cytostatic or cytotoxic to both kind of cells in a patient. Hence, there are many scientific research projects going on to design anticancer agents which will kill the tumor cells but will not

harm the normal ones (Avendaño & Menéndez, 2015). For example, Fe-bleomycin is a drug preferred in the treatment of certain cancer types and has antitumor activity by producing double strand breaks in particular DNAs. Cytidines are included in CpG islands in DNA and take part in gene regulation, development, and carcinogenesis. It was revealed that methylation in cytidines affects nucleosome organization and gene expression, thus prevents Fe-bleomycin from destroying DNA. As a result, while Fe-bleomycin destroys unmethylated tumor cells specifically, methylation protects healthy cells from the cytotoxic effects of this drug (Roy et al., 2014).

1.6 Interaction of DNA with Small Molecules

DNA is an essential part of the cellular organization and stores genetic data. It takes a significant part in replication, transcription, translation, and thus the cell viability (Bhaduri et al., 2018). Because DNA keeps codes for the production of all proteins and enzymes, it indirectly maintains conformation and function of the cell (Rehman et al., 2015). Therefore, it has been considered as a long-lasting target of different clinically valuable small molecules to identify and treat human diseases (Paul & Bhattacharya, 2012; Rehman et al., 2015). Direct binding of small molecules to a specific region on DNA duplex where regulatory proteins normally bind might give rise to alterations in various downstream processes such as the hinderance of significant enzymes and proteins with roles in regulation of the cellular conformation and activity, slowing down or inhibition of cell growth, or overproduction of a number of proteins and increased cell growth (Aleksić & Kapetanović, 2014; Rehman et al., 2015). In addition, small molecule stimulated alteration in physical parameters of DNA might affect cellular metabolism and growth (Afrin et al., 2017). If the alteration of DNA function by small molecule binding is used to treat or maintain the disease, this molecule is considered as a drug, if not it is called a cytotoxic molecule (Aleksić & Kapetanović, 2014). The research about the interaction of small molecules with DNA provides shed light on

the mechanism of action, unknown therapeutic potentials and dangerous side effects of known drugs, and supports the design of novel DNA binding drugs for the possible treatment of many diseases (Rehman et al., 2015; Afrin et al., 2017).

Many small molecules, inorganic or organic, biological or non-biological, bind to DNA, generally when it is in duplex configuration (Aleksić & Kapetanović, 2014). Interaction of DNA with small molecules is generally divided into two main groups as covalent and non-covalent interactions (Bhaduri et al., 2018).

1.6.1. Covalent Interaction

In covalent interactions, small molecules are bound to DNA irreversibly and with relatively high binding affinity. Such binding alters DNA structure, and thus interferes with protein-DNA interactions (Aleksić & Kapetanović, 2014). For instance, it can halt transcription contemporarily and result in cell collapse (Bhaduri et al., 2018).

Small molecules interact with DNA covalently in three ways: substitution of nitrogen-bearing bases, inter/intra-strand cross-linking, and alkylation of nitrogen-bearing bases. For instance, cisplatin ($Pt(NH_3)_2Cl_2$) is a common anticancer agent which is administered intravenously. Inside the cell, cisplatin confronts with a less chloride concentration compared to outside and chloride ligands are substituted by water molecules to produce two cations, cis-$[Pt(H_2O)(NH_3)_2Cl]^+$ and cis-$[Pt(H_2O)_2(NH_3)_2Cl]^{+2}$, which make covalent interaction with electron-rich regions of DNA, generally with N-7 of guanines (Aleksić & Kapetanović, 2014). The intra/interstrand crosslink produced between cisplatin and nitrogens of bases on neighboring strands prevent the opening of DNA for replication and/or transcription (Paul & Bhattacharya, 2012; Aleksić & Kapetanović, 2014). To give another example, temozolomide, chlorambucil, and nimustine are preferred for cancer therapy for many years. Donation of alkyl groups to DNA by these molecules causes DNA breakage (Aleksić & Kapetanović,

2014). Alkylation of DNA might also lead to the mispairing of nucleotides, thus mutations (Paul & Bhattacharya, 2012).

1.6.2. Non-covalent Interaction

In non-covalent interactions, small molecules are bound to DNA reversibly and might alter DNA configuration, DNA torsional stiffness, interfere with the protein-DNA association, and cause DNA breakage (Aleksić & Kapetanović, 2014). Non-covalent interactions can be classified mainly as intercalation and groove binding (Rorbach & Bobrowicz, 2014).

1.6.2.1. Intercalation

Intercalation is the penetration of planar aromatic or heteroaromatic units between neighboring nucleotides in DNA (Bhaduri et al., 2018). Hydrophobic and aromatic side groups within intercalator attract aromatic nucleotides and hydrogen bonding might be established between drug and DNA (Aleksić & Kapetanović, 2014). That's why, intercalation usually occurs autonomously from sequence but favorably at CG-rich regions (Paul & Bhattacharya, 2012). Water-mediated interactions are more common than the direct hydrogen bond formation. In any case, the amount of water on the surface is decreased after the intercalation (Aleksić & Kapetanović, 2014).

Although energy is needed to loosen the twist and separate the nucleotides for intercalation, intercalation could be a powerful and stable attraction mode (Paul & Bhattacharya, 2012). Intercalation is directed by electrostatic attractions, dipole-dipole forces, dispersive forces, and π–π interactions (Rorbach & Bobrowicz, 2014). DNA intercalation mostly obeys the nearest-neighbor exclusion model, which mentions that intercalators enter, at most, between alternating nucleotides (Goftar et al., 2014).

For the intercalation of a molecule in-between nucleotides, helix should unwind to decrease the stacking interactions between the nucleotides and open up the distance between them (Aleksić & Kapetanović, 2014). In order to counterbalance the resulting helix perturbation, the sugar-phosphate is readjusted such that the helical coil extension is reduced, and DNA length is increased (Aleksić & Kapetanović, 2014; Bhaduri et al., 2018). Conformational alteration of DNA structure intervenes with binding and action of drugs and DNA-related proteins such as polymerases, repair enzymes, topoisomerases and transcription factors. The majority of DNA intercalators hinders the synthesis of DNA and RNA and stimulates DNA damage (Mišković et al., 2013), thus are commonly preferred in chemotherapy (Bhaduri et al., 2018).

Intercalation can be categorized as classical and threading intercalation. Threading intercalators usually include two side groups on an aromatic ring (Paul & Bhattacharya, 2012). The difference between these two modes is that in threading intercalation the side groups are located at major and/or minor grooves while the aromatic ring is inserted in-between the bases in the classical intercalation (Banerjee et al., 2016). Due to the additional interactions between the side groups of the intercalator and the grooves of the DNA, the threading intercalation is generally more stable compared to the classical mode (Paul & Bhattacharya, 2012).

Ethidium bromide (EtBr) (Figure 3) is an example of classical intercalators (Banerjee et al., 2016) with a phenanthridinium ring (Benevides & Thomas, 2005). It is preferred as an antimicrobial agent (Nakamoto et al., 2008) and DNA coloring dye (Hayashi & Harada, 2007). EtBr-DNA interactions are investigated in detail using different analytic techniques. The structure of EtBr-DNA was revealed via X-ray analyses using two different dinucleoside monophosphates in two different studies, 5-iodouridylyl (3’-5’) adenosine and 5-iodocytidylyl (3’-5’) guanosine. In both studies, nucleoside monophosphates were paired with Watson-Crick base pairing. They were separated from each other by 6.7 Å and rotated by 8º because of structural alterations in the sugar-phosphate backbone after EtBr intercalation (Tsai

et al., 1977; Jain et al., 1977). Then, a modeling study was carried out with EtBr and B-DNA. Intercalation results with 1 Å dislocation and 10º twist of two strands, thus the helix was uncoiled by 26º and nucleotides were bent by 8º relative to each other at the binding region (Sobell et al., 1977). The EtBr spectrum shows a maximum absorbance at 479 nm in the visible range. After it intercalates into calf thymus DNA, the maximum absorbance wavelength shifts to the red region and the magnitude of the maximum absorbance decreases (Waring, 1965). In addition, EtBr increases the melting temperature (T_m) of DNA (Waring, 1964), the temperature in which double helix is converted to two single stranded DNAs (Neidle & Waring, 1983). According to Benevides and Thomas (2005), hydrogen bonding between the groups on the rings of EtBr and the oxygens on phosphates of DNA is one of the reason behind the increased the stability of DNA. Upon intercalation of EtBr into DNA, the fluorescence intensity of EtBr enhances significantly. No sequence preference is noticed in the binding of EtBr to DNA, thus the equilibrium constant obtained from fluorescence intensity is not specific to the GC-content (LePecq & Paoletti, 1967).

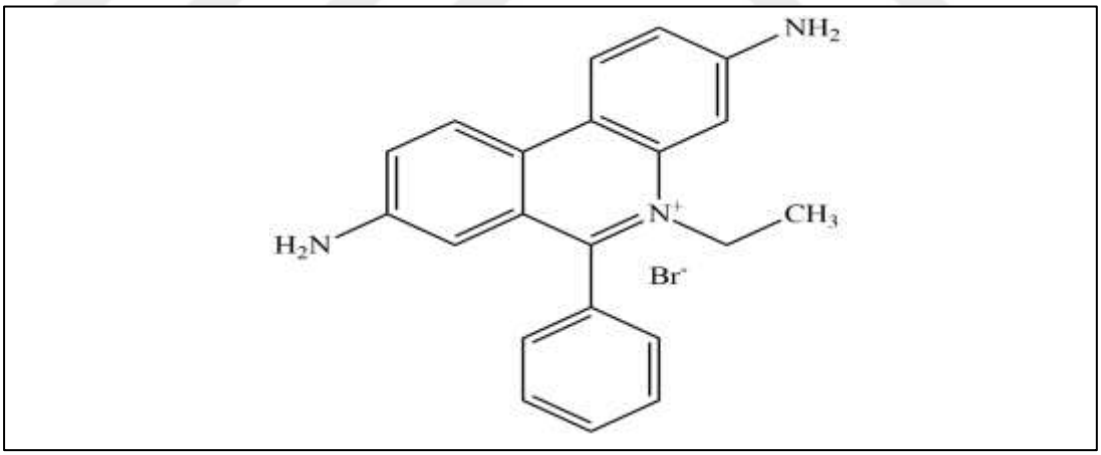

Figure 3.Chemical structure of EtBr

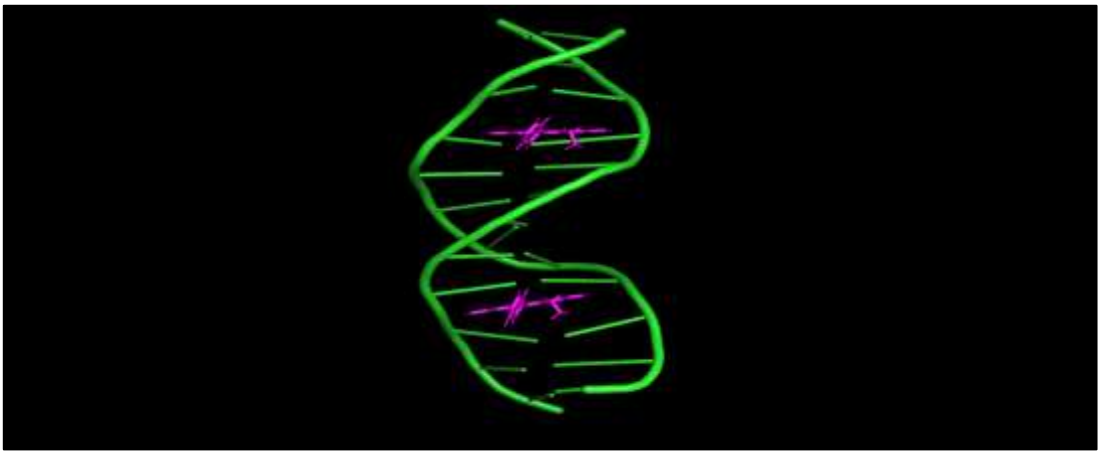

Figure 4. Intercalation of EtBr to DDD generated using PyMOL 2.4 and based on the model designed by the group of Assist. Prof. Antoine Marion

Doxorubicin (Dox) (Figure 5) is an example of threading intercalators (Aleksić & Kapetanović, 2014). It is involved in the anthracycline type of antibiotics which is considered as a powerful chemotherapeutic agent for numerous tumors (Tacar et al., 2013). Nevertheless, drug resistance and side effects such as cardiotoxicity are its disadvantages which may be developed upon Dox usage (Rubio et al., 2016). It has a planar aromatic chromophore formed from four rings (Frederick et al., 1990; Neidle & Waring, 1993). In addition, it has an amino sugar called daunosamine (Neidle & Waring, 1993) which is positively charged at pH=7 (Pérez-Arnaiz et al., 2014). Dox is threading in the minor groove with the help of ionic attraction of amine groups with the negatively charged DNA (Figure 6, Bhaduri et al., 2018). The chromophore intercalates into the DNA duplex (Frederick et al., 1990) while one of the rings projects into the major groove (Neidle & Waring, 1993). In the study of Porumb (1978), the binding of Dox to DNA caused red shift and hypochromism in both the visible and UV spectra of the drug. The wavelength in which maximum absorbance was observed shifted from 496 nm to 505 nm and the absorbance value at this wavelength decreased. According to Di Marco et al. (1976), reduction of fluorescence intensity at 550 nm with excitation at 470 nm indicates that the fluorescence intensities of anthracyclic drugs are quenched upon binding to duplex DNA. Dox enhances the T_m of double

stranded DNA by a value range from 14.8ºC (Zunino et al., 1972) to 17.8ºC (Henry, 1976), which is much more than the one observed after the binding of most classical intercalators. Increased T_m indicates the thermal stabilization of DNA upon Dox intercalation (Pérez-Arnaiz et al., 2014). In addition, Dox binding results with uncoiling of DNA by about 11º (Neidle & Waring, 1983).

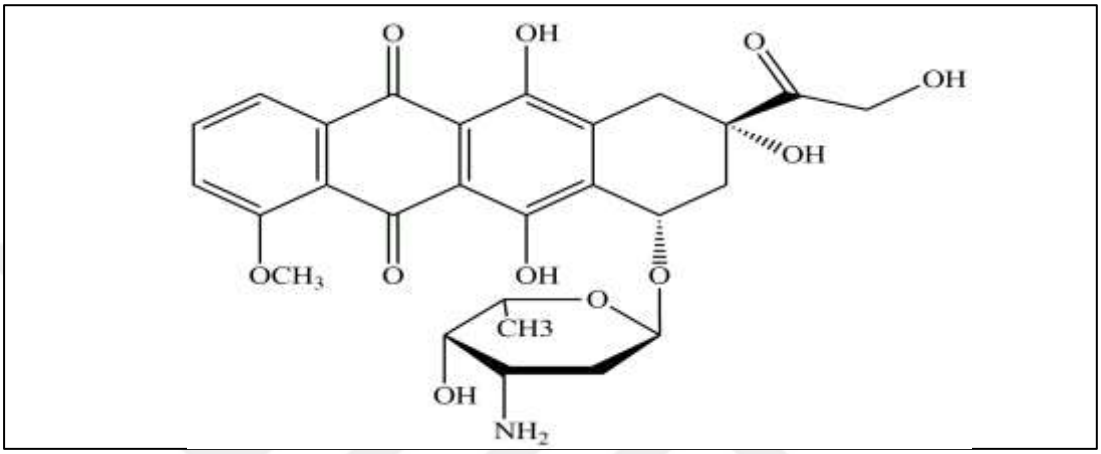

Figure 5. Chemical structure of Dox

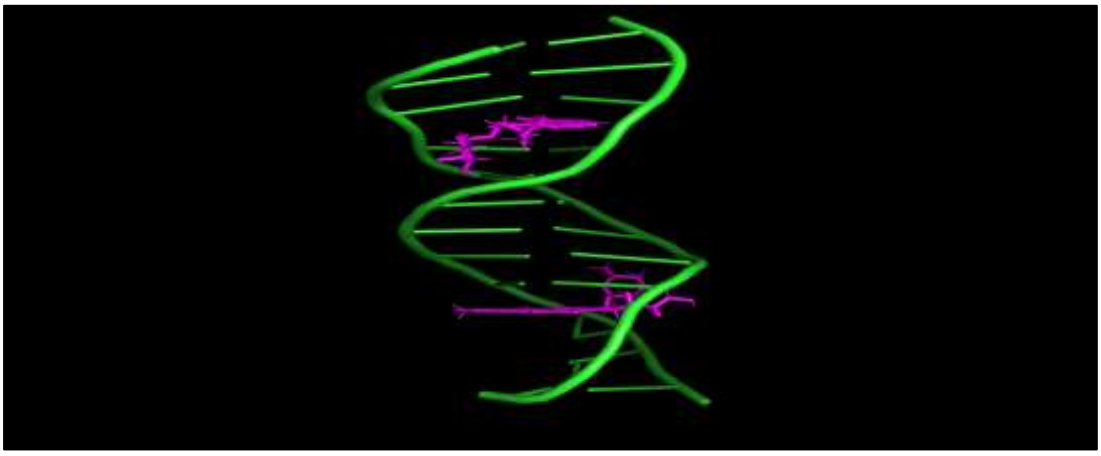

Figure 6. Intercalation of Dox to DDD generated using PyMOL 2.4 and based on the model designed by the group of Assist. Prof. Antoine Marion

1.6.2.2. Groove Binding

The essential information for DNA recognition by the other molecules is stored in the grooves of double stranded DNA, in which the edges of nucleotides are projected into (Barawkar & Ganesh, 1995). Groove binding is the insertion of an exogenous small molecule into the groove of DNA and the occupancy of the groove where normally other molecules, including enzymes, bind. Therefore, small molecules might interfere with the function of these essential molecules (Rorbach & Bobrowicz, 2014), and might, for instance, result in the hindrance of transcription (Clark et al., 1997).

Each groove binding molecule interacts with major or minor grooves of DNA. The main points which determine this preference are hydrogen bond formation between the molecule, nucleotides, and water; electrostatic forces between the positively charged zones of the molecules and the negatively charged grooves; van der Waals attractions; and the specifications of DNA depends on the nucleotide sequences such as groove size and base structure. The shape of a molecule might also be important for fitting to the curve of the groove (Clark et al., 1997). Furthermore, while bulky molecules generally interact with the major groove of DNA, smaller ones intercalate into nucleotides or bind to minor groove or do both (Barawkar & Ganesh, 1995).

Groove binding molecules fit onto the outside of DNA (Rehman et al., 2015), thus do result in little or no alteration in DNA conformation (Rorbach & Bobrowicz, 2014). In a study by Rehman et al. (2015), little or no change in the CD spectrum of duplex DNA was observed after the binding of a small molecule. Because groove binding molecules do not change the axial length of DNA, they also do not have a significant effect on the viscosity of DNA (Rehman et al., 2015). In addition, in a study by Cassina et al. (2011), netropsin (Net) which is a groove binding molecule did not alter the contour length of DNA significantly. However, according to Reinert et al. (1980), the interaction between Net and AT-rich DNA results in the formation of a more stable DNA with enhanced contour length. The

interactions of groove binders with DNA via non-covalent attractions lessen the structural autonomy of these molecules and entropy. With the hydrophobic transmission of molecules from solution to the DNA attachment region, these energy losses are balanced (Bhaduri et al., 2018).

Upon the small molecule interaction with the grooves of double stranded DNA, a blue shift is generally noticed in the UV-Vis spectrum of DNA (Weisenberger & Romano, 1999). When a molecule interacts with the grooves of DNA, the excited state of the molecule is generally deactivated and the emitted fluorescence intensity is enhanced (Afrin et al., 2017).

1.6.2.2.1. Major Groove Binding

For a regular B-form DNA, the major groove width is 11.6 Å, thus it is almost two-fold wider than the minor groove which is 6 Å. Because of this size variance, DNA associated proteins mostly bind to the major grooves of DNA (Paul & Bhattacharya, 2012). Nitrogens and oxygens in the nucleotides of the broad major grooves are projected through the centerline of the duplex (Aleksić & Kapetanović, 2014). Therefore, these atoms, generally in GC regions (Bhaduri et al., 2018), become available for specific recognition by proteins through the formation of van der Waals interactions and hydrogen bonding (Aleksić & Kapetanović, 2014; Bhaduri et al., 2018). Non-protein molecules help this recognition by interacting with the minor groove. It is necessary to design a molecule with an adequate level of affinity and selectivity towards a major groove in order to occupy the binding region of proteins on DNA and prevent their function. Currently, there are very few numbers of non-protein molecules which target the major groove (Paul & Bhattacharya, 2012) such as methyl green, antitumor molecules having a carboxamide frame, tobramycin, pluramycins, aflatoxins, azinomycins, and neocarzinostatin (Aleksić & Kapetanović, 2014).

1.6.2.2.2. Minor Groove Binding

Minor groove binding molecules have a specific bent shape in order to fit with the edges of the minor groove (Clark et al., 1996). The joined aromatic circles permit facilitated motility and rotation of these molecules (Mišković et al., 2013). The positive charge they carry at the termini is suitable for the electrostatic capacity of the binding region in the groove (Clark et al., 1996).

Hydrogen bond formation, electrostatic attractions, van der Waals forces, and hydrophobic interactions take part in the binding of molecules to the minor groove. The hydrogen bonding capacity of nucleotides maintains the positioning of molecules on the grooves. Electrostatic forces are important for the transfer of molecules into the center of the minor groove, in which the electrostatic capacity is the deepest. Apolar sites in the sugar groups are the places where van der Waals interactions take place. The relocation of water molecules after the interaction between a minor groove binder and DNA is important for conformational unity (Dolenc et al., 2005). Hydrogen bond formation, van der Waals forces, and electrostatic attractions are responsible for the AT-rich region preference of minor groove binders (Kakkar & Grover, 2005). An extra cumbersome amine group of cytosines and guanines placed in the minor groove might hinder interaction and hydrogen bonding (Vlieghe et al., 1999). AT-rich minor grooves are generally narrow (Clark et al., 1996) and the width of minor groove determines van der Waals forces between the minor groove binder and DNA. AT-rich regions are more negative than CG islands and can strongly interact with positive end groups of minor groove binders (Vlieghe et al., 1999). AT sequence bias of minor groove binding molecules might result in comprehensive conformational alterations in the major groove such as changing the availability of guanine alkylation (Neidle & Waring, 1993).

There are various minor groove binding molecules which have antitumor, antiviral, fungicidal, antimicrobial, anticancer, and antibiotic features (Clark et al., 1996; Mišković et al., 2013). The way they act includes prevention of the action of

DNA topoisomerases or binding of transcription factors upon interaction with minor groove (Clark et al., 1996). They interact with DNA generally with more affinity and greater nucleotide selectivity compared to intercalators (Paul & Bhattacharya, 2012).

Net (Figure 7) is a natural oligopeptide extracted from *Streptomyces netropsis* (Andac et al., 2011; Zasedatelev et al., 1974). It contains N-methylpyrrole and amide groups terminating with positively charged guanidinium and propylamidinium ions (Dolenc et al., 2005). The N-methylpyrrole group ensures hydrogen bonding attractions and van der Waals forces, hence takes a role in the specific binding of Net to the minor groove of AT-rich DNA regions (Kelly et al., 2009). Net interacts with the minor groove through relocating the H_2O molecules at the spine of hydration, while N-3 atoms of adenines and O-2 atoms of thymines placed in neighboring bps and complementary strands are connected by hydrogen bonding, and C-2 hydrogens of adenines and CH units of the pyrrole rings are attached by van der Waals forces (Kopka et al., 1985). The positive ends of Net give strength to DNA-Net binding (Kelly et al., 2009). Because the minor groove width is small, Net molecules are located symmetrically in the middle while non-coplanar pyrrole rings stay parallel to the edges of the groove (Figure 8, Kopka et al., 1985). Its arched structure helps its fitting to the curved surface of the minor groove (Kelly et al., 2009). It does not uncoil or lengthen the duplex (although there are some studies which criticize this evidence, as explained before) but the relaxation of the minor groove by 0.5-2.0 Å and twisting of the helix by 8° upon binding facilitate the binding of the molecule to DNA (Kopka et al., 1985). Net binds to DNA with high affinity (Marky & Breslauer, 1987) and increases the thermal stability of DNA (Patel et al., 1992).

Net has antibiotic, antifungal, and antiviral features, and an ability to eliminate the tumor viruses in mammals (Wartell et al., 1974). Although it is very toxic when consumed (Patel et al., 1992), it produced the basis of lexitropsins and some of the other anticancer medicines (Andac et al., 2011).

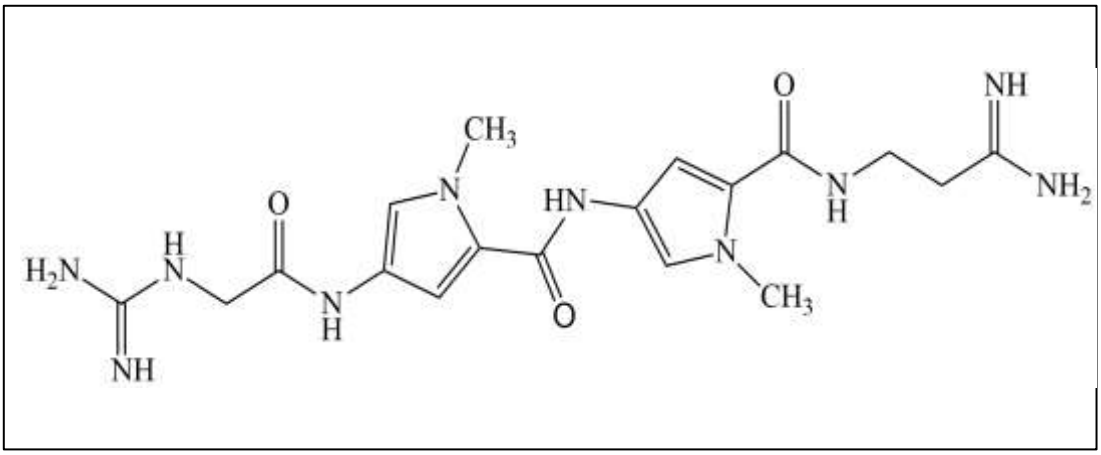

Figure 7. Chemical structure of Net

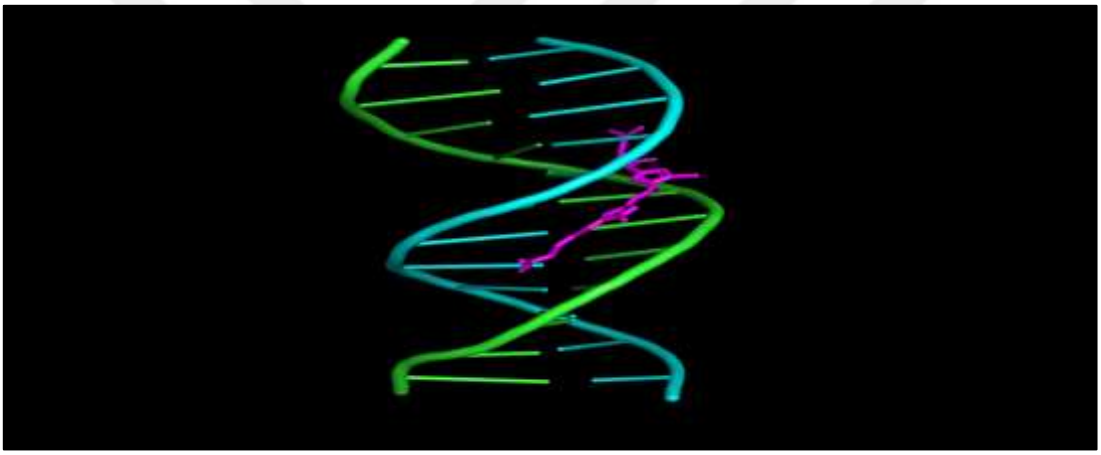

Figure 8. Binding of Net to the minor groove of DDD generated using PyMOL 2.4 and PDB file 1D86 adapted from Sriram et al. (1993)

Hoechst 33258 (Hoe) (Figure 9) is a fluorescent compound which is composed of two benzimidazole units connected head-to-tail, N-methylpiperazine, and a phenol unit (Mišković et al., 2013; Wellenzohn et al., 2001; Mann et al., 2001). Via an X-ray crystallographic analysis of Hoe and B-form of CGCGAATTCGCG sequence interaction applied by Pjura et al. (1987), it was investigated that while Hoe locates inside the minor groove of ATTC part of the DNA (Figure 10) and relocates the spine of hydration, imidogen units in benzimidazoles connect N-3 atoms of adenines and O-2 atoms of thymines by

hydrogen bonds. Hence, the benzimidazole groups of Hoe interact with three successive AT bps specifically (Mann et al., 2001). Nevertheless, a cumbersome piperazine ring cannot suit the small AT site (Neidle, 2008) and lies down the GC part of the DNA, which is larger. The amino group of guanines does not allow Hoe binding to GC rich regions (Wellenzohn et al., 2001). Because Hoe is a minor groove binder, its interaction with DNA is also stabilized by electrostatic, van der Waals, and hydrophobic forces beside hydrogen bonding (Han et al., 2005). Hoe fits the minor groove with the help of its curved structure (Wellenzohn et al., 2001).

Hoe has a local maximum UV absorbance at 338 nm, which shifts to ~350 nm upon binding to DNA. Hoe-DNA interaction results in the formation of an induced band at 355 nm in the CD spectrum. Hoe shows a maximum fluorescence emission at 505 nm (Pjura et al., 1987), while its interaction with DNA shifts this value to 461 nm and increases the fluorescence (Bucevičius et al., 2018). Hoe has a high binding affinity to B-form of DNA (Bhaduri et al., 2018). It does not significantly affect the double helix organization but enhances the stability and T_m of DNA (Mishra et al., 2009; Pjura et al., 1987).

Hoe can be used as an anthelminthic or antitumor drug, as an inhibitor of DNA topoisomerase I, as a cytological or chromosomal dye (Pjura et al., 1987; Paul & Bhattacharya, 2012).

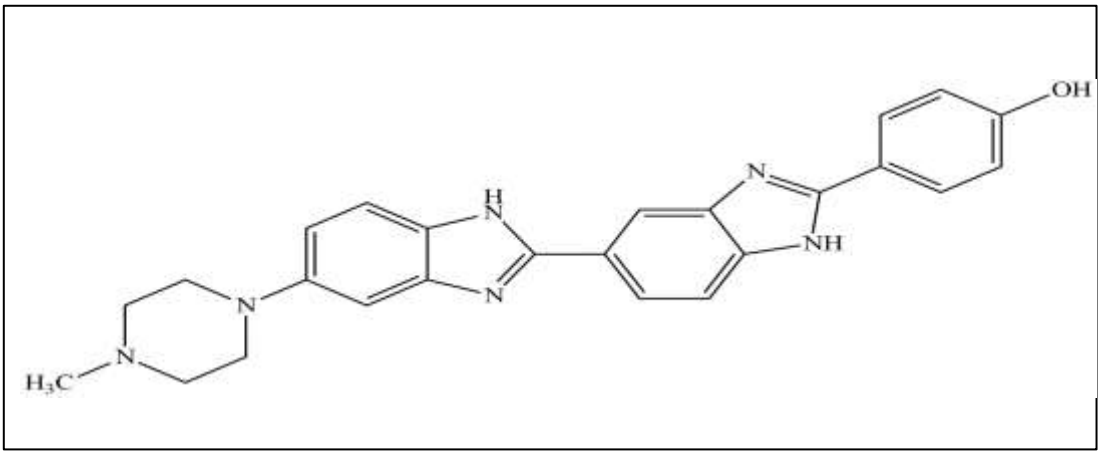

Figure 9. Chemical structure of Hoe

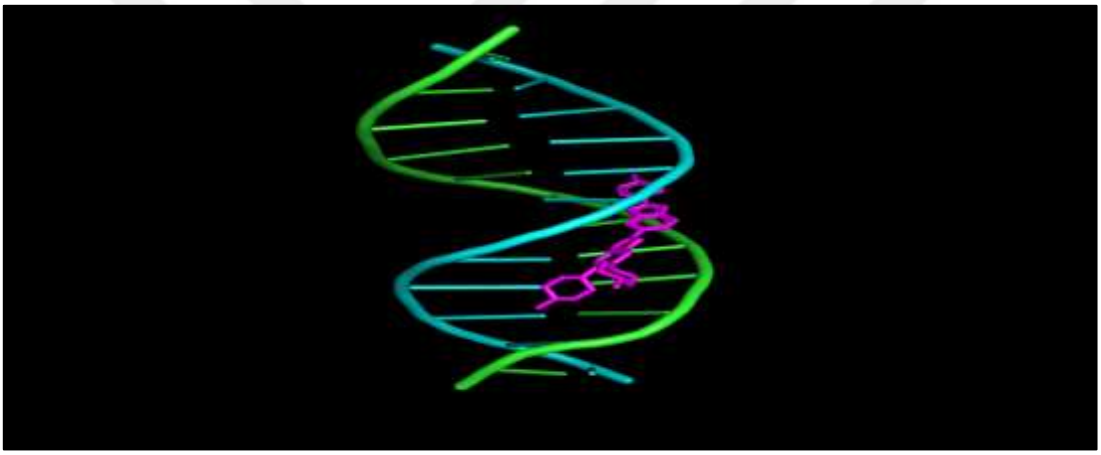

Figure 10. Binding of Hoe to the minor groove of DDD generated using PyMOL 2.4 and PDB file 8BNA adapted from Pjura et al. (1987)

1.7 Aim of the Study

Until now, most of the experiments about epigenetics have been performed *in-vivo*. The studies about the chemistry or biochemistry of epigenetic modifications are inadequate. In addition, there is too little research about the effect of these modifications on DNA structure and DNA-small molecule interactions. The main purpose of this study is to analyze how DNA conformation, DNA

stability, and DNA-small molecule attractions are altered with DNA methylation using biophysical methods and to shed light on epigenetic programming.

According to the studies performed before, a methyl group in the 5^{th} carbon of one of the cytosines in each strand increases the T_m of double stranded DNA slightly and enhances its stability compared to DNA lacking methyl groups (Thalhammer et al., 2011; Renciuk et al., 2013; Leavitt et al., 2015). On the contrary, in the study of Theruvathu et al. (2013), it was revealed that methyl groups in one or two of the cytosines in each strand did not alter neither the DNA structure nor its stability. These studies are contradictory to each other and therefore are not very conclusive. Within the scope of this thesis, the number and location of methyl groups in double stranded DNA helix were altered and the role of DNA methylation on DNA conformation and stability was analyzed systematically.

The drugs which are preferred in chemotherapy such as Dox, mitoxantrone, actinomycin act by targeting DNA structure and its biological role (Mišković et al., 2013). However, most of these drugs are cytotoxic molecules and do not differentiate the malignant and non-malignant cells. Nevertheless, targeting the epigenetic modifications observed only in cancerous cells should be considered as a novel approach in drug design studies. For instance, hypermethylation is dominant in some of the cancer types but hypomethylation in others. Chemotherapeutic agents which are specific to hypermethylated or hypomethylated DNA regions should be designed for adjusting cellular routes. To make this aim come true, it is fundamental to become familiar with the interaction of these drugs with DNA. According to our knowledge, the effect of DNA methylation on DNA-bleomycin interaction is the only study about this topic (Roy et al., 2014). In the course of this thesis, the interactions of two intercalators (EtBr and Dox) and two minor-groove binders (Net and Hoe) with methylated and non-methylated DNA duplexes were investigated. The binding affinities of these molecules and the alterations in the stability of DNAs upon binding were determined. The outcomes

of these experiments might give rise to the design of novel and specific drugs according to the methylation level of diseases.

CHAPTER 2

MATERIALS AND METHODS

2.1 Materials

Dickerson dodecamer (DDD) DNA sequences (Table 1) were obtained from Integrated DNA Technologies (Europe) in a lyophilized manner and used without purification. The lyophilized DDD was dissolved in millipore water to produce the stock solutions. The concentrations of solutions were quantified by UV-Vis absorbance at 260 nm using the extinction coefficients provided by the supplier. The extinction coefficients (ε) provided by IDT (Europe) were 110700 $M^{-1}.cm^{-1}$ for DDD, 109000 $M^{-1}.cm^{-1}$ for DDD2a and DDD2b, 107300 $M^{-1}.cm^{-1}$ for DDD4a, DDD4b, and DDD4c, 105600 $M^{-1}.cm^{-1}$ for DDD6a and DDD6b, and 103900 $M^{-1}.cm^{-1}$ for DDD8.

Table 1. Oligonucleotides used in the experiments

Abbreviation for the DNAs	*DNA Sequences*	*DNA Double Helices*
DDD	5’-CGCGAATTCGCG-3’	5’-CGCGAATTCGCG-3’ 3’-GCGCTTAAGCGC-5’
DDD2a	5’-^{me}CGCGAATTCGCG-3’	5’-^{me}CGCGAATTCGCG-3’ 3’-GCGCTTAAGCG^{me}C-5’
DDD2b	5’-CG^{me}CGAATTCGCG-3’	5’-CG^{me}CGAATTCGCG-3’ 3’-GCGCTTAAG^{me}CGC-5’
DDD4a	5’-^{me}CG^{me}CGAATTCGCG-3’	5’-^{me}CG^{me}CGAATTCGCG-3’ 3’-GCGCTTAAG^{me}CG^{me}C-5’
DDD4b	5’-^{me}CGCGAATTCG^{me}CG-3’	5’- ^{me}CGCGAATTCG^{me}CG-3’ 3’-G^{me}CGCTTAAGCG^{me}C-5’
DDD4c	5’-CG^{me}CGAATT^{me}CGCG-3’	5’-CG^{me}CGAATT^{me}CGCG-3’ 3’-GCG^{me}CTTAAG^{me}CGC-5’
DDD6a	5’-^{me}CG^{me}CGAATT^{me}CGCG-3’	5’-^{me}CG^{me}CGAATT^{me}CGCG-3’ 3’-GCG^{me}CTTAAG^{me}CG^{me}C-5’
DDD6b	5’-^{me}CG^{me}CGAATTCG^{me}CG-3’	5’-^{me}CG^{me}CGAATT^{me}CGCG-3’ 3’-G^{me}CGCTTAAG^{me}CG^{me}C-5’
DDD8	5’-^{me}CG^{me}CGAATT^{me}CG^{me}CG-3’	5’-^{me}CG^{me}CGAATT^{me}CG^{me}CG-3’ 3’-G^{me}CG^{me}CTTAAG^{me}CG^{me}C-5’

EtBr, Net, and Hoe were obtained from Sigma. Dox was obtained from Zhejiang Hisun Pharmaceutical CO., LTD (Zhejiang, China). Weighed quantities of molecules were dissolved in distilled water to produce the stock solutions. They were stored in the dark at 4ºC until used. Concentrations of stock solutions were calculated by UV-Vis absorbance at 478 nm for EtBr (ε = 5680 $M^{-1}.cm^{-1}$) (Garbett et al., 2004), at 480 nm for Dox (ε = 11500 $M^{-1}.cm^{-1}$) (Agrawal et al., 2009), at 296 nm for Net (ε = 21500 $M^{-1}.cm^{-1}$) (Degtyareva et al., 2007), and at 338 nm for Hoe (ε =42000 $M^{-1}.cm^{-1}$) (Han et al., 2005).

Each experiment was performed in BPES buffer (pH = 7.0) containing 6 mM Na_2HPO_4, 2 mM NaH_2PO_4, 1 mM Na_2EDTA, and 185 mM NaCl.

2.2 Methods

In UV-Vis and CD experiments, the ratio of DNA to intercalators, EtBr or Dox, was maintained as 4 DNA bases:1 small molecule in agreement with the 'nearest neighbor exclusion' model (Avendaño & Menéndez, 2015). The ratio of DNA to groove binding molecules, Net and Hoe, was maintained as 1 DNA duplex:1 small molecule in agreement with the crystal structures (Goodsell et al., 1995; Pjura et al., 1987). The samples included 60 μM of DNA in base and/or a selected small molecule in a quantity with respect to the rules mentioned. To guarantee the formation of the proper secondary structure, each oligonucleotide was annealed by heating until 95˚C and kept at this temperature for 3 min in a water bath and let cool down to room temperature for overnight. The small molecules were added to the samples including annealed DNAs just before the experiments.

2.2.1. Clarification of Alterations in Secondary Structure of DNA Duplex by Circular Dichroism Spectrophotometry

The spectrum of each sample was obtained by JASCO J-815 Circular Dichroism (CD) spectrophotometer combined with a Peltier temperature control item (PTC-423S/15). For thermal denaturation measurements, the samples were heated from 5 to 95°C, with 2°C intervals, 200 nm/min scanning speed and 1 nm bandwidth. The spectra of samples between 215 and 500 nm were obtained during heating. The samples were maintained at the same temperature for 2 min before the collection of the spectrum. Each CD spectrum was baseline corrected using the buffer solution. Data were obtained as an average of two values. Thermal denaturation curves were drawn by analyzing the alteration in ellipticity at 250 nm with respect to temperature and T_m of DNAs were determined from the thermal denaturation curves.

2.2.2. Determination of DNA Stability by UV-Visible Spectrophotometry

Thermal denaturation measurements were also carried out using Jasco V-730 UV-Vis spectrophotometer combined with an ETCS-761 temperature control item and a programmable heated cell holder. First, the absorbance of samples was collected in plugged quartz cuvettes between 190 and 800 nm, at 15°C. The solution including 1X BPES buffer was used as a blank for baseline correction. Then, the samples were heated from 15 to 85°C with 1°C intervals per min. 1-min delay time was given between each temperature. During heating, UV-Vis absorbance values at 260 nm with varying temperature were collected. To determine if the thermal denaturation was reversible, the measurement was repeated while the samples were cooled down from 85 to 15°C. The experiment was repeated twice. Then, thermal denaturation curves were obtained from the data

of the absorbance change at 260 nm with respect to temperature and T_ms were calculated from these thermal denaturation curves.

2.2.3. Verification of Binding Affinities by Fluorescence Spectroscopy

The samples including 1.0 μM of the selected small molecule were titrated with the sample containing 1.0 μM of the same molecule and 400.0 μM (in bp) DDD or DDD8. After each titration, emission spectrums were collected by Agilent Cary Eclipse Fluorescence Spectrophotometer, using excitation wavelengths of 510 nm for EtBr, 480 nm for Dox, and 365 nm for Hoe, and emission spectra were collected from 525 to 800 nm for EtBr, 500 to 750 nm for Dox, and 375 to 675 nm for Hoe. Excitation and emission slits were set to 10.0 and 10.0 for EtBr, 5.0 and 10.0 for Dox, and 2.5 and 5.0 for Hoe, respectively. The experiments were performed in triplicate and average value of fluorescence intensity was determined for each emission wavelength in each titration. For EtBr and Dox, the binding constants were determined by fitting the integrated fluorescence intensity as a function of DNA concentration applying the least squares equations as stated before (Horowitz & Hud, 2006; Qu & Chaires, 2000). For Hoe, the data was suitable to a sigmoidal curve fitting better, and the binding constants were determined from the middle points of the curves.

CHAPTER 3

RESULTS AND DISCUSSION

3.1 Determination of the Effect of DNA Methylation on DNA Structure and Stability

3.1.1. Determination of Secondary Structure of Oligonucleotides Using Circular Dichroism Spectroscopy

CD is the measurement of the difference between the molar absorption of the left and right-handed polarized light by photosensitive chiral molecules (Nejedlý et al., 2005; Reddy et al., 1999). CD spectroscopy is a precise method which is used for the assessment of alterations in the secondary structure of polypeptides, proteins, and DNA (Husain et al., 2013). Hence, to observe the outcome of the existence of the methyl groups in the secondary conformation of DNA, CD spectroscopy was preferred.

In Figure 11, the CD spectra of DDD and modified DDD duplexes with different number of deoxy-5-methylcytosines (*d5mC*s) at different positions were displayed. The CD spectrum of a classical B-form DNA is associated with a positive band at around 280 nm and a negative band at around 250 nm with a midpoint around 260 nm (Bloomfield et al., 2000; Renciuk et al., 2013). The CD spectrum of DDD at 5°C (black line) was consistent with the previously published CD spectrum for DDD (Renciuk et al., 2013). DDD oligonucleotides with several *d5mC*s have similar CD spectra because of having similar folding patterns, in the same way as also formerly stated by Renciuk et al. (2013) and Theruvathu et al. (2013). The major features of the B-form DNA were preserved. However, in the spectra of DDD with greater number of methyl groups, notable alterations in the

wavelength and the intensity of the maximum ellipticity were observed compared to DDD. The CD spectra of DDD, DDD2a (red line), DDD2b (light green line), and DDD4a (light blue line) were not significantly different from each other as do the spectra of DDD4b (pink line), DDD4c (purple line), DDD6a (yellow line), and DDD6b (dark green line). The negative band was red shifted about 2 nm and its intensity was decreased about 1.5 mdeg in DDD4b, DDD4c, DDD6a, and DDD6b. The DNA with a spectrum which presents these alterations the most recognizably is DDD8 in which all the cytosines were substituted with *d5mC*s. The negative band of DDD8 (dark blue line) was red shifted about 4 nm and its intensity was decreased about 4 mdeg, from ~-11.6 mdeg to ~-15.6 mdeg, compared to the negative band of DDD at around 250 nm. These changes indicate that, even though the *d5mC* substitution does not alter the B form helical structure, it does affect π-π* transitions in the plane of the bases. The methyl groups might be interfering with the π-π stacking between DNA bases. The reduced energy level of the π-π* transitions are previously reported as triggering a red shift and a hypochromic effect (Hajian et al., 2009). Although the changes observed were more clear in DDD8, they were not directly correlated with the number of *d5mC* substitutions. In addition, the position of the methyl groups in the sequence does not have a significant effect on π-π* transitions as revealed from the CD spectra of DDD sequences with the same number of *d5mC*s such as DDD6a and DDD6b.

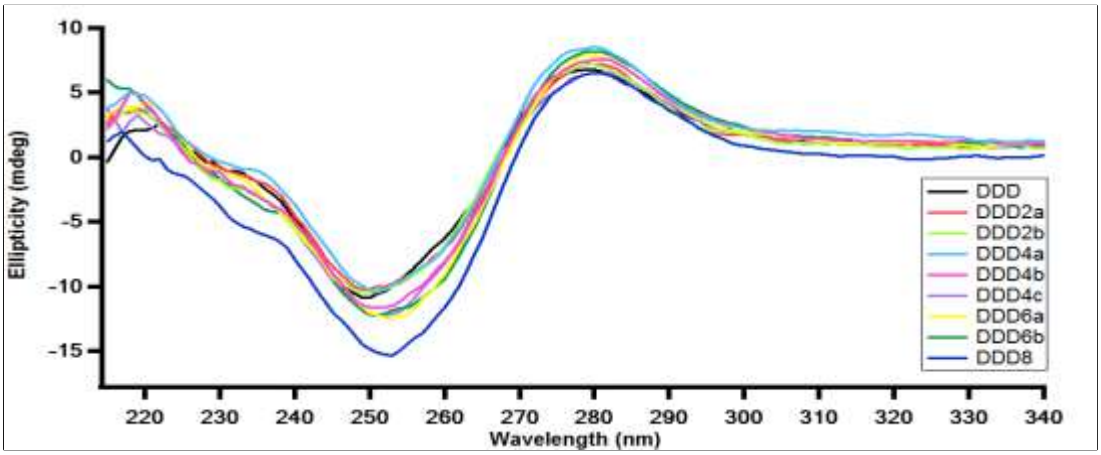

Figure 11. CD spectra of DDD and d5mC substituted DDDs (given in Table 1) at 5°C

3.1.2. Determination of Thermal Denaturation Temperatures of Oligonucleotides Using UV-Visible and Circular Dichroism Spectroscopy

So as to establish the effect of methyl groups on the stability of double stranded DNAs, thermal denaturation studies were performed by UV-Vis and CD spectrophotometers.

Thermal denaturation experiments are used to determine the stability of DNA. The heating of the double stranded DNA solution results in the separation of two strands (denaturation) into single strands. This alters the absorbance of light at 260 nm by DNA. The temperature at which 50% of duplex DNA is converted to single stranded DNA is named the melting temperature or the thermal denaturation temperature (T_m) of DNA. While the T_m is increased during DNA stabilization, it will decrease during destabilization (Rehman et al., 2015). In other words, the greater the T_m, the more stable the DNA is (Żołek & Maciejewska, 2010).

UV-Vis spectroscopy is a straightforward and efficient technique which is preferred to analyze the stability of DNA. Any alteration in the conformation of DNA changes its UV-Vis spectrum. While the destabilization of secondary

structure of DNA results with hyperchromic shift, the stabilization causes hypochromic shift (Rehman et al., 2015).

UV-Vis thermal denaturation profiles of DDDs are given in Figure 12. No direct correlation between the stability of double stranded DNAs and the number or the place of methyl groups on cytosines was observed. However, the association between the stability of DNA and the number of methyl groups was obvious (Figure 12). ~3°C increase in T_m of DDD8 in which all the cytosines were substituted with *d5mC* compared to DDD noticeably states that the methyl groups enhance the strength and stability of double stranded DNA (Table 2). Yet, the effect of *d5mC* substitution was not clear in CD thermal denaturation curves (Figure 13).

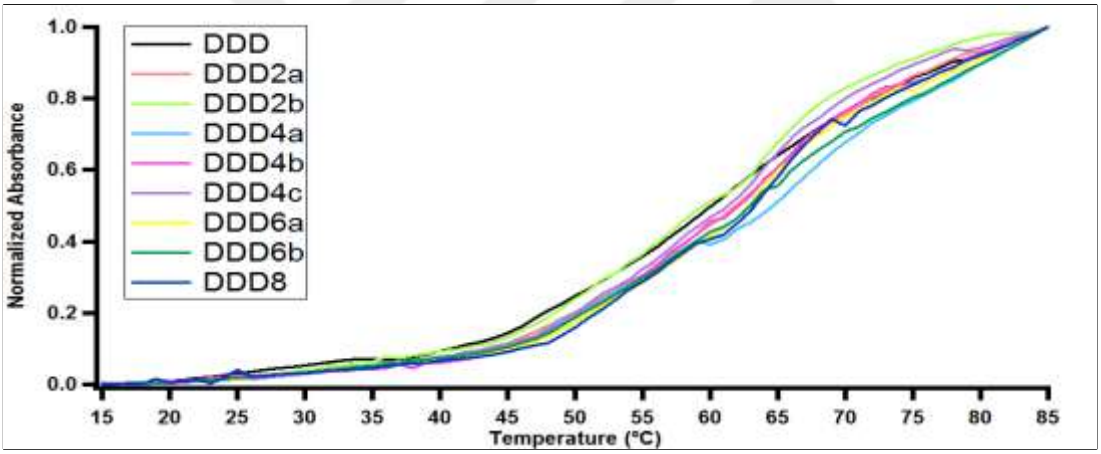

Figure 12. Average normalized thermal denaturation curves of DDD and d5mC substituted DDDs (given in Table 1) obtained by monitoring the UV-Vis absorbance at 260 nm with varying temperature

Table 2. T_m of DDD and d5mC substituted DDDs (given in Table 1) determined from the thermal denaturation profiles in Figure 12

Sequence	T_m (°C)
DDD	60.0 ± 0.5
DDD2a	62.0 ± 1.0
DDD2b	59.5 ± 0.1
DDD4a	64.8 ± 0.3
DDD4b	62.3 ± 0.8
DDD4c	61.3 ± 0.3
DDD6a	62.8 ± 0.3
DDD6b	62.8 ± 0.3
DDD8	63.3 ± 0.3

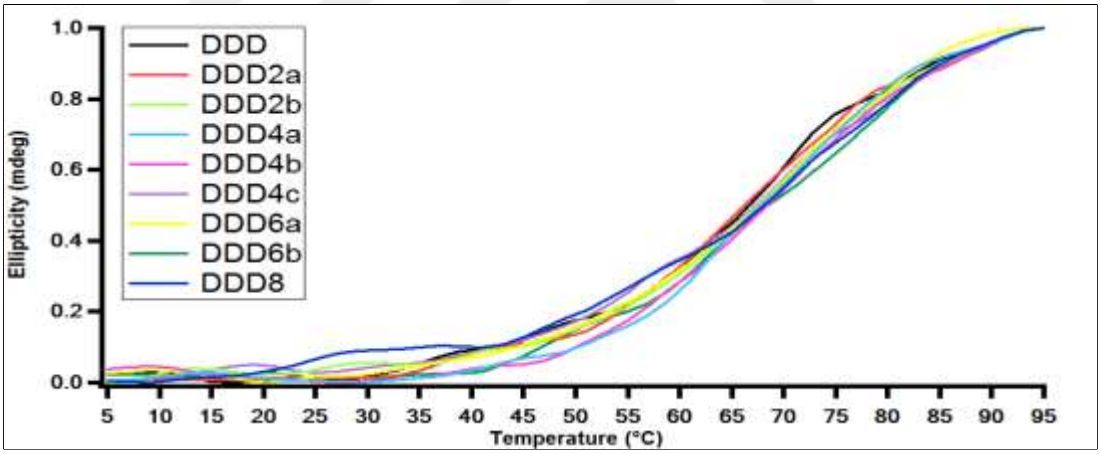

Figure 13. Normalized thermal denaturation curves of DDD and d5mC substituted DDDs (given in Table 1) obtained by monitoring the CD ellipticity at 250 nm with increasing temperature

3.2 Determination of the Effect of DNA Methylation on DNA-Small Molecule Interactions

To evaluate the effect of DNA methylation on DNA-small molecule interactions, the interactions of DDD and DDD8 with DNA intercalators and minor groove binders were investigated by UV-Vis and CD spectroscopy. DDD and DDD8 were chosen because one can monitor the effect of methyl groups on the conformation of DNA clearly by comparing the CD spectra of DDD and DDD8 in which none or all of the cytosines are methylated, respectively.

3.2.1. Determination of Interaction Using UV-Visible Spectroscopy

The UV-Vis spectra of DDD and DDD8 in the presence and absence of intercalators and groove binders were given in Figure 14 and 15, respectively. The alteration of absorption maximums in the longer wavelength regions of the UV-Vis spectra of the small molecules upon binding to DDD or DDD8 reveals the presence of interaction between the small molecules and DNAs (Figure 14 and 15 insets). The absorption maximums in the longer wavelength region of all small molecules were progressively shifted to the red upon binding to DDD or DDD8. Furthermore, there was a decrease in the magnitudes of maximum absorbance of intercalators in that region, EtBr and Dox, (hypochromism) while a significant increase was observed for Hoe, as a minor groove binder (hyperchromism). Hypochromism or hyperchromism are not induced upon the binding of Net to DDD or DDD8. The hypochromic effect was slightly higher upon the interaction of Dox with DDD8 compared to DDD. No difference in maximum absorbance values of EtBr and Hoe was observed upon their interactions with DDD or DDD8.

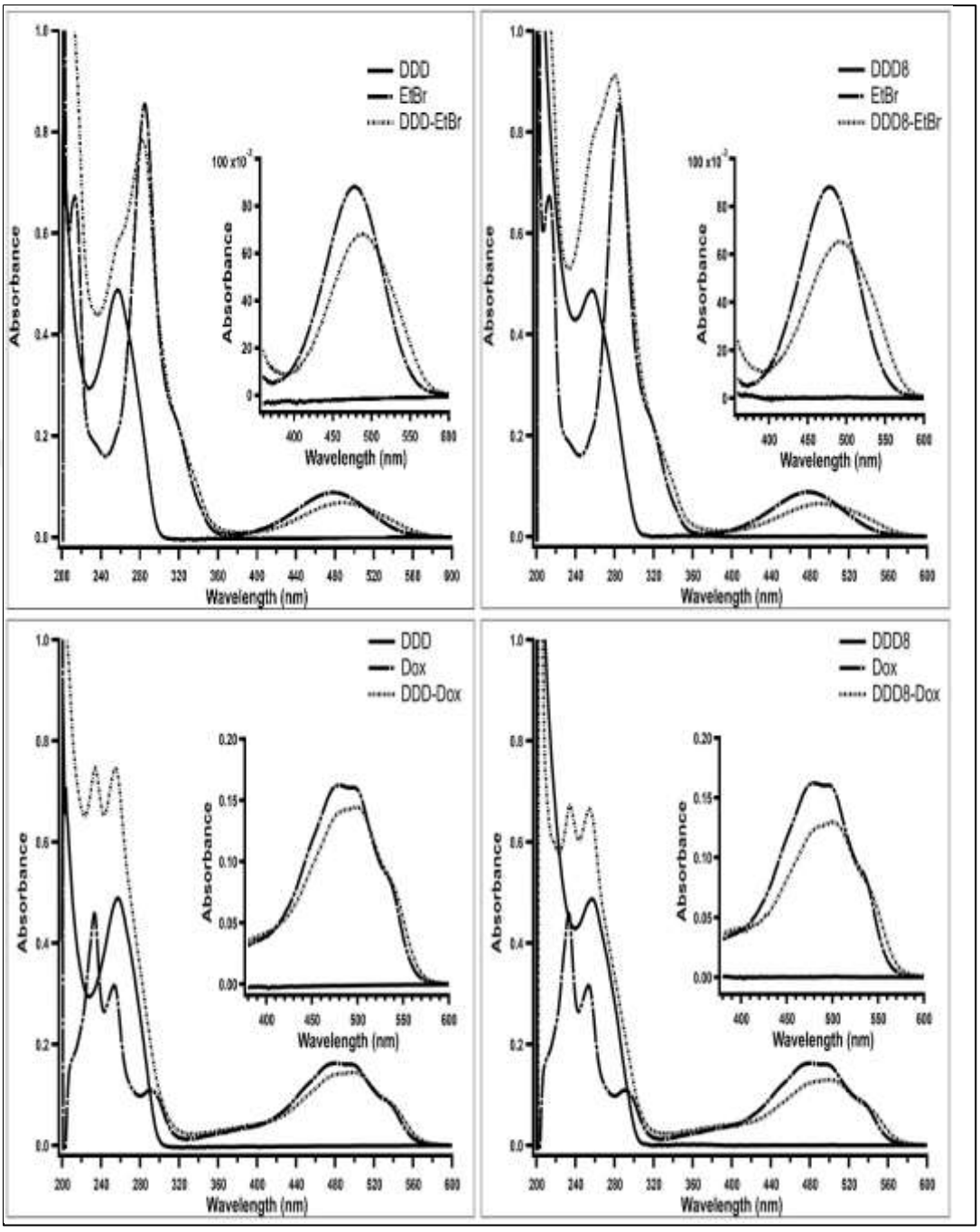

Figure 14. UV-Vis spectra of DDD and DDD8 in the absence and presence of intercalators at 15°C. The insets demonstrate the longer wavelength region of the UV-Vis spectra.

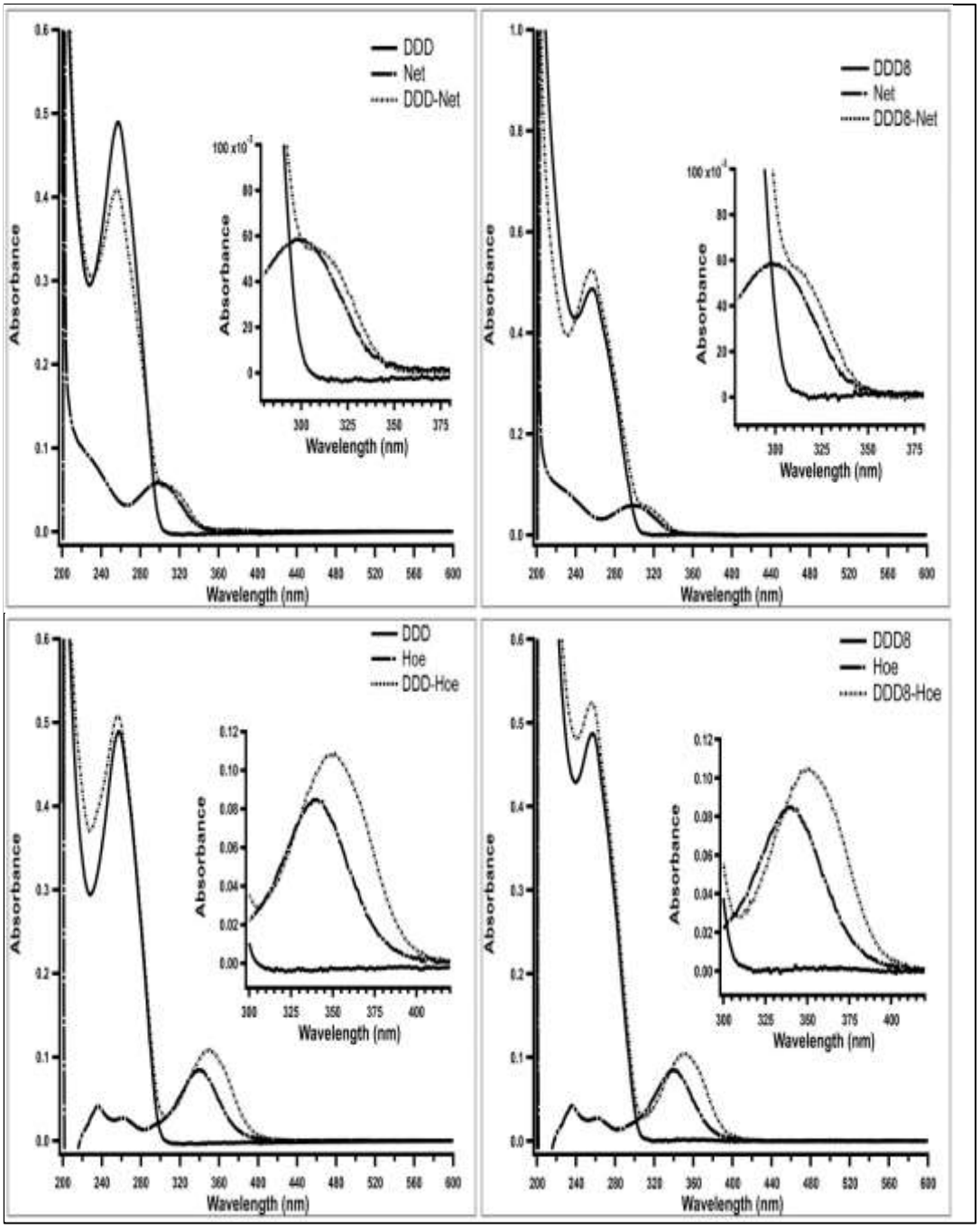

Figure 15. UV-Vis spectra of DDD and DDD8 in the absence and presence of groove binders at 15°C. The insets demonstrate the longer wavelength region of the UV-Vis spectra.

3.2.2. Determination of Interaction Using Circular Dichroism Spectroscopy

In Figure 16 and 17, the CD spectra of DDD and DDD8 in the presence and absence of intercalators and groove binders were displayed, respectively. Achiral small molecules do not give a CD-spectrum. As stated above, the CD spectrum of DDD and DDD8 were consistent with the spectrum of a B-form DNA with a negative peak at around 250 nm and a positive peak at around 280 nm (Bloomfield et al., 2000; Renciuk et al., 2013). While the interaction with small molecules does not change the B-form structure, it alters the conformation slightly, thus the CD spectrum. EtBr, Net, and Hoe affect both the CD spectra of DDD and DDD8 in a similar way. However, Dox changes the CD spectra of DDD and DDD8 in a significantly different way.

In Figure 16a, the CD spectra of DDD and DDD8 in the presence and absence of EtBr is demonstrated. EtBr binding caused an increase in the intensity of ellipticity in the negative peak at ~250 and ~280 nm, and blue shift in the positive peak at ~280 nm of both DDD and DDD8. The blue shift observed at 280 nm for DDD-EtBr was much notable than the blue shift observed for DDD8-EtBr. Yet, the intensity changes at 250 and 280 nm upon EtBr binding were more significant for DDD8 compared to DDD. Moreover, upon EtBr binding, an additional local minimum at ~228 nm and a new induced band between 300 and 370 nm were formed, as stated before (Huang & Baserga, 1976; Parodi et al., 1975). The induced CD band indicates the interaction of achiral EtBr with the chiral environment of DNAs.

In Figure 16b, the CD spectra of DDD and DDD8 in the presence and absence of Dox were observed. Interaction with Dox significantly altered the spectrum of DDD. Upon Dox binding, the peak which has a local minimum at ~250 nm was splitted up to two peaks with local minimums at ~233 and ~243 nm with an increase in the intensity. Similarly, the peak which has a local maximum at

~280 nm was splitted up to two peaks with local maximums at ~262 and ~274 nm. Moreover, a new induced band was formed with a local minimum at 300 nm. Agudelo et al. (2016) reported that Dox altered the CD spectrum of calf thymus DNA in the same way. According to their comments, the increase in the intensity of ellipticity was related to base destacking, and the blue shift and splits of the peaks were related with a conformational change from B to A form. In contrast, Dox did not change the spectrum of DDD8 as much as DDD. The peak split at 250 nm was not spotted and the increase in the intensity of the peak at this wavelength was very small compared to the one observed in DDD's spectrum. In addition, the new local minimum at 300 nm was not spotted. As a result, Dox binding to DDD8 did not cause a transition from B to A form and causes a less important base destacking compared to DDD.

The ellipticity change upon Dox binding was much more than EtBr binding. Dox, as a threading intercalator, increased the stability of DNAs more than the classical intercalator, EtBr (Paul & Bhattacharya, 2012).

Even though the effect of Net on the conformation of DNA could not be detected from UV-Vis spectra (Figure 15), its effect was obvious from CD spectra (Figure 17a). As explained before, groove binding molecules might slightly alter the conformation of DNA, thus its CD spectrum (Rehman et al., 2015). Net might open the minor groove of DNA by 0.5-2.0 Å and bend the helix by 8° in order to make hydrogen bonds (Kopka et al., 1985; Aleksić & Kapetanović, 2014). Yet, in comparison to intercalators, its effect on DNA conformation is not noteworthy.

Similar to Dox, Net affects the structure of DDD more noticeably than the structure of DDD8. Upon Net binding, while the intensity of ellipticity at ~250 nm was increased significantly in the spectrum of DDD, the increase was lower in the spectrum of DDD8. In addition, while Net binding significantly decreased the ellipticity of DDD at ~280 nm, it did not change it in the spectrum of DDD8. The weak induced band formed upon Net binding between 300 – 340 nm was similar for DDD-Net and DDD8-Net complexes.

In Figure 17b, the alterations in the CD spectra of DDD and DDD8 upon Hoe binding were displayed. Hoe does not significantly change the secondary conformations of DDD and DDD8. As mentioned before, the bulky piperazine ring of Hoe results with a slightly disrupted minor groove (Wellenzohn et al., 2001). As a result, minor intensity changes in the ellipticities in ~250 nm, slight red shift (~3 nm), and induced band formation between 300 – 400 nm were observed in the spectra of both DDD and DDD8, upon Hoe binding.

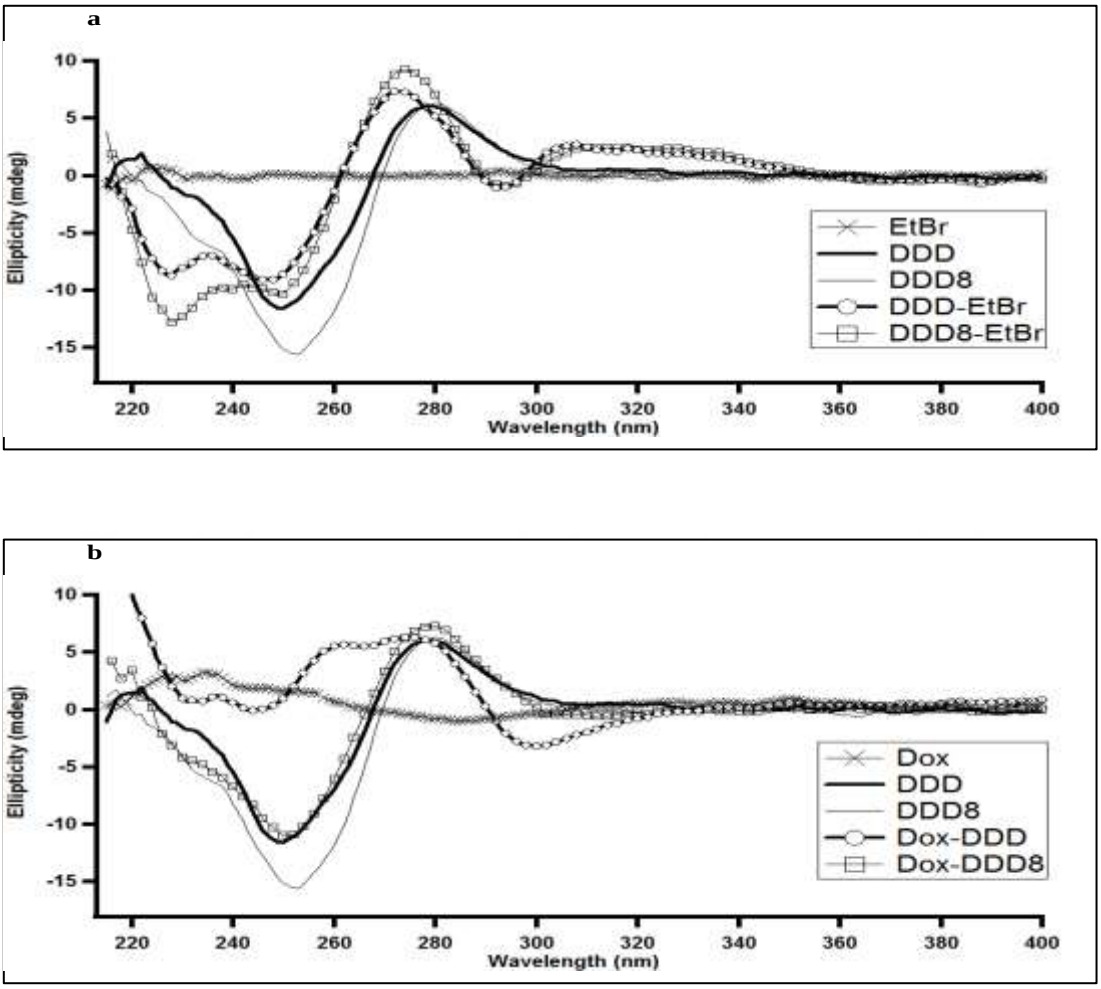

Figure 16. CD spectra of DDD and DDD8 in the absence and presence of intercalators at 5^{o}C

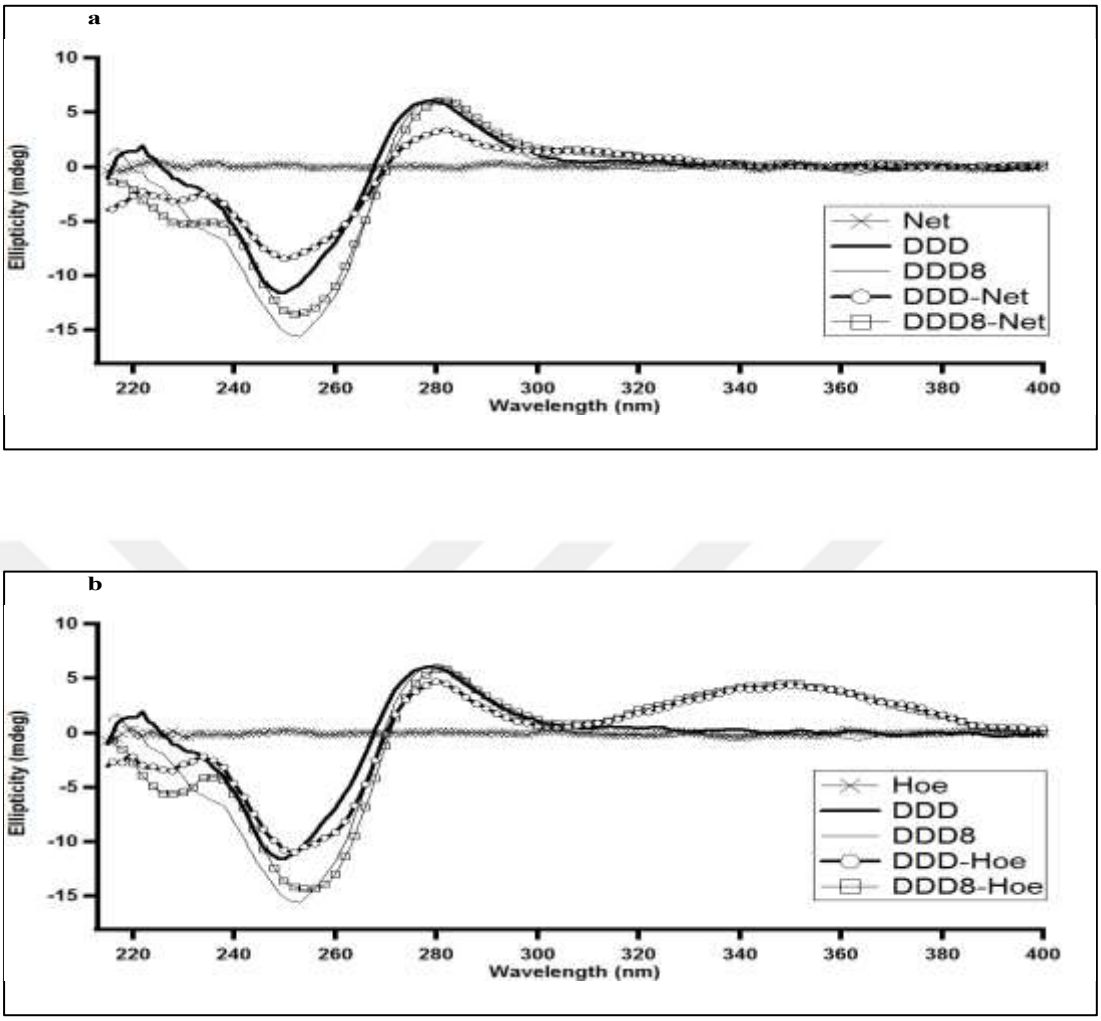

Figure 17. CD spectra of DDD and DDD8 in the absence and presence of groove binders at 5^{o}C

3.2.3. Determination of Thermal Denaturation Temperatures of Oligonucleotides in Interaction with Small Molecules Using UV-Visible Spectroscopy

Thermal denaturation experiments of DDD and DDD8 were also carried out in the presence of small molecules via UV-Vis spectrophotometer (Figure 18 insets, Table 3). All the small molecules chosen in the scope of this thesis, except EtBr, were looked as if they stabilized both DDD and DDD8. EtBr was observed as destabilizing both DDD and DDD8 structures to some extent. While EtBr is commonly known to increase the stability of DNA (Benevides and Thomas, 2005), its destabilizing effect which develops based on environmental conditions and the sequence of nucleic acid was also reported in former studies (Shchyolkina & Borisova, 1997; Vardevanyan et al., 2001). The considerable increase in the distance between the minor and major grooves upon intercalation is known to promote the destabilization of DNA. But we cannot exclude the possibility that the slight decrease in T_m of DNA upon EtBr binding might also be due to our experimental error or the weak binding affinity of EtBr to DNA. On the other hand, groove binding does not change the distance between the major and minor grooves of DNA (Yang et al., 2019) and are also known to increase the stability of DNA (Mishra et al., 2009). Here we observed that Dox, Net and Hoe, had a more stabilizing affect on DNA in contrast to EtBr.

While Dox, as an intercalator, increased the T_m of both DDD and DDD8 as ~3 °C, Net, as a minor groove binder, increased the T_m of these DNAs as ~9 °C. Also Hoe is a minor groove binder and increased the T_m of DDD and DDD8 as 8 and 7.3 °C, respectively. The minor groove binders, increased the stability of both DDD and DDD8 more than intercalators did.

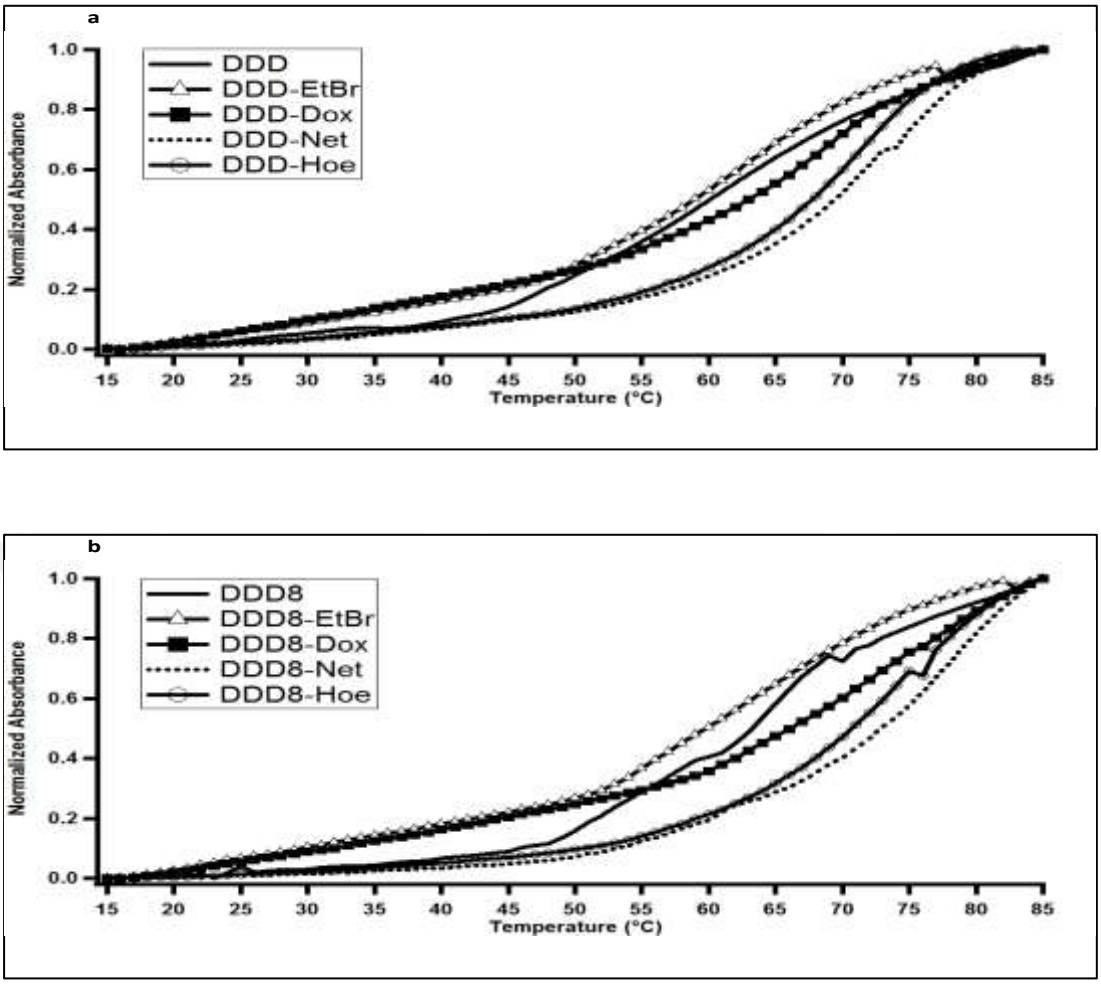

Figure 18. Average normalized heating traces of DDD (a) and DDD8 (b) in the absence and presence of small molecules obtained by observing the UV-Vis absorbance changes at 260 nm with increasing temperature

Table 3. T_m of double helical structures of DDD and DDD8 in the absence and presence of small molecules obtained from the thermal denaturation profiles in Figure 18

Sample	T_m (°C)	Sample	T_m (°C)
DDD	60.0 ± 0.5	DDD8	63.5 ± 0.1
DDD-EtBr	59.0 ± 0.1	DDD8-EtBr	59.8 ± 0.3
DDD-Dox	63.3 ± 0.3	DDD8-Dox	66.3 ± 0.3
DDD-Net	69.5 ± 0.5	DDD8-Net	72.8 ± 1.3
DDD-Hoe	68.0 ± 0.0	DDD8-Hoe	70.8 ± 0.3

3.2.4. Determination of Binding Constants Using Fluorescence Spectroscopy

Lastly, to establish the effect of DNA methylation on the binding ability of the small molecules to DNA, association constants (K_a) were determined via fluorescence titrations. The K_as obtained for the titrations of EtBr, Dox, and Hoe with DDD or DDD8 are given in Table 4, and the representative titration curves are given in Figure 19, 20, 21, 22, 23, and 24. The K_as for the titrations of Net with DNAs could not be obtained because of insignificant alteration in fluorescence of Net upon interaction with DNA, as being consistent with the report of Wartell et al. (1974). All of the small molecules chosen in the scope of this thesis were observed to be binding to DDD8 slightly better than DDD.

K_a of EtBr interacting with DDD and DDD8 was obtained to be much lower than the other small molecules. It indicates that EtBr binds to DNAs weaker than Dox and Hoe. Its weaker binding is probably the reason behind its insignificant effect on DNA stability compared to other small molecules (Figure 18, Table 3).

Hoe had a higher binding affinity towards DDD compared to EtBr and Dox while Dox was binding to DDD8 stronger than EtBr or Hoe. Although Hoe was binding to DNAs with high binding affinity, it was not able to alter their

conformation as much as the intercalators as evident from the UV-Vis and CD results.

As mentioned above, Dox was found to be altering the conformation of DDD significantly upon binding. However, it was not able to change the structure of DDD8. The reason might be the fact that the stability of DDD8 is higher than the stability of DDD. The enhanced stability of DDD8 with methyl groups might be decreasing the possible structural alteration upon Dox binding.

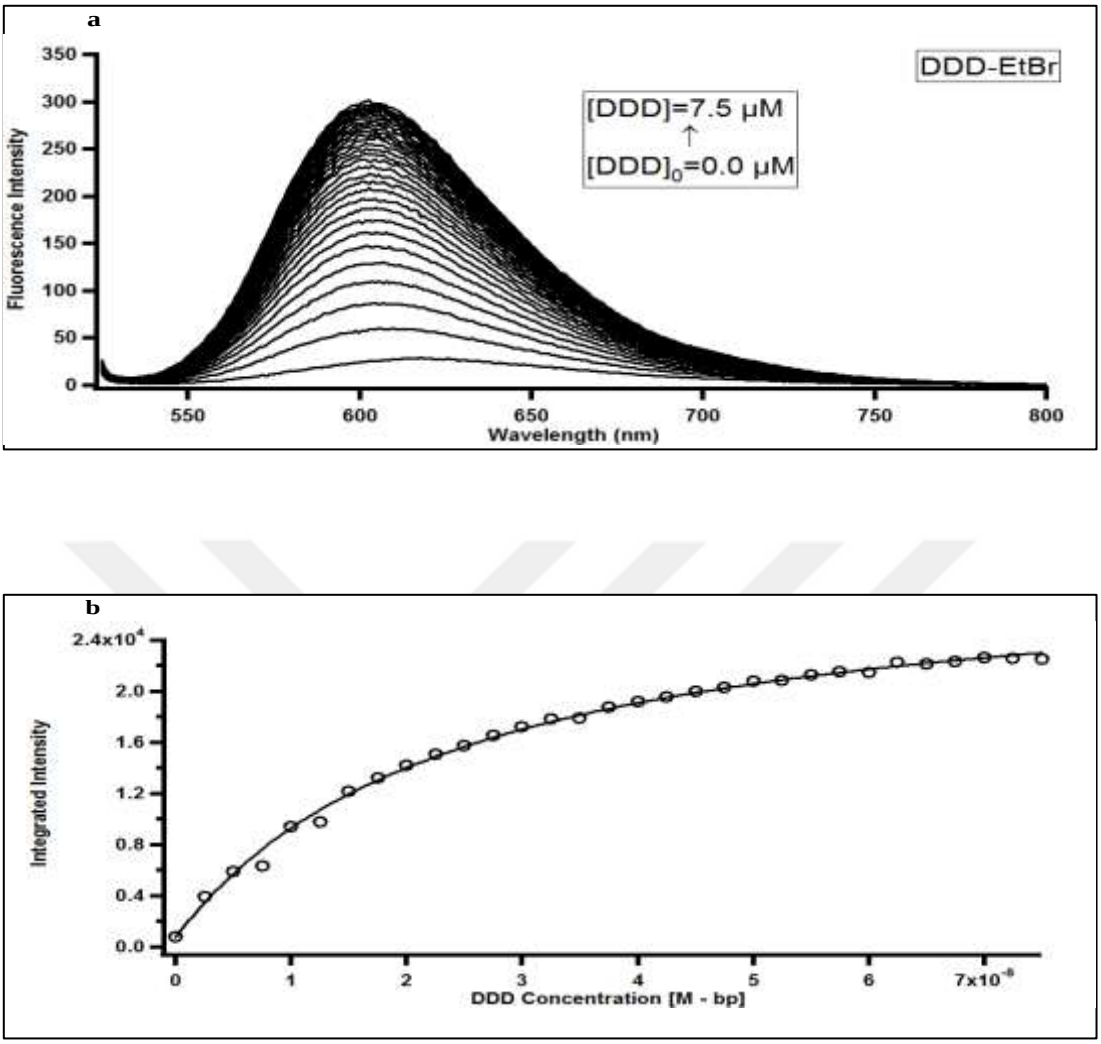

Figure 19. Average fluorescence intensity vs wavelength spectrum of EtBr which was titrated with DDD solution including 1.0 μM of EtBr (a) and the plot of integrated fluorescence intensity vs DDD concentration (b)

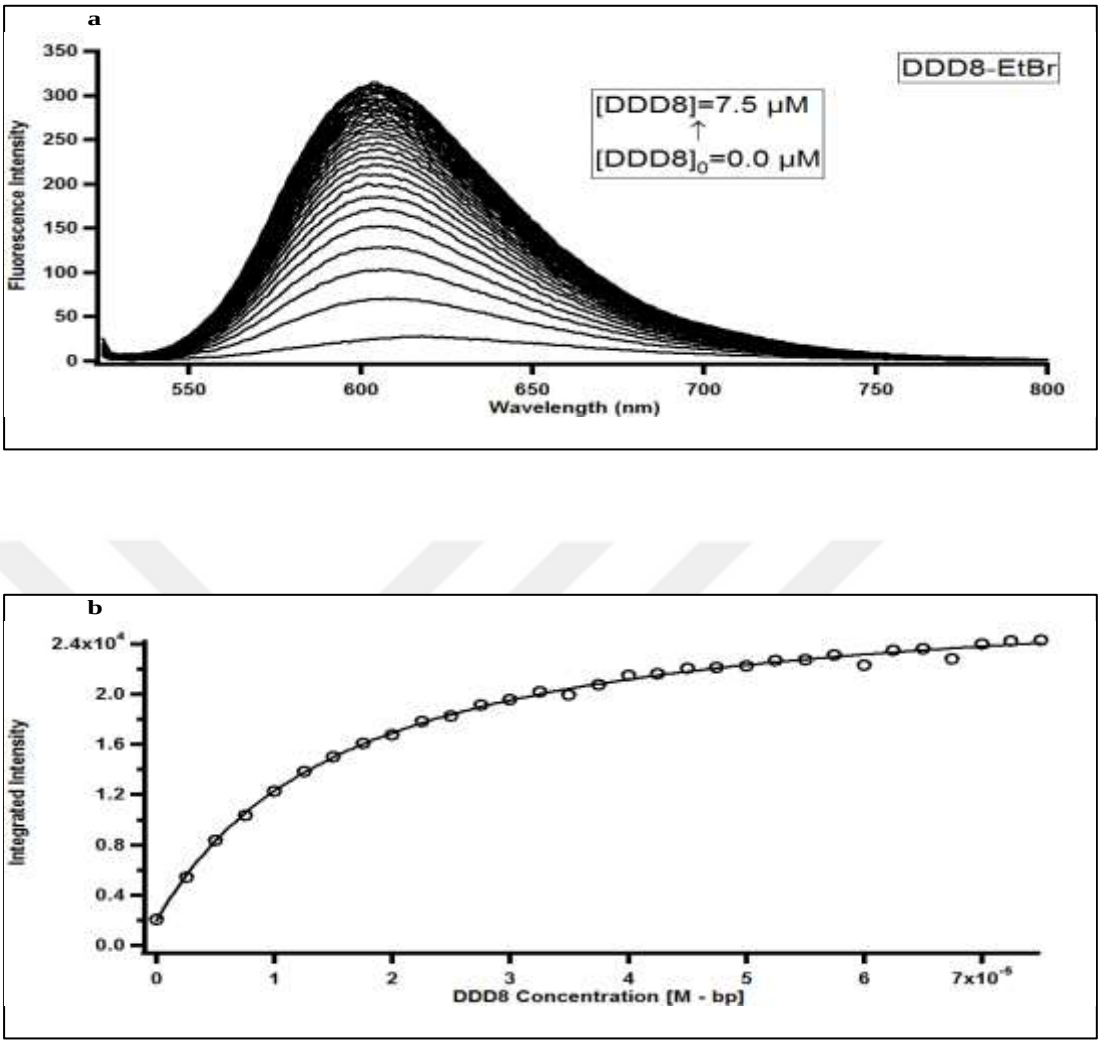

Figure 20. Average fluorescence intensity vs wavelength spectrum of EtBr which was titrated with DDD8 solution including 1.0 μM of EtBr (a) and the plot of integrated fluorescence intensity vs DDD8 concentration (b)

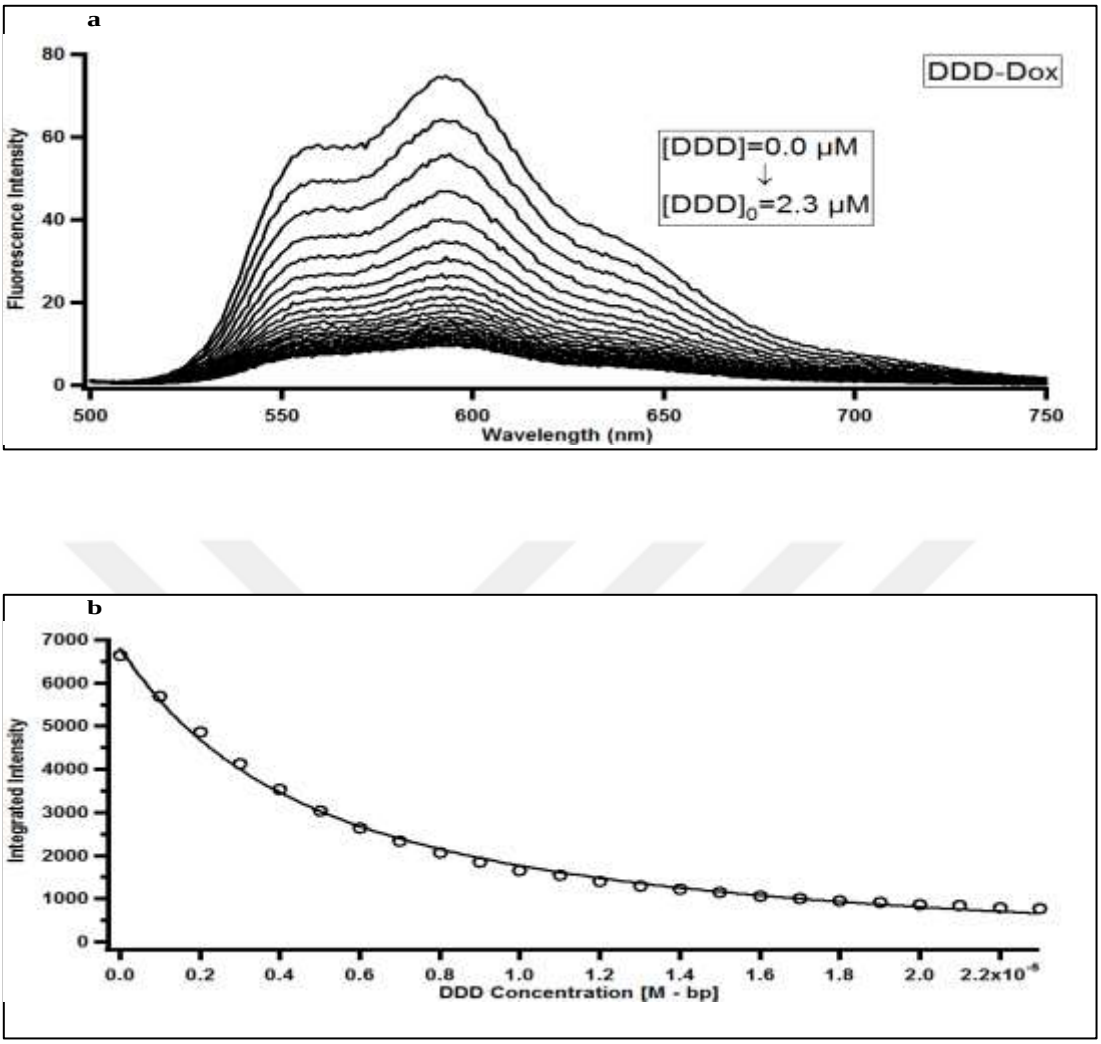

Figure 21. Average fluorescence intensity vs wavelength spectrum of Dox which was titrated with DDD solution including 1.0 μM of Dox (a) and the plot of integrated fluorescence intensity vs DDD concentration (b)

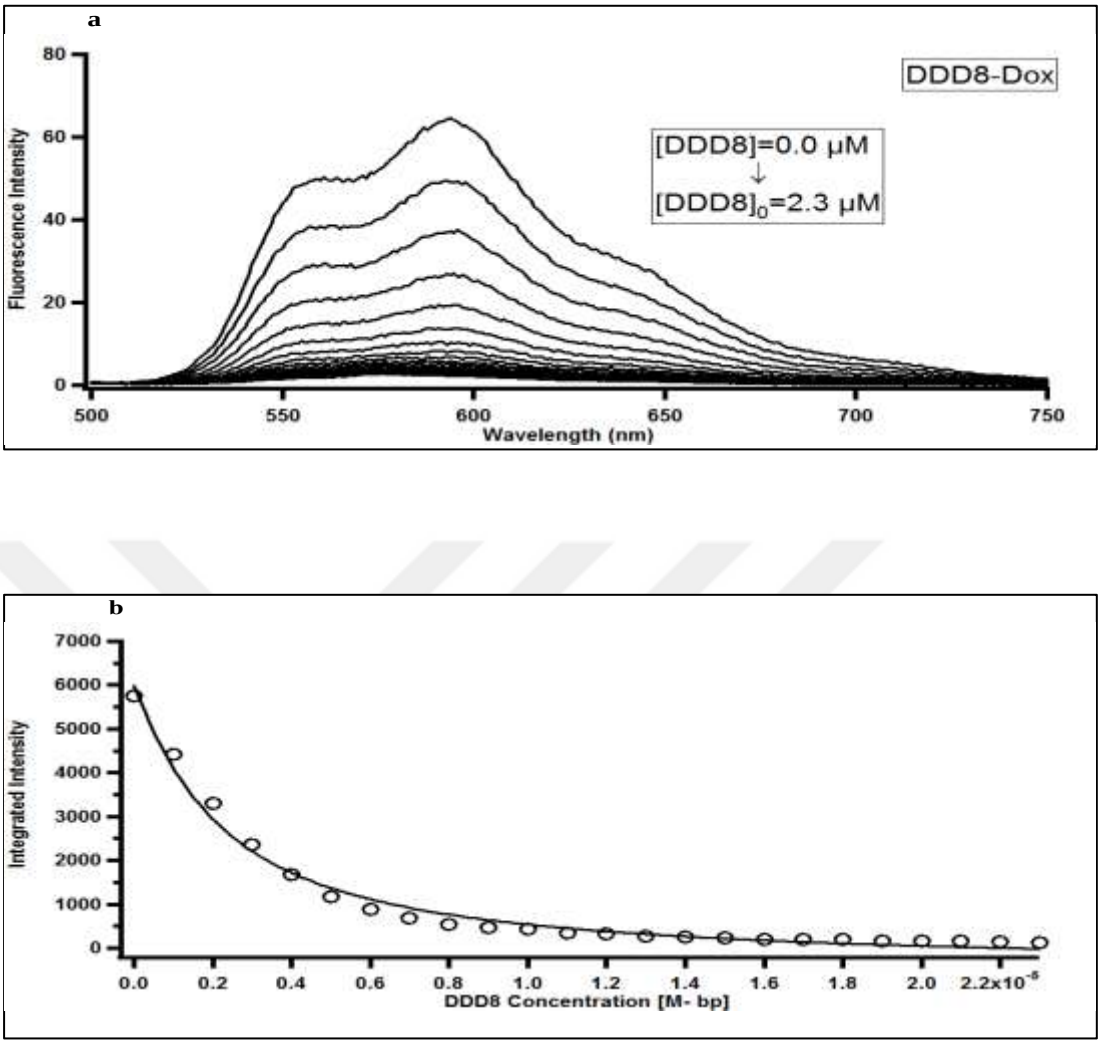

Figure 22. Average fluorescence intensity vs wavelength spectrum of Dox which was titrated with DDD8 solution including 1.0 μM of Dox (a) and the plot of integrated fluorescence intensity vs DDD8 concentration (b)

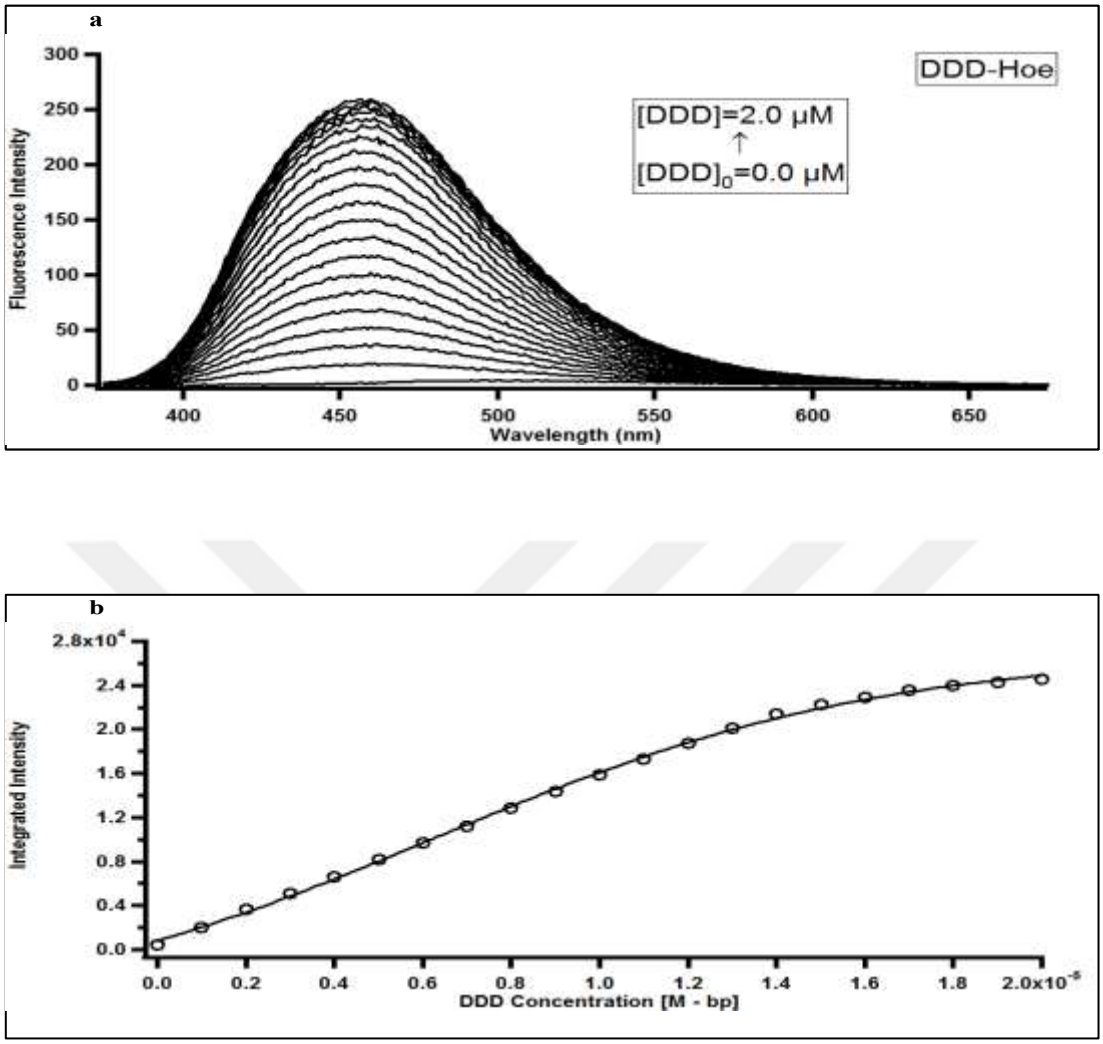

Figure 23. Average fluorescence intensity vs wavelength spectrum of Hoe which was titrated with DDD solution including 1.0 μM of Hoe (a) and the plot of integrated fluorescence intensity vs DDD concentration (b)

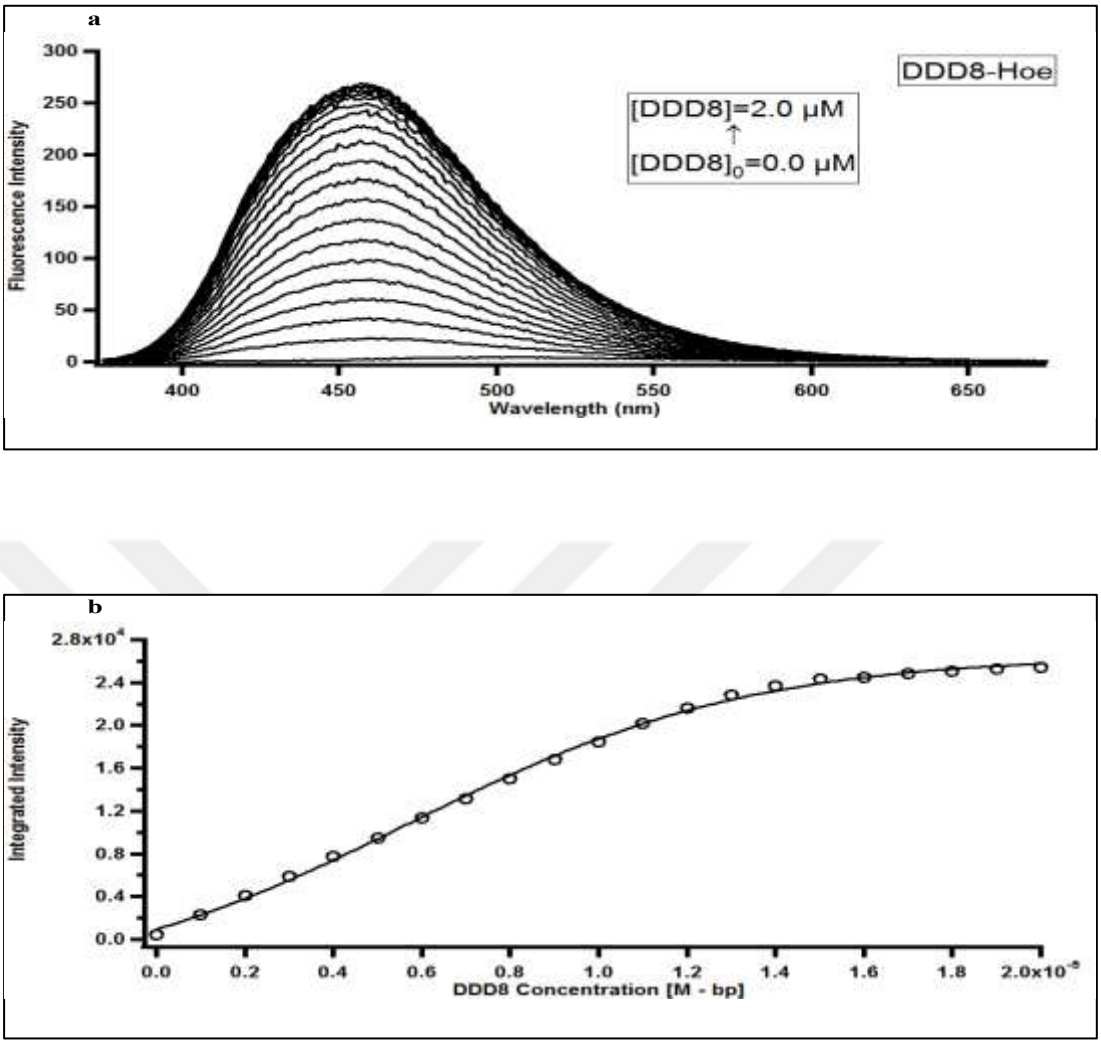

Figure 24. Average fluorescence intensity vs wavelength spectrum of Hoe which was titrated with DDD8 solution including 1.0 μM of Hoe (a) and the plot of integrated fluorescence intensity vs DDD8 concentration (b)

Table 4. Association constants (K_a) determined for small molecules-DDD or DDD8 complexes

Sample	K_a*10^5 (M^{-1})
DDD-EtBr	0.42 ± 0.02
DDD8-EtBr	0.67 ± 0.03
DDD-Dox	2.38 ± 0.12
DDD8-Dox	5.80 ± 0.59
DDD-Hoe	3.60 ± 0.36
DDD8-Hoe	4.50 ± 0.19

CHAPTER 4

CONCLUSION

With this thesis, firstly, the effect of *d5mC* on DNA, in terms of stability and secondary structure was revealed. It was investigated that the secondary structures of DDD, DDD2a, DDD2b, and DDD4a were similar while the CD spectra of DDD4b, DDD4c, DDD6a, and DDD6b were also not significantly different. DDD4b, DDD4c, DDD6a, and DDD6b present 2 nm red shift and 1.5 mdeg ellipticity alterations compared to DDD, DDD2a, DDD2b, and DDD4a. In addition, 4 nm red shift and 4 mdeg ellipticity change was observed in the CD spectrum of DDD8 compared to DDD. These changes explain the effect of *d5mC* on the structure of DNA. Yet it was not a linear relationship, the ~3°C increase in T_m of DDD8 compared to DDD can be an evidence of increase in the stability of DNA with increasing number of *d5mC* substitutions. On the other hand, the change in *d5mC* location in a sequence really altered neither the thermal stability nor the conformation of DNA.

Secondly, the effect of *d5mC* on the binding ability of intercalating and groove binding small molecules was assessed. EtBr, as an intercalator have a lower binding affinity to DNA compared to the other small molecules investigated so it did not really alter the stability of DNA. The decrease in T_m of DNA upon EtBr binding might possibly be due to the environmental conditions or the sequence of DNA (Shchyolkina & Borisova, 1997; Vardevanyan et al., 2001) or our undeniable experimental error. Although EtBr cannot strongly bind and considerably change the stability of DNA, it can significantly alter the secondary structure of DNA. According to the X-ray diffraction studies of Fuller and Waring (1964), the intermolecular separations for calf thymus sodium DNA and DNA-ethidium are 26.6 Å and 23.9 Å, respectively. In addition, the molecular model presented in the

same article shows that the nucleotides in DNA rotate by the helix axis of 24° and relocate by 6.6 Å, upon EtBr intercalation. Dox, as a threading intercalator, noticeably affects the secondary structure of DDD more than DDD8 although it binds to DDD8 with higher K_a than it does to DDD and increases the stability of both DDD and DDD8. Net, as a groove binder, changes the structure of DDD more significantly than DDD8 while it increases the stability of both DDD and DDD8, as Dox does. The alteration in secondary structure of DNA upon Net binding is not as noticeable as the one upon EtBr and Dox binding. Hoe binds to DDD8 slightly stronger than it does to DDD and increases the stability of both DDD and DDD8. However, compared to other small molecules, Hoe does not have a significant effect on the secondary structure of DDD and DDD8. Our results revealed that while EtBr was not able to significantly alter the stability of DNA and bound to DNA with low K_a, the effect of both EtBr and Dox on the secondary structures of DNA was higher than the effect of minor groove binders. In other words, the effect of groove binders on the secondary structure of DNA was not as notable as the effect of intercalators. These results are consistent with the previous literature (Rorbach & Bobrowicz, 2014; Mišković et al., 2013). And, although the groove binders could not considerably change the structure of DNA, they were able to increase its thermal stability more than intercalators because of their high binding ability to DNA. In addition, all the small molecules, especially Dox, affected the thermal stability of both DDD and DDD8 while altering the structure of DDD more than DDD8. One can say that methyl groups give strength and stability to DNA and prevent the change in secondary conformation of DNA upon small molecule binding.

In their studies, Fernandez et al. (2012) reported the comparison of the CpG islands of different tumor tissues and non-cancerous tissue and the DNA methylation profiles of tumors were determined. Two-thirds of these CpG islands were hypermethylated while the rest of them were hypomethylated. This result is illuminative to understand that each cancer cell has specific DNA methylation profile. Our findings suggest that the groove binders, because of their high binding

ability and capability to increase the stability of DNA without changing the structure of DNA, could be preferred instead of intercalators for targeting hypermethylated regions. This result might be useful to design drugs which are specific to cancer types.

REFERENCES

Afrin, S., Rahman, Y., Sarwar, T., Amir, M., Ali, A., & Tabish, M. (2017). Molecular spectroscopic and thermodynamic studies on the interaction of anti-platelet drug ticlopidine with calf thymus DNA. *Spectrochimica Acta Part A: Molecular and Biomolecular Spectroscopy*, *186*, 66–75.

Agrawal, P., Barthwal, S. K., & Barthwal, R. (2009). Studies on self-aggregation of anthracycline drugs by restrained molecular dynamics approach using nuclear magnetic resonance spectroscopy supported by absorption, fluorescence, diffusion ordered spectroscopy and mass spectrometry. *European Journal of Medicinal Chemistry*, *44*(4), 1437–1451.

Agudelo, D., Bourassa, P., Bérubé, G., & Tajmir-Riahi, H. A. (2016). Review on the binding of anticancer drug doxorubicin with DNA and tRNA: Structural models and antitumor activity. *Journal of Photochemistry and Photobiology B: Biology*, *158*, 274–279.

Aleksić, M. M., Kapetanović, V. (2014). An overview of the optical and electrochemical methods for detection of DNA – drug interactions. *Acta Chimica Slovenica*, *61*, 555–573.

Andac, C. A., Miandji, A. M., Hornemann, U., & Noyanalpan, N. (2011). Use of the parmbsc0 force field and trajectory analysis to study the binding of netropsin to the DNA fragment (5′CCAATTGG)2 in the presence of excess NaCl salt in aqueous solution. *International Journal of Biological Macromolecules*, *48*(4), 531–539.

Avendaño, C., Menéndez, C. A. (2015). Medicinal Chemistry of Anticancer Drugs, 2nd edition; Elsevier.

Banerjee, T., Banerjee, S., Sett, S., Ghosh, S., Rakshit, T., & Mukhopadhyay, R. (2016). Discriminating intercalative effects of threading intercalator nogalamycin, from classical intercalator daunomycin, using single molecule atomic force spectroscopy. *PLoS ONE*, *11*(5), 1–14.

Bannister, A. J., & Kouzarides, T. (2011). Regulation of chromatin by histone modifications. *Cell Research*, *21*(3), 381–395.

Barawkar, D. A., & Ganesh, K. N. (1995). Fluorescent d(CGCGAATTCGCG): Characterization of major groove polarity and study of minor groove interactions through a major groove semantophore conjugate. *Nucleic Acids Research*, *23*(1), 159–164.

Benevides, J. M., & Thomas, G. J. (2005). Local conformational changes induced in B-DNA by ethidium intercalation. *Biochemistry*, *44*, 2993–2999.

Berg, J. M., Tymoczko, J. L., Stryer, L. (2002). Biochemistry, 5th edition; W. H. Freeman: New York.

Bhaduri, S., Ranjan, N., & Arya, D. P. (2018). An overview of recent advances in duplex DNA recognition by small molecules. *Beilstein Journal of Organic Chemistry*, *14*, 1051–1086.

Bhatla, T., Wang, J., Morrison, D. J., Raetz, E. A., Burke, M. J., Brown, P., & Carroll, W. L. (2012). Epigenetic reprogramming reverses the relapse-specific gene expression signature and restores chemosensitivity in childhood B-lymphoblastic leukemia. *Blood*, *119*(22), 5201–5210.

Bird, A. (2007). Perceptions of epigenetics. *Nature*, *447*(7143), 396–398.

Bloomfield, V. A., Crothers, D. M., Tinoco, I. (2000). Nucleic Acids: Structures, Properties, and Functions; University Science Books: Sausalito, California.

Bonasio, R., Tu, S., Reinberg, D. (2010). Molecular signals of epigenetic states. *Science, 330*(6004), 612–616.

Bora, G., Yurter, H. E. (2007). Epigenetik hastalıklar ve tedavi yaklaşımları. *Hacettepe Tıp Dergisi*, *38*, 48–54.

Bucevičius, J., Lukinavičius, G., & Gerasimaite, R. (2018). The use of hoechst dyes for DNA staining and beyond. *Chemosensors, 6*(18), 1–12.

Cassina, V., Seruggia, D., Beretta, G. L., Salerno, D., Brogioli, D., Manzini, S., … Mantegazza, F. (2011). Atomic force microscopy study of DNA conformation in the presence of drugs. *European Biophysics Journal*, *40*(1), 59–68.

Castillo-Aguilera, O., Depreux, P., Halby, L., Arimondo, P. B., Goossens, L. (2017). DNA methylation targeting: The DNMT/HMT crosstalk challenge. *Biomolecules*, *7*(3), 1–21.

Chargaff, E. (1950). Chemical specificity of nucleic acids and mechanism of their enzymatic degradation. *Experientia*, *6*(6), 201-240.

Cheung, P., & Lau, P. (2005). Epigenetic regulation by histone methylation and histone variants. *Molecular Endocrinology, 19*(3), 563–573.

Clark, G. R., Boykin, D. W., Czarny, A., & Neidle, S. (1997). Structure of a bis-amidinium derivative of Hoechst 33258 complexed to dodecanucleotide d(CGCGAATTCGCG)2: The role of hydrogen bonding in minor groove drug-DNA recognition. *Nucleic Acids Research*, *25*(8), 1510–1515.

Clark, G. R., Squire, C. J., Gray, E. J., Leupin, W., & Neidle, S. (1996). Designer DNA-binding drugs: The crystal structure of a meta-hydroxy analogue of hoechst 33258 bound to d(CGCGAATTCGCG)2. *Nucleic Acids Research*, *24*(24), 4882–4889.

Dahm, R. (2008). Discovering DNA: Friedrich Miescher and the early years of nucleic acid research. *Human Genetics*, *122*, 565–581.

Degtyareva, N. N., Wallace, B. D., Bryant, A. R., Loo, K. M., & Petty, J. T. (2007). Hydration changes accompanying the binding of minor groove ligands with DNA. *Biophysical Journal*, *92*(3), 959–965.

Di Marco, A., Casazza, A. M., Gambetta, R., Supino, R., & Zunino, F. (1976). Relationship between activity and amino sugar stereochemistry of daunorubicin and adriamycin derivatives. *Cancer Research*, *36*(6), 1962–1966.

Dodd, I. B., Micheelsen, M. A., Sneppen, K., & Thon, G. (2007). Theoretical analysis of epigenetic cell memory by nucleosome modification. *Cell*, *129*(4), 813–822.

Dolenc, J., Borštnik, U., Hodošček, M., Koller, J., & Janežič, D. (2005). An ab initio QM/MM study of the conformational stability of complexes formed by netropsin and DNA. The importance of van der Waals interactions and hydrogen bonding. *Journal of Molecular Structure: THEOCHEM*, *718*(1–3), 77–85.

Feinberg, A. P. (2004). The epigenetics of cancer etiology. *Seminars in Cancer Biology*, *14*(6), 427–432.

Fernandez, A. F., Assenov, Y., Martin-Subero, J. I., Balint, B., Siebert, R., Taniguchi, H., … Esteller, M. (2012). A DNA methylation fingerprint of 1628 human samples. *Genome Research*, *22*(2), 407–419.

Frederick, C. A., Williams, L. D., Ughetto, G., van der Marel, G. A., van Boom, H. J., Rich, A., & Wang, A. H. J. (1990). Structural comparison of anticancer drug-DNA complexes: Adriamycin and daunomycin. *Biochemistry*, *29*(10), 2538–2549.

Garbett, N. C., Hammond, N. B., & Graves, D. E. (2004). Influence of the amino substituents in the interaction of ethidium bromide with DNA. *Biophysical Journal*, *87*(6), 3974–3981.

Goftar, M. K., Kor, N. M., & Kor, Z. M. (2014). DNA intercalators and using them as anticancer drugs. *International Journal of Advanced Biological and Biomedical Research*, *2*(3), 811–822.

Goldberg, A. D., Allis, C. D., & Bernstein, E. (2007). Epigenetics: A landscape takes shape. *Cell*, *128*(4), 635–638.

Gonzalo, S. (2010). Epigenetic alterations in aging. *Journal of Applied Physiology*, *109*(2), 586–597.

Goodsell, D. S., Kopka, M. L., & Dickerson, R. E. (1995). Refinement of netropsin bound to DNA: Bias and feedback in electron density map interpretation. *Biochemistry*, *34*(15), 4983–4993.

Gros, C., Fahy, J., Halby, L., Dufau, I., Erdmann, A., Gregoire, J. M., … Arimondo, P. B. (2012). DNA methylation inhibitors in cancer: Recent and future approaches. *Biochimie*, *94*(11), 2280–2296.

Güler, C., & Balcı Peynircioğlu, B. (2016). DNA metilasyonu ve hastalıklarla ilişkisi. *Acıbadem Üniversitesi Sağlık Bilimleri Dergisi*, *7*(2), 61–68.

Hajian, R., Shams, N., & Mohagheghian, M. (2009). Study on the interaction between doxorubicin and deoxyribonucleic acid with the use of methylene blue as a probe. *Journal of the Brazilian Chemical Society*, *20*(8), 1399–1405.

Han, F., Taulier, N., & Chalikian, T. V. (2005). Association of the minor groove binding drug Hoechst 33258 with d(CGCGAATTCGCG)2: Volumetric, calorimetric, and spectroscopic characterizations. *Biochemistry*, *44*(28), 9785–9794.

Hayashi, M., & Harada, Y. (2007). Direct observation of the reversible unwinding of a single DNA molecule caused by the intercalation of ethidium bromide. *Nucleic Acids Research, 35*(19), 1–7.

Heerboth, S., Lapinska, K., Snyder, N., Leary, M., Rollinson, S., & Sarkar. (2014). Use of epigenetic drugs in disease: An overview. *Genetics & Epigenetics, 6*, 9–19.

Henry, D. W. (1976). Adriamycin. *Cancer Chemotherapy, 2*, 15–57.

Herman, J. G., & Baylin, S. B. (2003). Gene silencing in cancer in association with promoter hypermethylation. *New England Journal of Medicine, 349*(21), 2042–2054.

Horowitz, E. D., & Hud, N. V. (2006). Ethidium and proflavine binding to a 2′,5′-linked RNA duplex. *Journal of the American Chemical Society, 128*(48), 15380–15381.

Huang, C., & Baserga, R. (1976). Circular dichroism studies of ethidium bromide binding to the isolated nucleolus. *Nucleic Acids Research, 3*(8), 1857–1873.

Hurd, P. J. (2010). The era of epigenetics. *Briefings in Functional Genomics, 9*(6), 425–428.

Husain, M. A., Yaseen, Z., Rehman, S. U., Sarwar, T., & Tabish, M. (2013). Naproxen intercalates with DNA and causes photocleavage through ROS generation. *FEBS Journal, 280*(24), 6569–6580.

Jain, S. C., Tsai, C., Sobell, H. M. (1977). Visualization of drug-nucleic acid interactions at atomic resolution: II. Structure of an ethidium/dinucleoside monophosphate crystalline complex, ethidium: 5-iodocytidylyl (3’-5’) guanosine. *Journal of Molecular Biology, 144*, 317–331.

Jones, P. A., & Baylin, S. B. (2002). The fundamental role of epigenetic events in cancer. *Nature Reviews Genetics*, *3*, 415–428.

Kakkar, R., Suruchi, & Grover, R. (2005). Theoretical study of molecular recognition by hoechst 33258 derivatives. *Journal of Biomolecular Structure and Dynamics*, *23*(1), 37–47.

Kaneda, A., Tsukada, Y. (2017). DNA and Histone Methylation as Cancer Targets; Humana Press: Cham.

Kelly, C. B., Hill, H., Bartolotti, L., & Varadarajan, S. (2009). Molecular dynamics of d(CGCGAATTCGCG)2 complexed with netropsin and its minor groove methylating analog, Me-lex, using explicit and implicit water models. *Journal of Molecular Structure: THEOCHEM*, *894*(1–3), 50–58.

Khan S. & Hilliker A. (2014). DNA Methylation and Cancer. Molecular Life Sciences; Springer: New York.

Kim, H. J., & Bae, S. C. (2011). Histone deacetylase inhibitors: Molecular mechanisms of action and clinical trials as anti-cancer drugs. *American Journal of Translational Research*, *3*(2), 166–179.

Kopka, M. L., Yoon, C., Goodsell, D., Pjura, P., & Dickerson, R. E. (1985). The molecular origin of DNA-drug specificity in netropsin and distamycin. *Proceedings of the National Academy of Sciences of the United States of America*, *82*(5), 1376–1380.

Kosova, B. (2011). Prostat kanseri tanısında DNA metilasyonunun yeri var mı? *Üroonkoloji Bülteni*, *2*(6), 33–40.

Lardenoije, R., Iatrou, A., Kenis, G., Kompotis, K., Steinbusch, H. W. M., Mastroeni, D., … Rutten, B. P. F. (2015). The epigenetics of aging and neurodegeneration. *Progress in Neurobiology*, *131*, 21–64.

Leavitt, R., Yen, J., & Jia, X. (2015). The double helix epigenetic switch: 5-methylcytosine and 5-hydroxymethylcytosine exert opposite forces on base pairing of DNA double helix. *Peanuts: A Biotechnical Newsletter*, *12*(1), 6–7.

Lepecq, J. B., & Paoletti, C. (1967). A fluorescent complex between ethidium bromide and nucleic acids: Physical-chemical characterization. *Journal of Molecular Biology*, *27*(1), 87–106.

Levene, P. A. (1919). The structure of yeast nucleic acid: IV. Ammonia hydrolysis. *Journal of Biological Chemistry*, *40*, 415–424.

Lim, D. H. K., & Maher, E. R. (2010). SAC review DNA methylation: A form of epigenetic control of gene expression. *The Obstetrician and Gynaecologist*, *12*, 37–42.

Lodish, H., Berk, A., Zipursky, S.L., et al. (2000). Molecular Cell Biology, 4th edition; W. H. Freeman: New York.

Luszczek, W., Cheriyath, V., Mekhail, T. M., & Borden, E. C. (2010). Combinations of DNA methyltransferase and histone deacetylase inhibitors induce DNA damage in small cell lung cancer cells: Correlation of resistance with IFN-stimulated gene expression. *Molecular Cancer Therapeutics*, *9*(8), 2309–2322.

Machado, A. C. D., Zhou, T., Rao, S., Goel, P., Rastogi, C., Lazarovici, A., … Rohs, R. (2014). Evolving insights on how cytosine methylation affects protein-DNA binding. *Briefings in Functional Genomics*, *14*(1), 61–73.

Mann, J., Baron, A., Opoku-Boahen, Y., Johansson, E., Parkinson, G., Kelland, L. R., & Neidle, S. (2001). A new class of symmetric bisbenzimidazole-based DNA minor groove-binding agents showing antitumor activity. *Journal of Medicinal Chemistry*, *44*(2), 138–144.

Marky, L. A., & Breslauer, K. J. (1987). Origins of netropsin binding affinity and specificity: Correlations of thermodynamic and structural data. *Proceedings of the National Academy of Sciences of the United States of America*, *84*(13), 4359–4363.

Mishra, K., Bhardwaj, R., & Chaudhury, N. K. (2009). Netropsin, a minor groove binding ligand: A potential radioprotective agent. *Radiation Research*, *172*(6), 698–705.

Mišković, K., Bujak, M., Baus Lončar, M., Glavaš-Obrovac, L. (2013). Antineoplastic DNA-binding compounds: Intercalating and minor groove binding drugs. *Archives of Industrial Hygiene and Toxicology*, *64*, 593–602.

Moore, L. D., Le, T., & Fan, G. (2013). DNA methylation and its basic function. *Neuropsychopharmacology*, *38*(1), 23–38.

Nakamoto, K., Tsuboi, M., & Strahan, G. D. (2008). Drug-DNA Interactions: Structures and Spectra. Wiley.

Nanney, D. L. (1958). Epigenetic control systems. *Proceedings of the National Academy of Sciences*, *44*(7), 712–717.

Neidle, S. (2008). Principles of Nucleic Acid Structure. London: Academic Press.

Neidle, S., & Waring, M. J. (1983). Molecular Aspects of Anti-cancer Drug Action. London: The Macmillan Press.

Neidle, S., & Waring, M. J. (1993). Molecular Aspects of Anticancer Drug-DNA Interactions: Volume 1. London: The Macmillan Press.

Nejedlý, K., Chládková, J., Vorlíčková, M., Hrabcová, I. & Kypr, J. (2005). Mapping the B-A conformational transition along plasmid DNA. *Nucleic Acids Research*, *33*(1), 1–8.

Ngo, T. T. M., Yoo, J., Dai, Q., Zhang, Q., He, C., Aksimentiev, A., & Ha, T. (2016). Effects of cytosine modifications on DNA flexibility and nucleosome mechanical stability. *Nature Communications*, *7*, 1–9.

Parodi, S., Kendall, F., & Nicolini, C. (1975). A clarification of the complex spectrum observed with the ultraviolet circular dichroism of ethidium bromide bound to DNA. *Nucleic Acids Research*, *2*(4), 477–486.

Patel, N., Berglund, H., Nilsson, L., Rigler, R., McLaughlin, L. W., & Graslund, A. (1992). Thermodynamics of interaction of a fluorescent DNA oligomer with the anti-tumour drug netropsin. *European Journal of Biochemistry*, *203*(3), 361–366.

Paul, A., & Bhattacharya, S. (2012). Chemistry and biology of DNA-binding small molecules. *Current Science*, *102*(2), 212–231.

Pauling, L., Corey, R. B. (1953). A proposed structure for the nucleic acids. *Proceedings of the National Academy of Sciences*, *39*, 84–97.

Pérez-Arnaiz, C., Busto, N., Leal, J. M., & García, B. (2014). New insights into the mechanism of the DNA/doxorubicin interaction. *Journal of Physical Chemistry B*, *118*(5), 1288–1295.

Phillips, T. (2008). The role of methylation in gene expression. *Nature Education*, *1*(1), 1–5.

Pierce, B. A. (2005). Genetics: A Conceptual Approach, 2nd edition; W. H. Freeman: New York.

Pjura, P. E., Grzeskowiak, K., & Dickerson, R. E. (1987). Binding of hoechst 33258 to the minor groove of B-DNA. *Journal of Molecular Biology*, *197*(2), 257–271.

Porumb, H. (1978). The solution spectroscopy of drugs and the drug-nucleic acid interactions. *Progress in Biophysics & Molecular Biology*, *34*, 175–195.

Pray, L. A. (2008). Discovery of DNA structure and function: Watson and Crick. *Nature Education, 1(1),* 100.

Qu, X. & Chaires, J. B. (2000). Analysis of drug-DNA binding data. *Methods in Enzymology*, *321*, 353-369.

Reddy, B. S. P., Sondhi, S. M., & Lown, J. W. (1999). Synthetic DNA minor groove-binding drugs. *Pharmacology and Therapeutics*, *84*(1), 1–111.

Rehman, S. U., Sarwar, T., Husain, M. A., & Ishqi, H. M. (2015). Studying non-covalent drug – DNA interactions. *Archives of Biochemistry and Biophysics*, *576*, 49–60.

Reinert, K. E., Thrum, H., & Sarfert, E. (1980). Counterion dependent variation of DNA secondary structure in (A-T) clusters: evidence by use of netropsin as a structural probe. *Nucleic Acids Research*, *8*(22), 5519–5532.

Renciuk, D., Blacque, O., Vorlickova, M., & Spingler, B. (2013). Crystal structures of B-DNA dodecamer containing the epigenetic modifications 5-hydroxymethylcytosine or 5-methylcytosine. *Nucleic Acids Research, 41*(21), 9891–9900.

Římal, V., Socha, O., Štěpánek, J., & Štěpánková, H. (2015). Spectroscopic study of cytosine methylation effect on thermodynamics of DNA duplex containing CpG motif. *Journal of Spectroscopy*, 2015.

Robertson, K. D. (2005). DNA methylation and human disease. *Nature Reviews Genetics, 6*(8), 597–610.

Rorbach, J., & Bobrowicz, A. J. (Eds.). (2014). Poly-adenylation Methods and Protocols. Humana Press.

Rosu, F., Gabelica, V., Houssier, C., Colson, P., & De Pauw, E. (2002). Triplex and quadruplex DNA structures studied by electrospray mass spectrometry. *Rapid Communications in Mass Spectrometry*, *16*, 1729–1736.

Roy, S. (2014). DNA methylation reduces binding and cleavage by bleomycin. *Biochemistry*, 53, 6103-6112.

Rubio, A. R., Busto, N., Leal, J. M., & García, B. (2016). Doxorubicin binds to duplex RNA with higher affinity than ctDNA and favours the isothermal denaturation of triplex RNA. *RSC Advances*, *6*(103), 101142–101152.

Russo, V. E., Martienssen, R. A., & Riggs, A. D. (1996). Epigenetic Mechanisms of Gene Regulation. Cold Spring Harbor Laboratory Press: New York.

Sarkar, S., Horn, G., Moulton, K., Oza, A., Byler, S., Kokolus, S., & Longacre, M. (2013). Cancer development, progression, and therapy: An epigenetic overview. *International Journal of Molecular Sciences*, *14*(10), 21087–21113.

Sawan, C., Vaissière, T., Murr, R., & Herceg, Z. (2008). Epigenetic drivers and genetic passengers on the road to cancer. *Mutation Research - Fundamental and Molecular Mechanisms of Mutagenesis*, *642*(1–2), 1–13.

Shchyolkina, A. K., & Borisova, O. F. (1997). Stabilizing and destabilizing effects of intercalators on DNA triplexes. *FEBS Letters*, *419*(1), 27–31.

Sobell, H. M., Tsai, C., Jain, S. C., Gilbert, S. G. (1977). Visualization of drug-nucleic acid interactions at atomic resolution: III. Unifying structural concepts in understanding drug-DNA interactions and their broader implications in understanding protein-DNA interactions. *Journal of Molecular Biology*, *144*, 333–365.

Sriram, M., Van Der Marel, G.A., Roelen, H.L.P.F., Van Boom, J.H., Wang, A.H.-J. Structural Consequences Of A Carcinogenic Alkylation Lesion On Dna: Effect of O6-ethyl-guanine on the molecular structure of D(CGC[E6G]AATTCGCG)-netropsin complex. *Biochemistry*, 31, 11823-11834.

Suzuki, M. M., & Bird, A. (2008). DNA methylation landscapes: Provocative insights from epigenomics. *Nature Reviews Genetics*, *9*(6), 465–476.

Tacar, O., Sriamornsak, P., & Dass, C. R. (2013). Doxorubicin: An update on anticancer molecular action, toxicity and novel drug delivery systems. *Journal of Pharmacy and Pharmacology*, *65*(2), 157–170.

Taqi, M. M., Wärmländer, S. K. T. S., Yamskova, O., Madani, F., Bazov, I., Luo, J., … Bakalkin, G. (2012). Conformation effects of CpG methylation on single-stranded DNA oligonucleotides: Analysis of the opioid peptide dynorphin-coding sequences. *PLoS ONE*, *7*(6).

Thalhammer, A., Hansen, A. S., El-Sagheer, A. H., Brown, T., & Schofield, C. J. (2011). Hydroxylation of methylated CpG dinucleotides reverses stabilisation of DNA duplexes by cytosine 5-methylation. *Chemical Communications*, *47*(18), 5325–5327.

Theruvathu, J. A., Yin, Y. W., Pettitt, B. M., & Sowers, L. C. (2013). Comparison of the structural and dynamic effects of 5-methylcytosine and 5-chlorocytosine in a CpG dinucleotide sequence. *Biochemistry*, 52(47), 8590–8598.

Tollefsbol, T. (2018). Translational Epigenetics: Epigenetics in Human Disease, 2nd edition; Academic Press.

Tsai, C., Jain, S. C., Sobell, H. M. (1977). Visualization of drug-nucleic acid interactions at atomic resolution: I. Structure of an ethidium/dinucleoside monophosphate crystalline complex, ethidium:5-iodouridylyl (3'-5') adenosine. *Journal of Molecular Biology, 114*, 301–315.

Van Dyke, M. W. (2005). Do DNA triple helices or quadruplexes have a role in transcription? In *DNA Conformation and Transcription* (pp. 105–126). Landes Bioscience.

Vardevanyan, P. O., Antonyan, A. P., Manukyan, G. A., & Karapetyan, A. T. (2001). Study of ethidium bromide interaction peculiarities with DNA. *Experimental and Molecular Medicine*, *33*(4), 205–208.

Vlieghe, D., Sponer, J., & Van Meervelt, L. (1999). Crystal structure of d(GGCCAATTGG) complexed with DAPI reveals novel binding mode. *Biochemistry*, *38*(50), 16443–16451.

Waddington, C. H. (1939). An Introduction to Modern Genetics; The Macmillan Company, New York.

Wang, J., Yu, J. T., Tan, M. S., Jiang, T., & Tan, L. (2013). Epigenetic mechanisms in Alzheimer's disease: Implications for pathogenesis and therapy. *Ageing Research Reviews*, *12*(4), 1024–1041.

Waring, M. J. (1964). Complex formation with DNA and inhibition of Escherichia coli RNA polymerase by ethidium bromide. *Biochimica et Biophysica Acta*, *87*, 358–361.

Waring, M. J. (1965). Complex formation between ethidium bromide and nucleic acids. *Journal of Molecular Biology*, *13*(1), 269–282.

Wartell, R. M., Larson, J. E., & Wells, R. D. (1974). Netropsin: A specific probe for A-T regions of duplex deoxyribonucleic acid. *The Journal of Biological Chemistry*, *21*, 6719–6731.

Watson, J. D., Crick, F. H. C. (1953). Molecular structure of nucleic acids: a structure for deoxyribose nucleic acid. *Nature, 171*, 737–738.

Weisenberger, D. J., & Romano, L. J. (1999). Cytosine methylation in a CpG sequence leads to enhanced reactivity with benzo[a]pyrene diol epoxide that correlates with a conformational change. *Journal of Biological Chemistry*, *274*(34), 23948–23955.

Wellenzohn, B., Flader, W., Winger, R. H., Hallbrucker, A., Mayer, E., & Liedl, K. R. (2001). Significance of ligand tails for interaction with the minor groove of B-DNA. *Biophysical Journal*, *81*(3), 1588–1599.

Yang, B., Qin, C., Hu, X., Xia, K., Lu, C., Gudda, F. O., … Gao, Y. (2019). Enzymatic degradation of extracellular DNA exposed to chlorpyrifos and chlorpyrifos-methyl in an aqueous system. *Environment International*, *132*(105087), 1–9.

Zasedatelev, A. S., & Gursky, G. V. (1974). Binding of netropsin to DNA and synthetic polynucleotides. *Molecular Biology Reports*, *1*, 337–342.

Żołek, T., & Maciejewska, D. (2010). Theoretical models of pentamidine analogs activity based on their DNA minor groove complexes. *European Journal of Medicinal Chemistry*, *45*(5), 1991–1999.

Zunino, F., Gambetta, R., Di Marco, A., & Zaccara, A. (1972). Interaction of daunomycin and its derivatives with DNA. *Biochimica et Biophysica Acta*, *277*(3), 489–498.

APPENDICES

A. Fluorescence Spectra

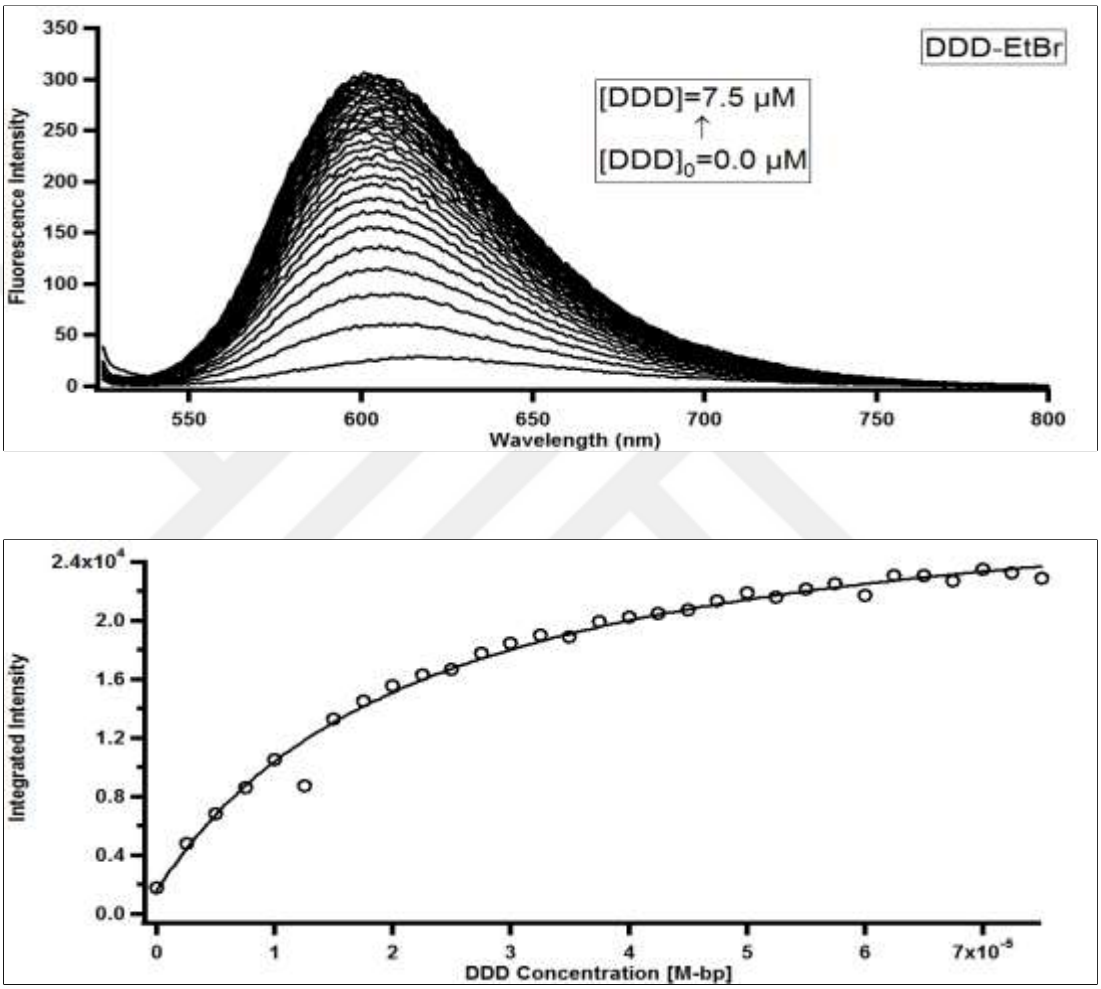

Figure A1. Fluorescence intensity vs wavelength spectrum of EtBr which was titrated with DDD solution including 1.0 µM of EtBr and the plot of integrated fluorescence intensity vs DDD concentration (1st replicate)

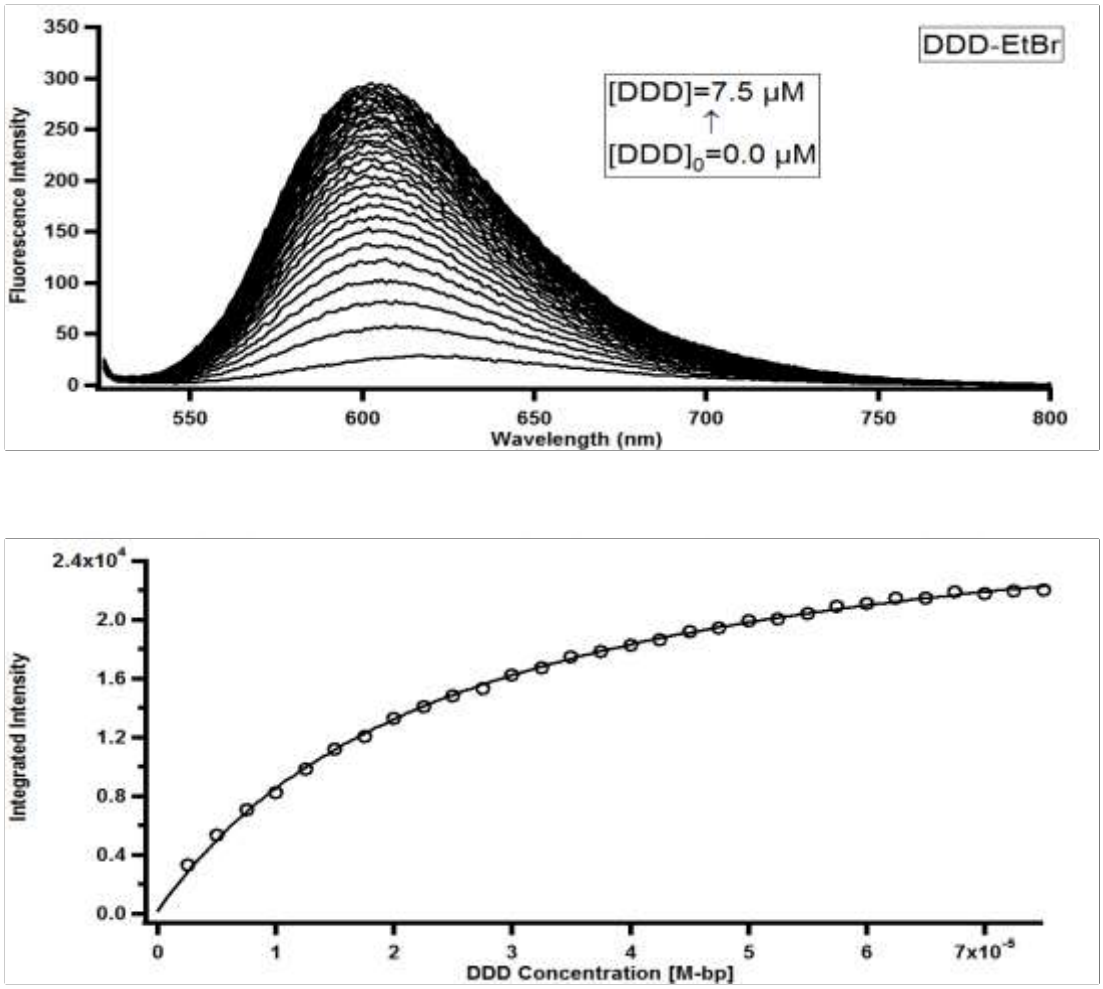

Figure A2. Fluorescence intensity vs wavelength spectrum of EtBr which was titrated with DDD solution including 1.0 μM of EtBr and the plot of integrated fluorescence intensity vs DDD concentration (2nd replicate)

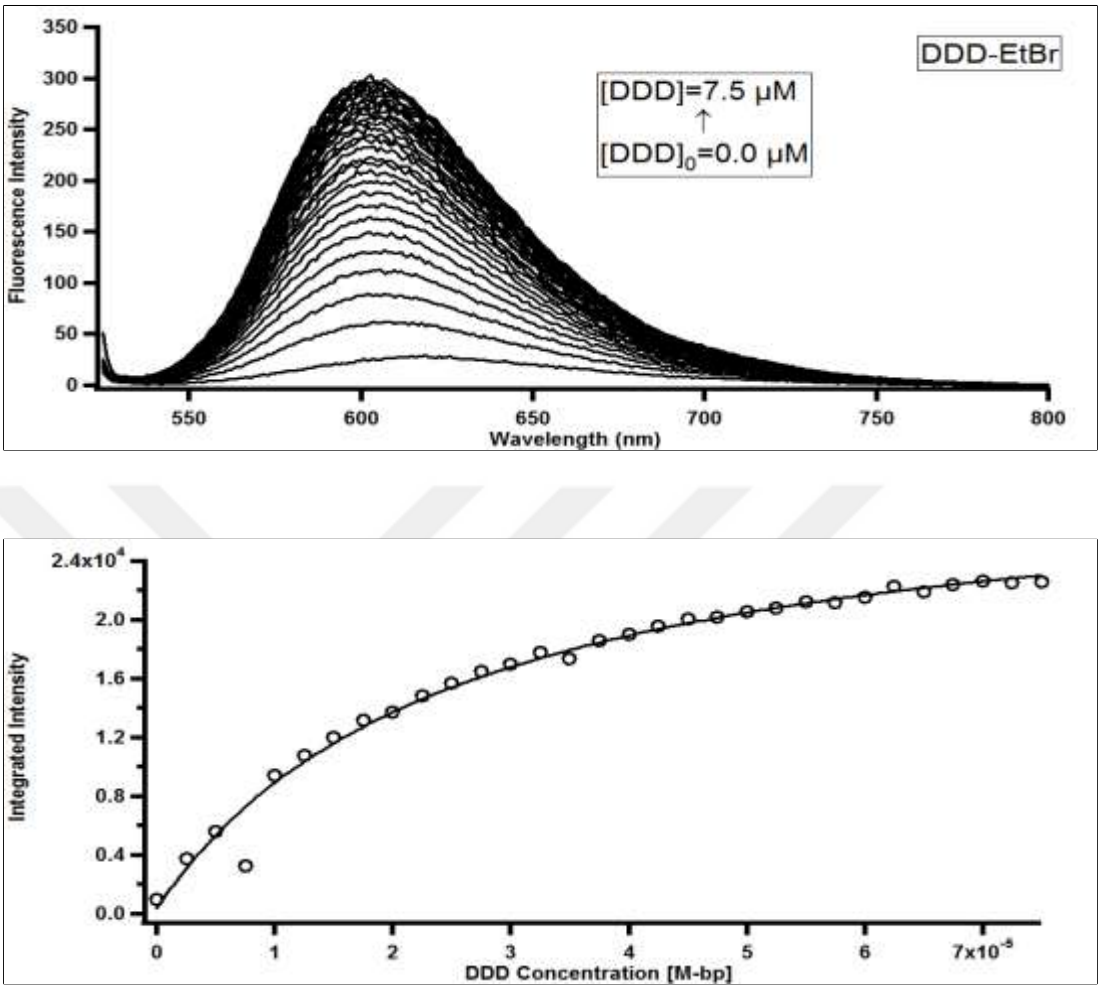

Figure A3. Fluorescence intensity vs wavelength spectrum of EtBr which was titrated with DDD solution including 1.0 µM of EtBr and the plot of integrated fluorescence intensity vs DDD concentration (3rd replicate)

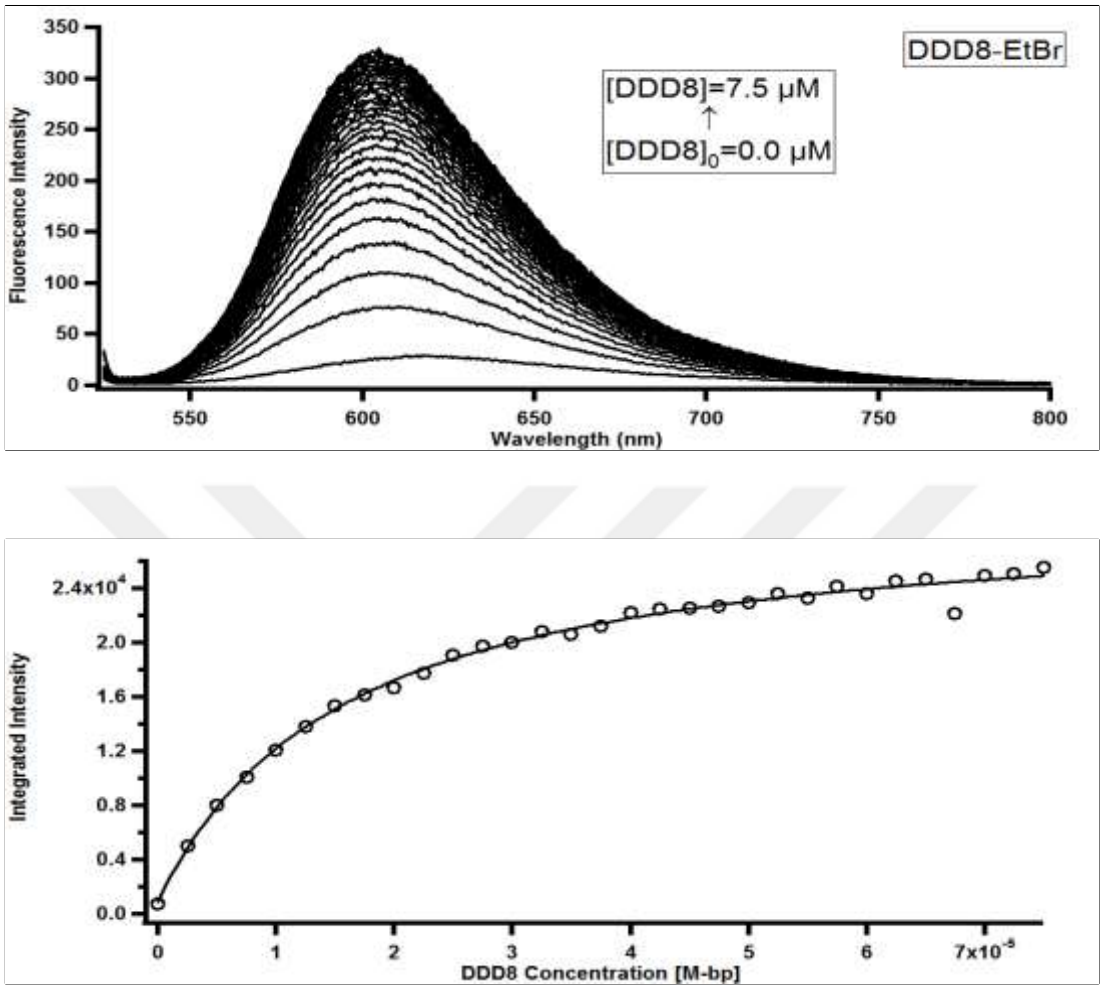

Figure A4. Fluorescence intensity vs wavelength spectrum of EtBr which was titrated with DDD8 solution including 1.0 µM of EtBr and the plot of integrated fluorescence intensity vs DDD8 concentration (1st replicate)

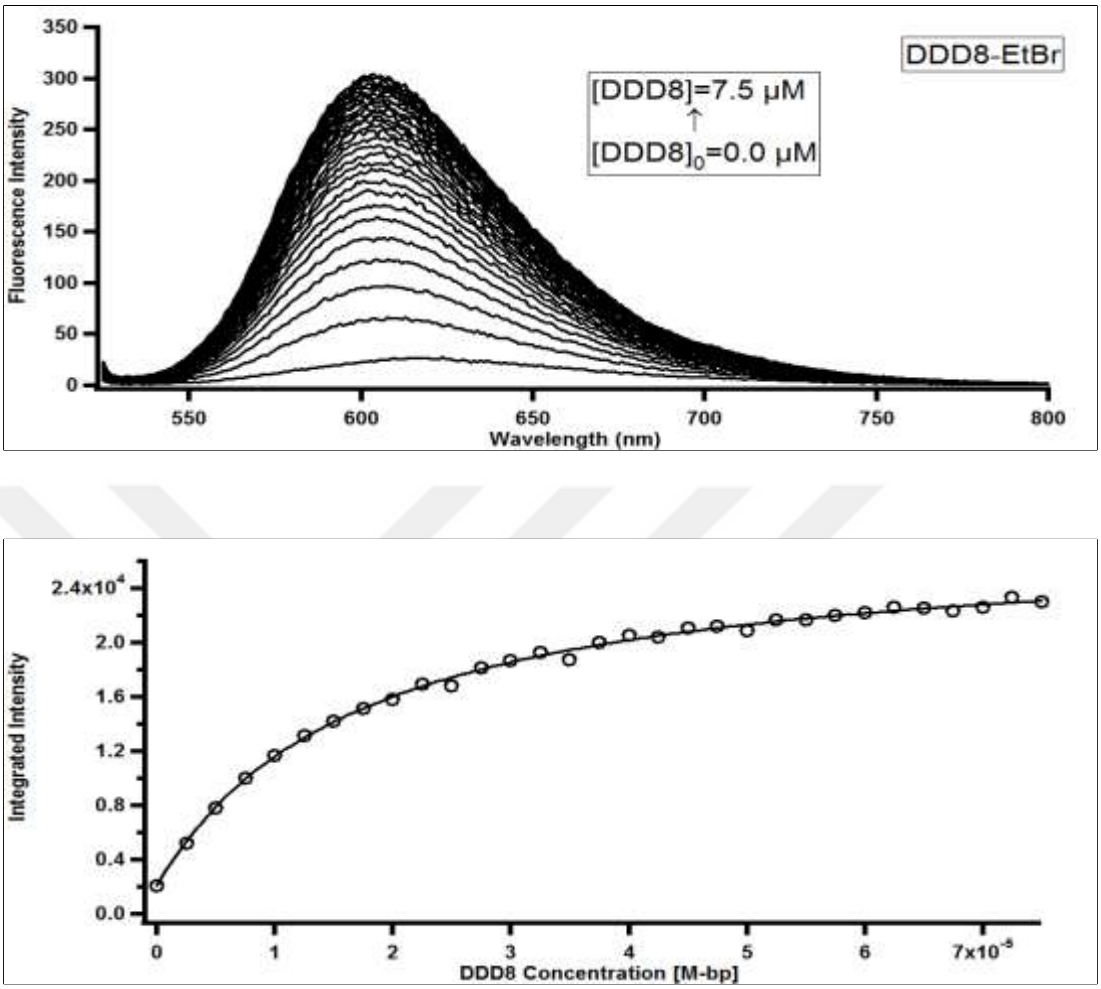

Figure A5. Fluorescence intensity vs wavelength spectrum of EtBr which was titrated with DDD8 solution including 1.0 µM of EtBr and the plot of integrated fluorescence intensity vs DDD8 concentration (2nd replicate)

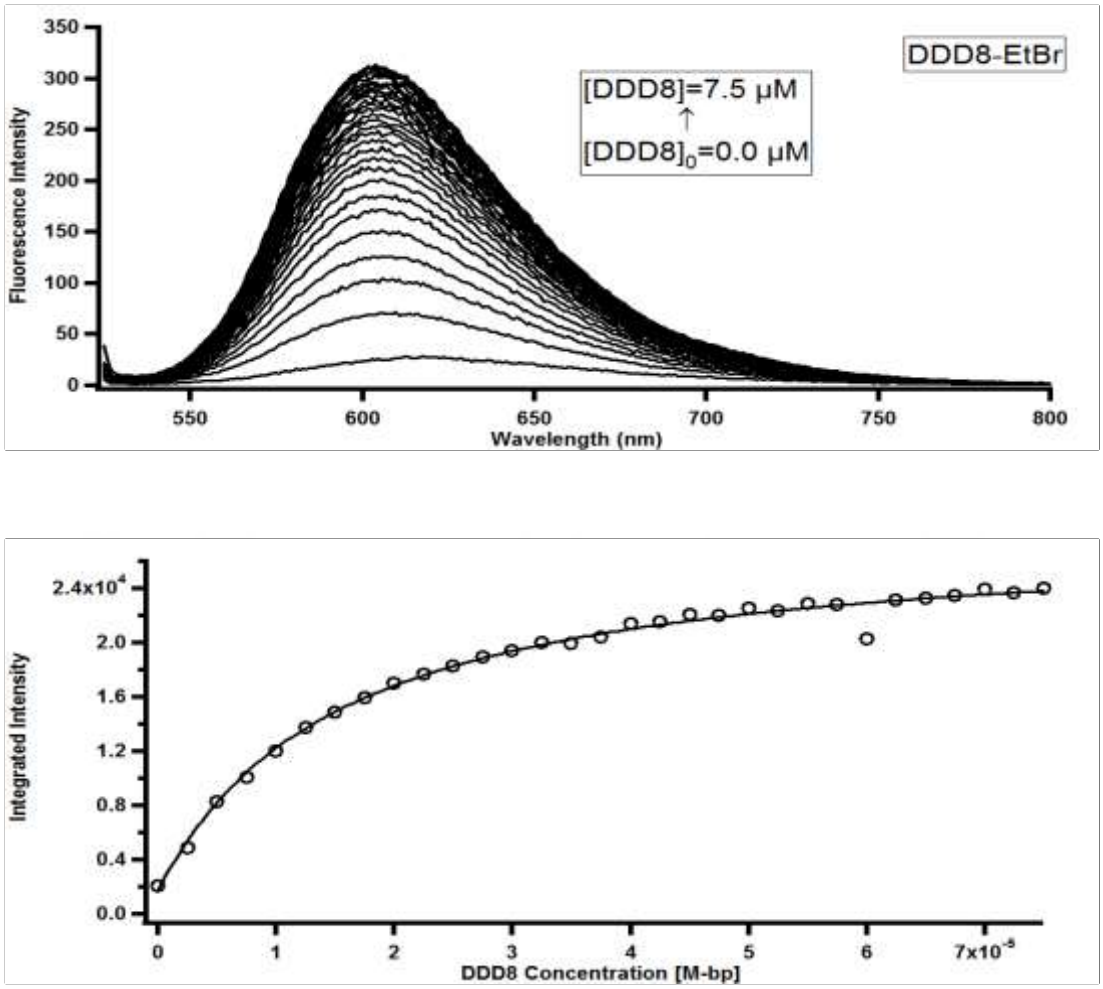

Figure A6. Fluorescence intensity vs wavelength spectrum of EtBr which was titrated with DDD8 solution including 1.0 µM of EtBr and the plot of integrated fluorescence intensity vs DDD8 concentration (3rd replicate)

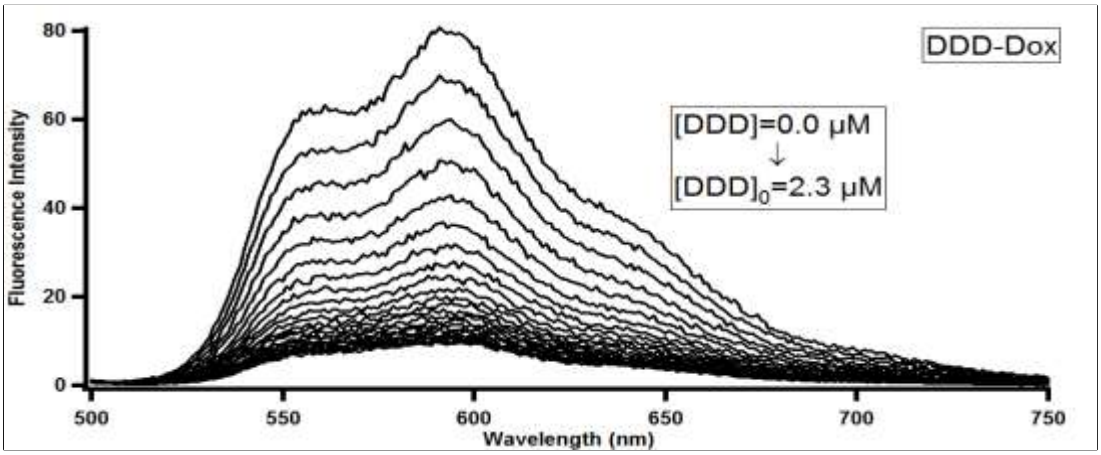

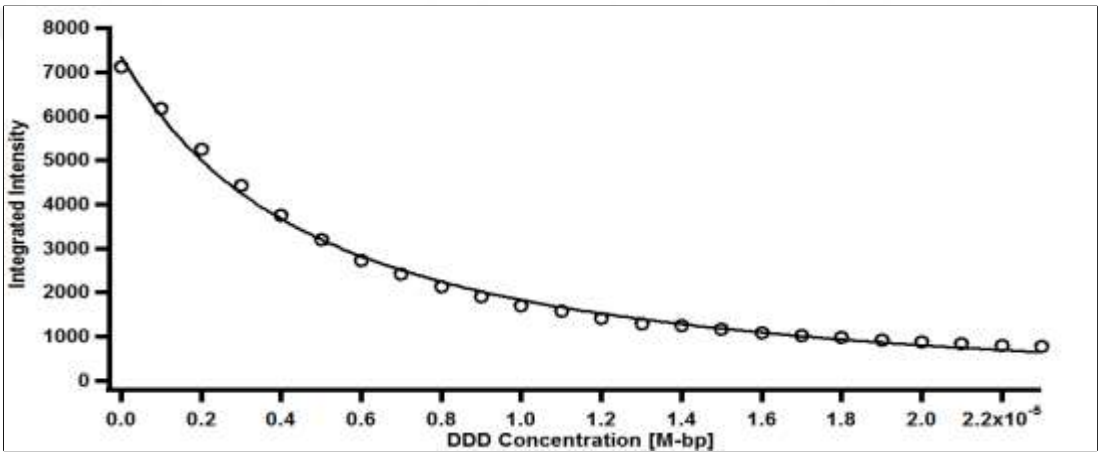

Figure A7. Fluorescence intensity vs wavelength spectrum of Dox which was titrated with DDD solution including 1.0 µM of Dox and the plot of integrated fluorescence intensity vs DDD concentration (1st replicate)

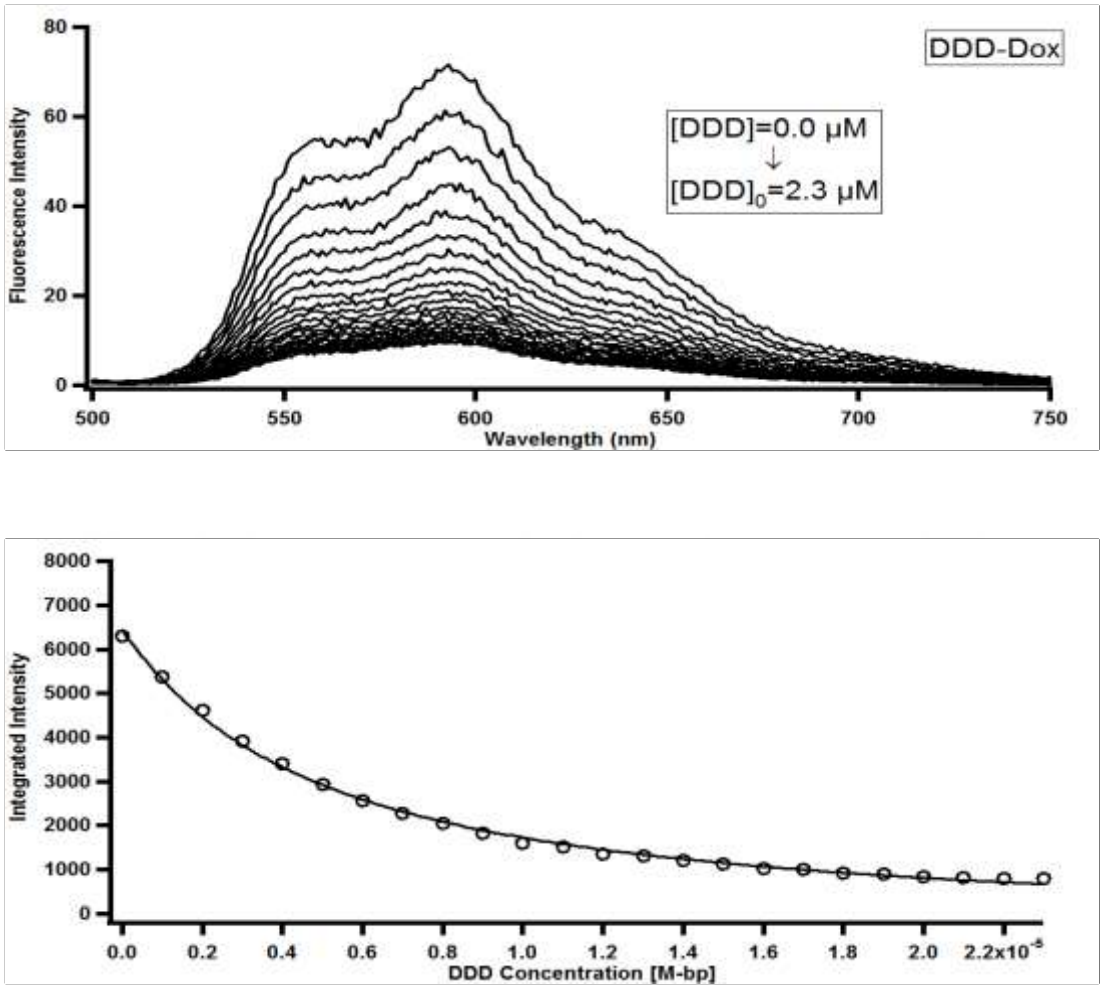

Figure A8. Fluorescence intensity vs wavelength spectrum of Dox which was titrated with DDD solution including 1.0 µM of Dox and the plot of integrated fluorescence intensity vs DDD concentration (2nd replicate)

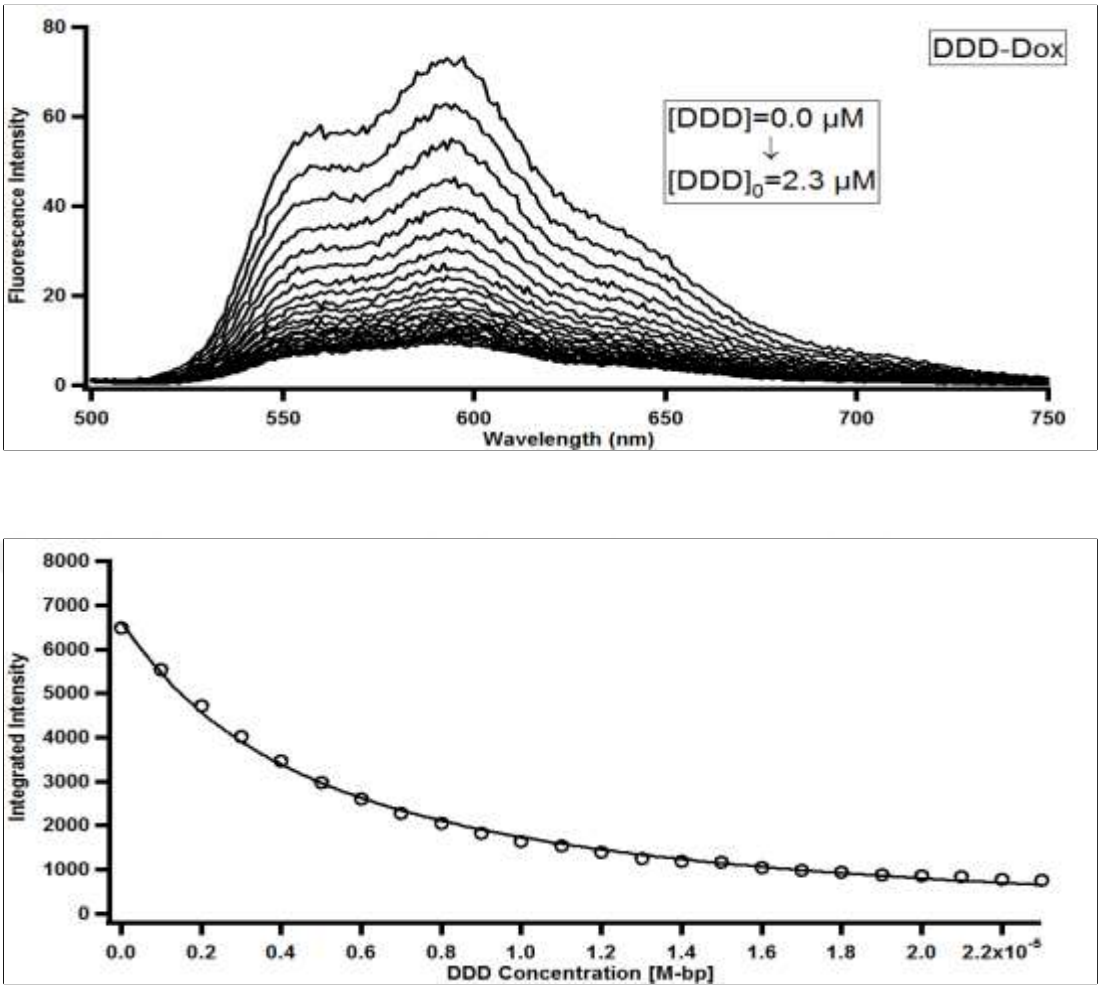

Figure A9. Fluorescence intensity vs wavelength spectrum of Dox which was titrated with DDD solution including 1.0 µM of Dox and the plot of integrated fluorescence intensity vs DDD concentration (3rd replicate)

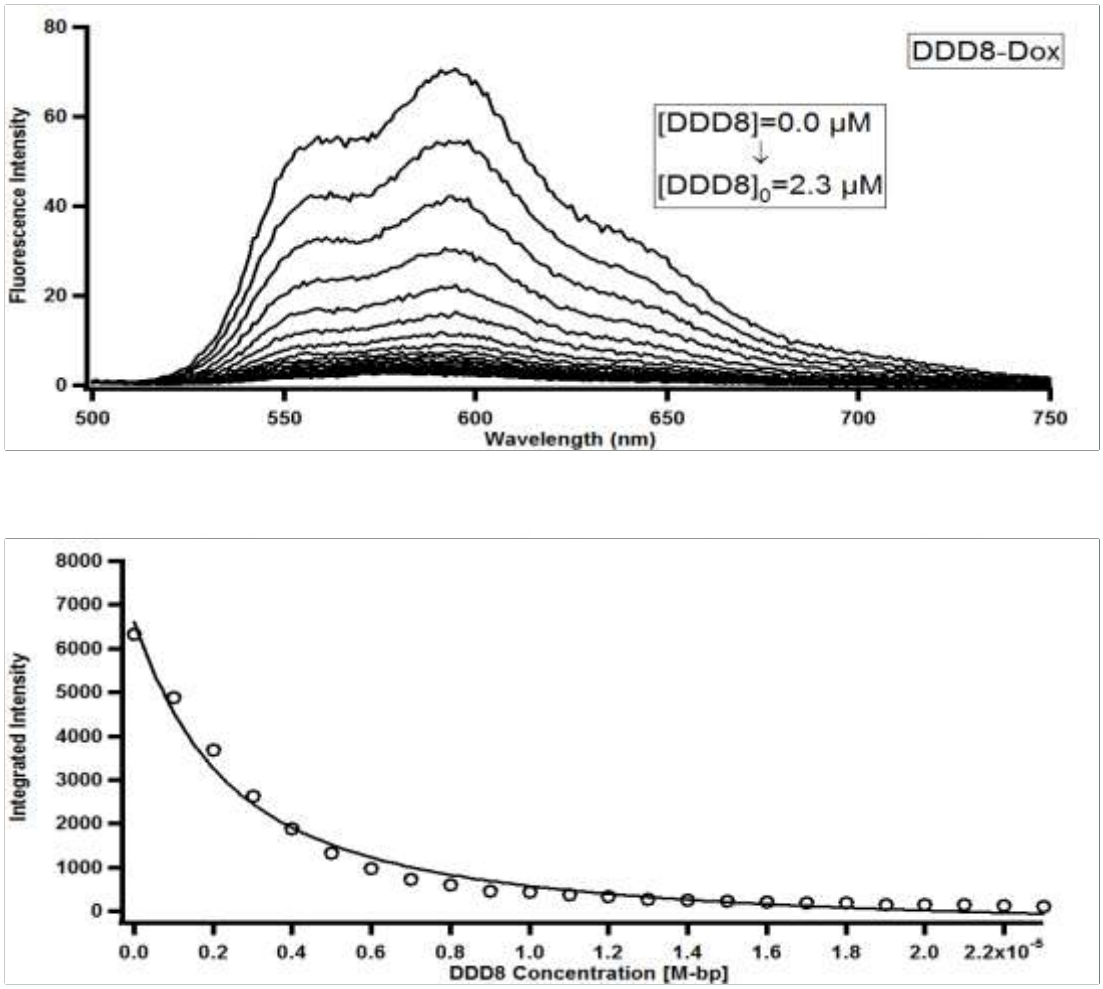

Figure A10. Fluorescence intensity vs wavelength spectrum of Dox which was titrated with DDD8 solution including 1.0 µM of Dox and the plot of integrated fluorescence intensity vs DDD8 concentration (1st replicate)

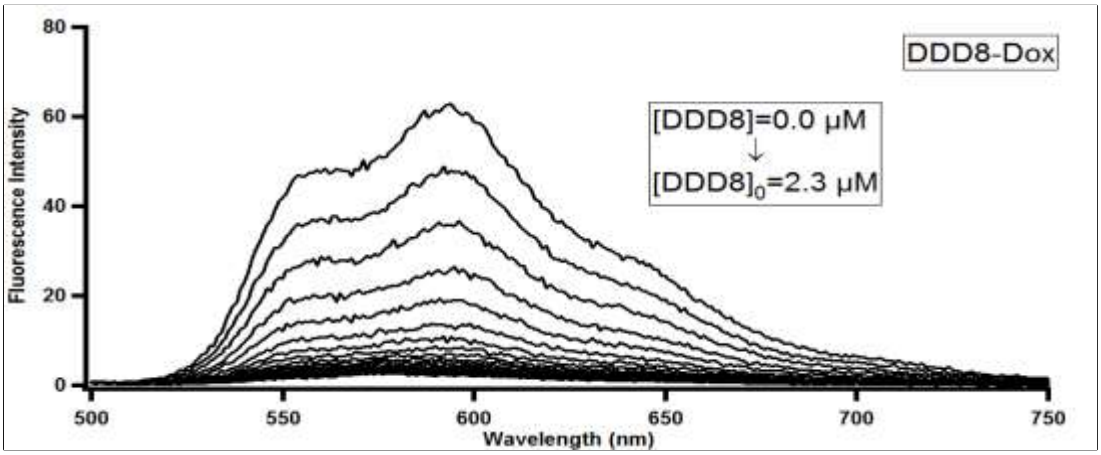

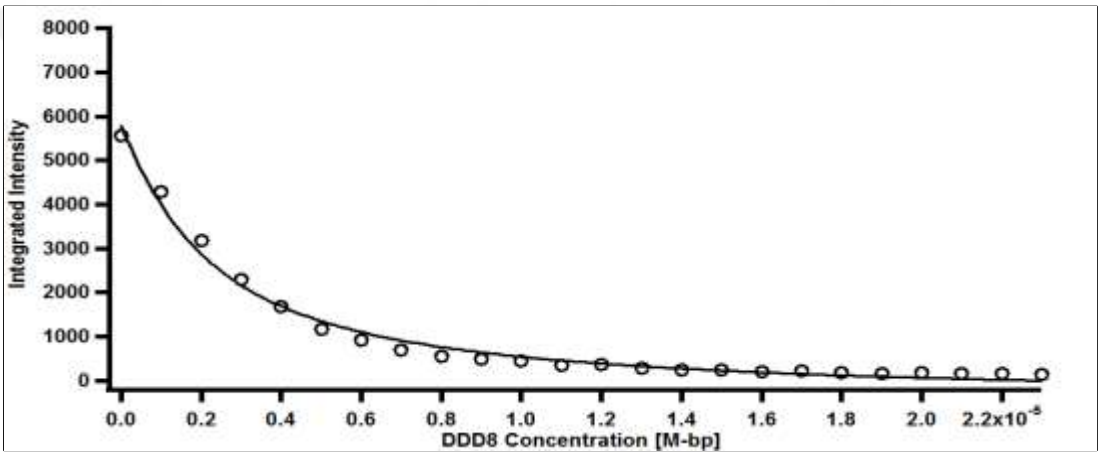

Figure A11. Fluorescence intensity vs wavelength spectrum of Dox which was titrated with DDD8 solution including 1.0 μM of Dox and the plot of integrated fluorescence intensity vs DDD8 concentration (2nd replicate)

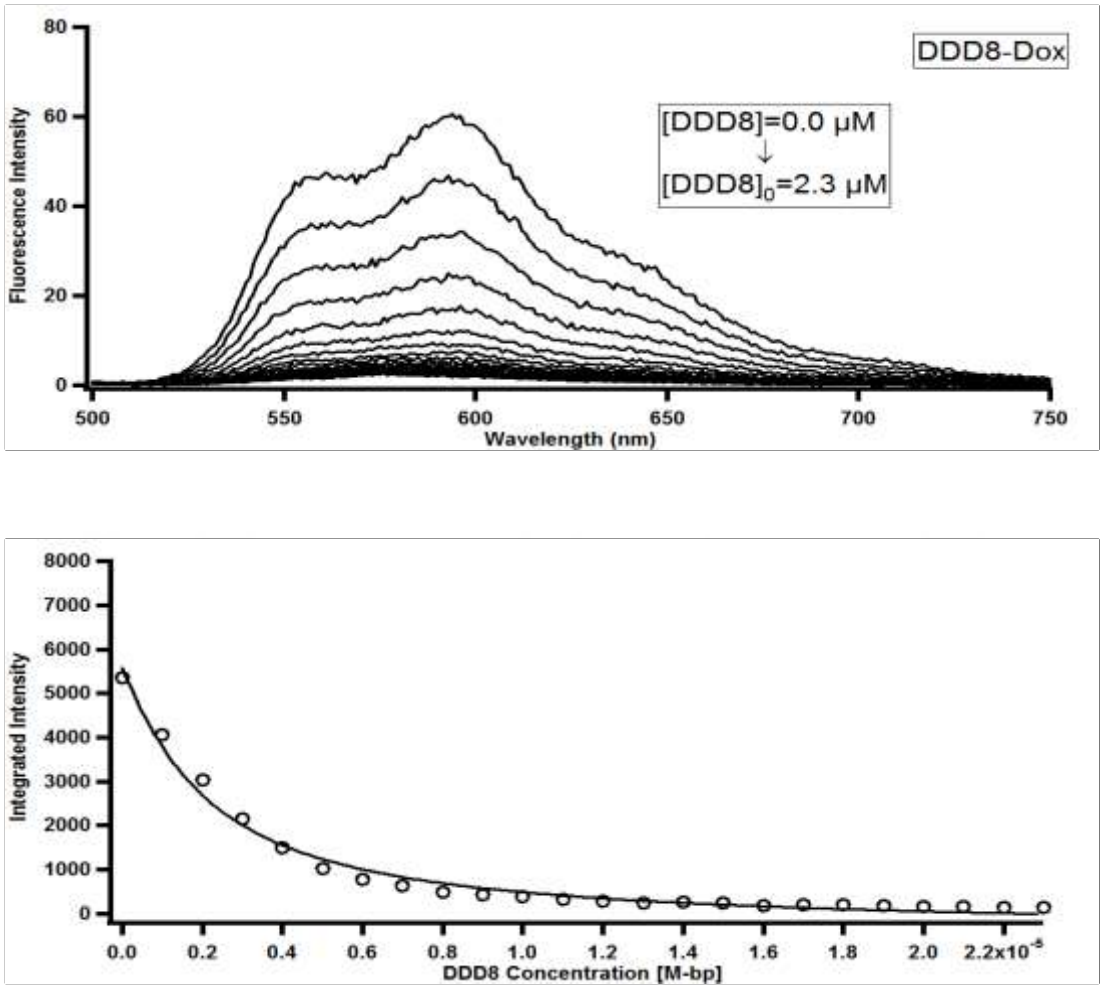

Figure A12. Fluorescence intensity vs wavelength spectrum of Dox which was titrated with DDD8 solution including 1.0 μM of Dox and the plot of integrated fluorescence intensity vs DDD8 concentration (3rd replicate)

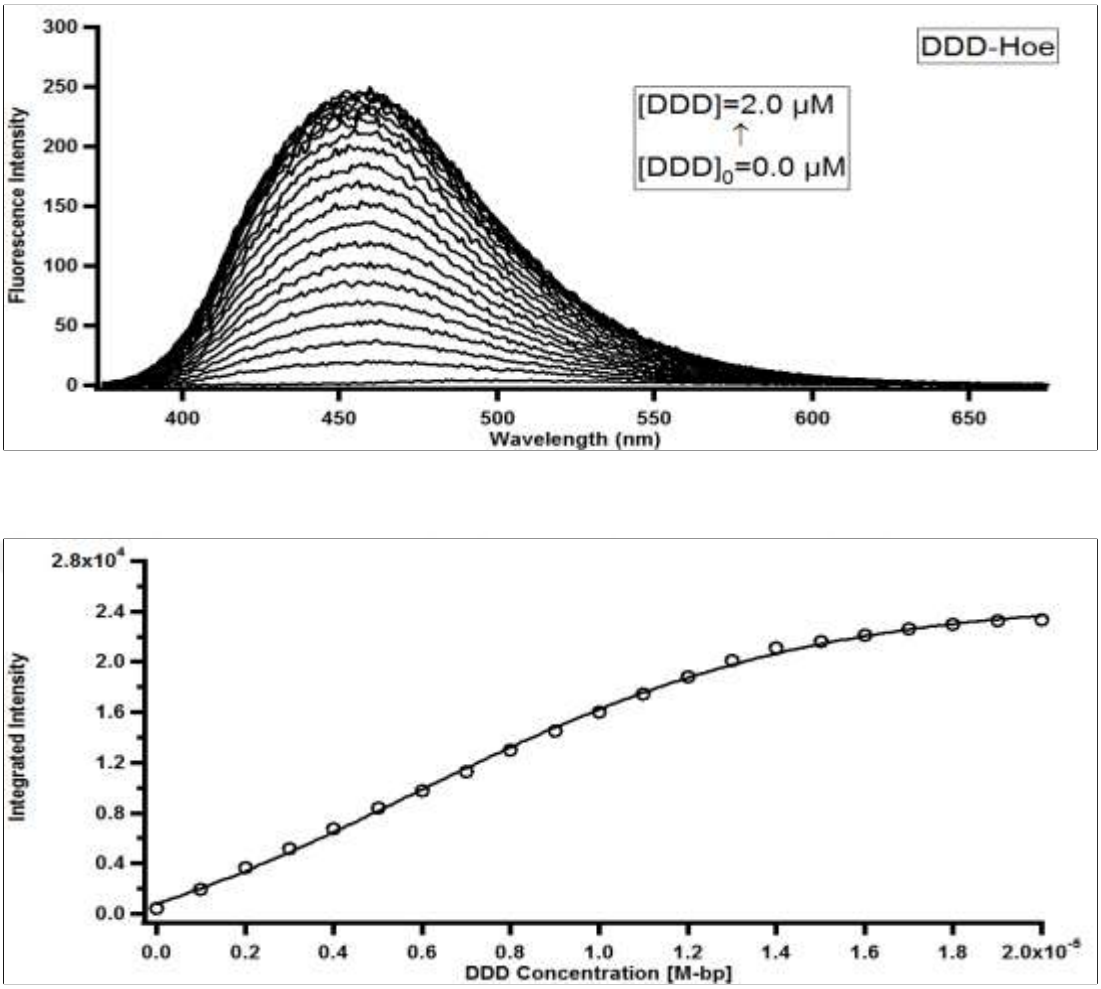

Figure A13. Fluorescence intensity vs wavelength spectrum of Hoe which was titrated with DDD solution including 1.0 μM of Hoe and the plot of integrated fluorescence intensity vs DDD concentration (1st replicate)

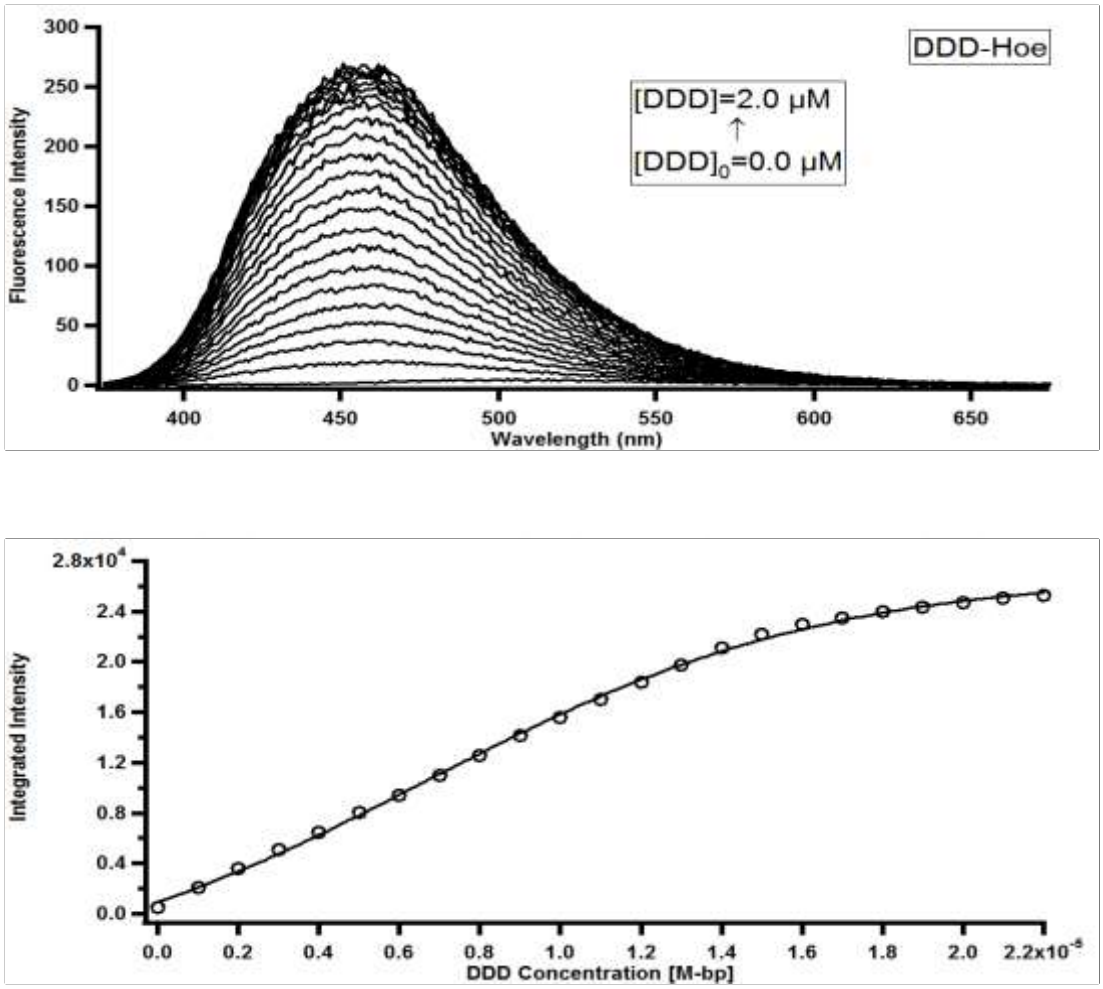

Figure A14. Fluorescence intensity vs wavelength spectrum of Hoe which was titrated with DDD solution including 1.0 µM of Hoe and the plot of integrated fluorescence intensity vs DDD concentration (2nd replicate)

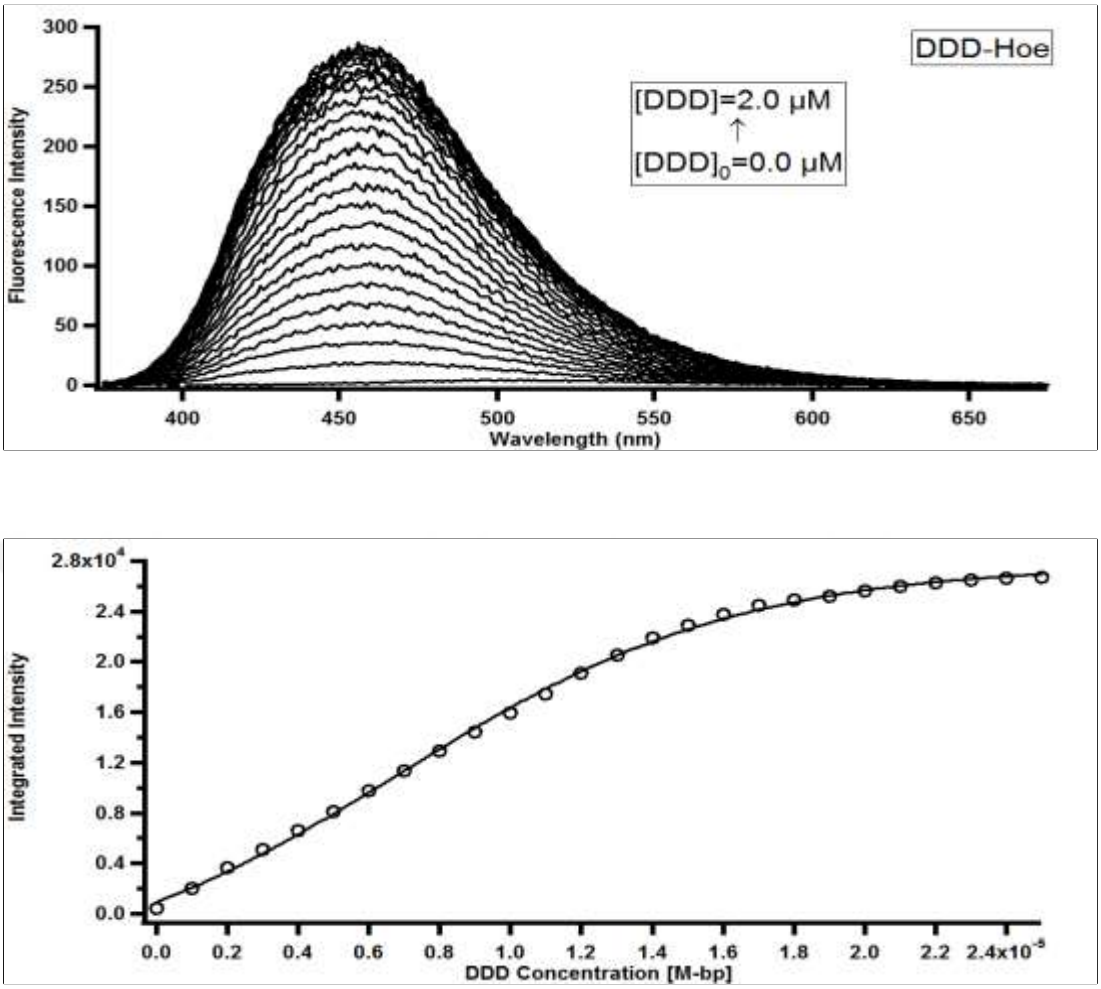

Figure A15. Fluorescence intensity vs wavelength spectrum of Hoe which was titrated with DDD solution including 1.0 µM of Hoe and the plot of integrated fluorescence intensity vs DDD concentration (3rd replicate)

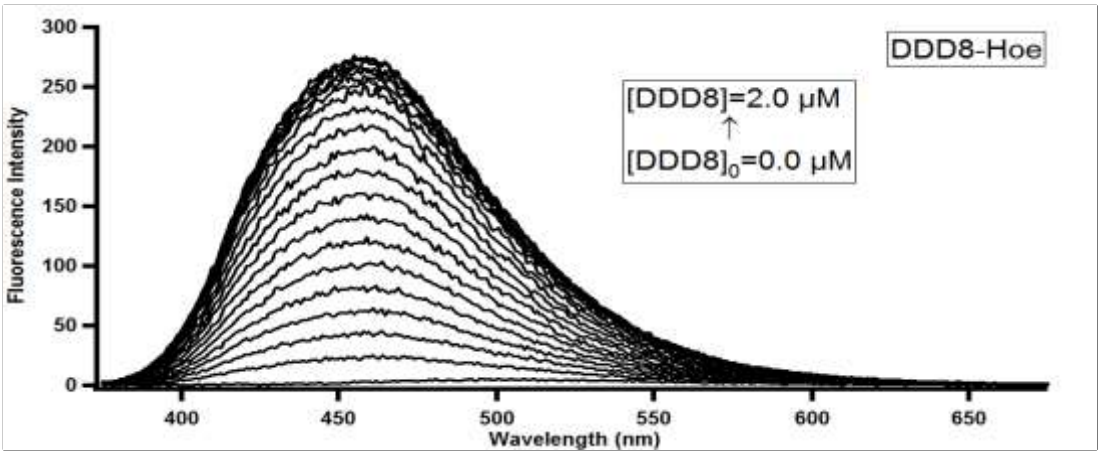

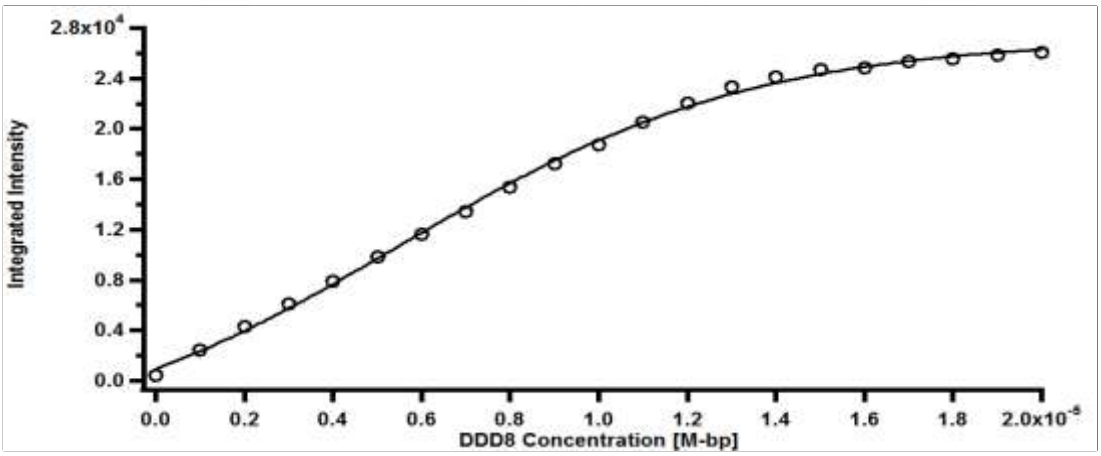

Figure A16. Fluorescence intensity vs wavelength spectrum of Hoe which was titrated with DDD8 solution including 1.0 μM of Hoe and the plot of integrated fluorescence intensity vs DDD8 concentration (1st replicate)

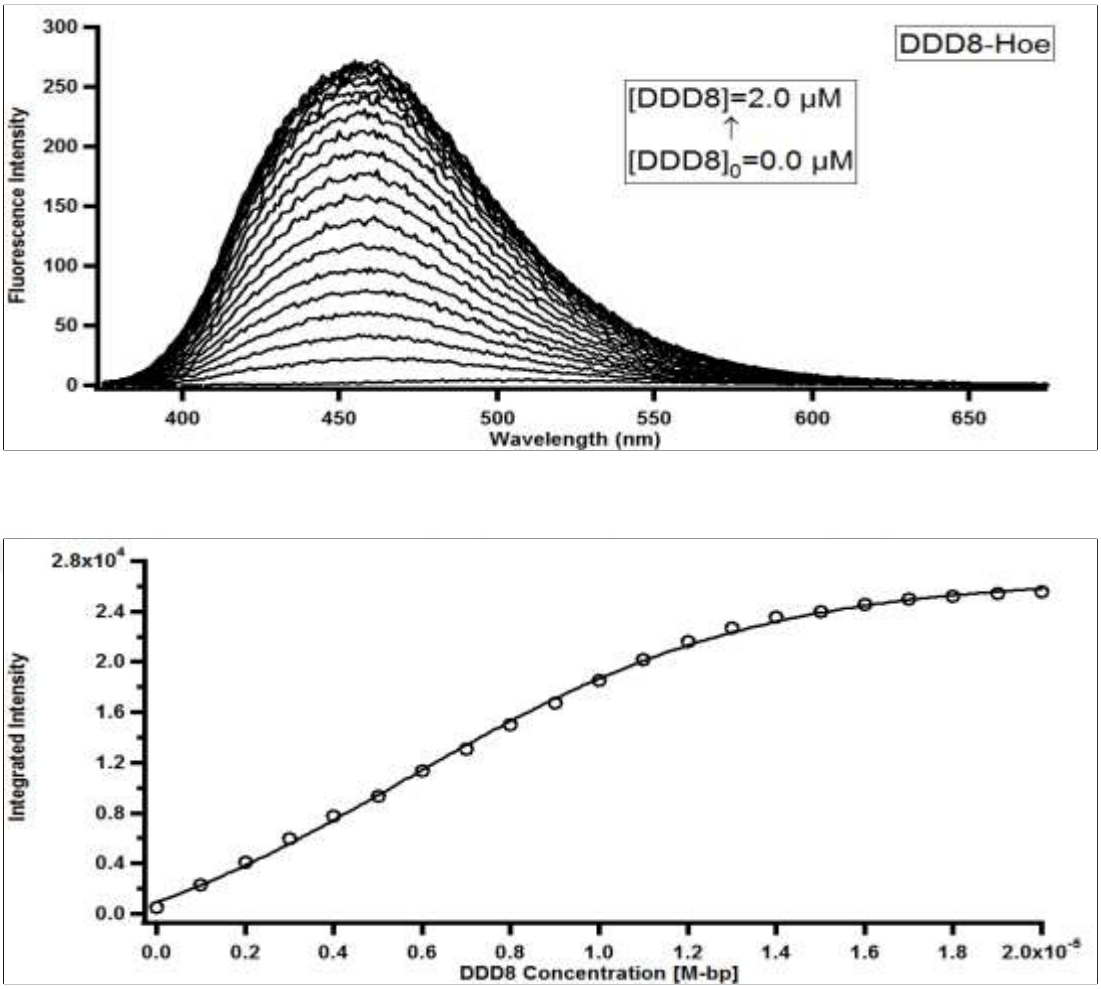

Figure A17. Fluorescence intensity vs wavelength spectrum of Hoe which was titrated with DDD8 solution including 1.0 μM of Hoe and the plot of integrated fluorescence intensity vs DDD8 concentration (2nd replicate)

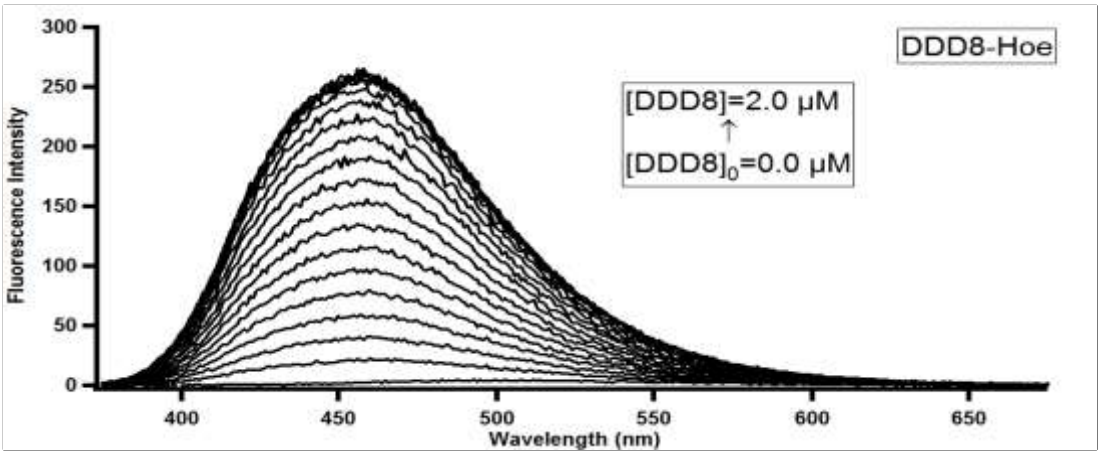

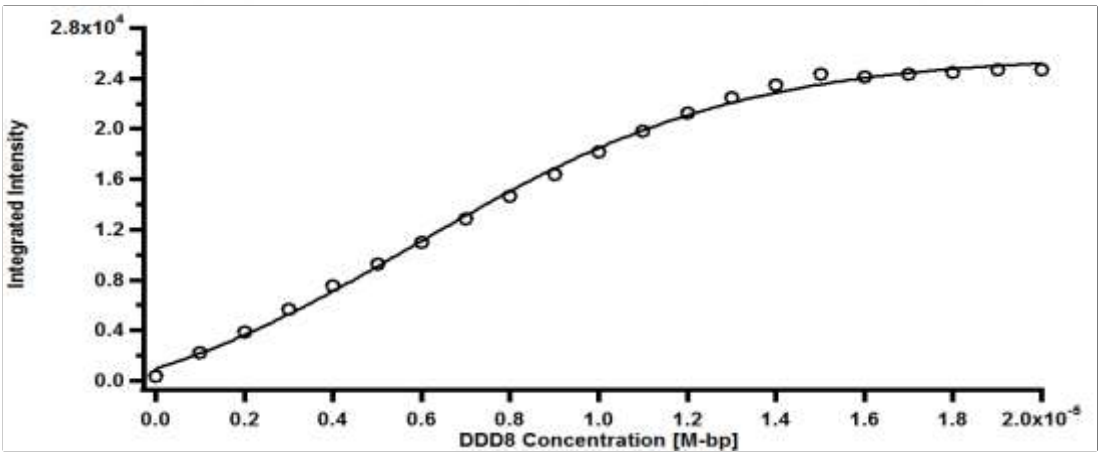

Figure A18. Fluorescence intensity vs wavelength spectrum of Hoe which was titrated with DDD8 solution including 1.0 μM of Hoe and the plot of integrated fluorescence intensity vs DDD8 concentration (3rd replicate)

B. Normalized Thermal Denaturation Curves of DDD and *d5mC* Substituted DDDs

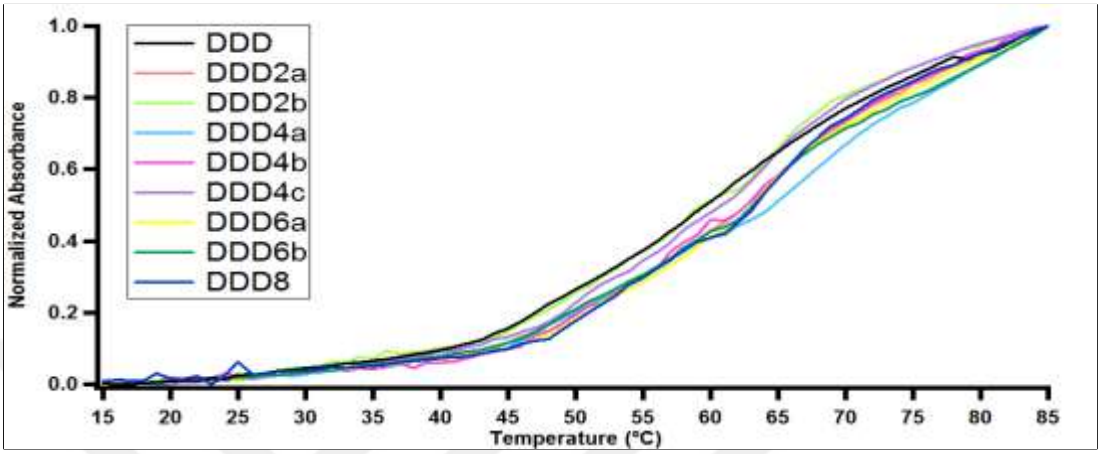

Figure B1. Normalized thermal denaturation curves of DDD and d5mC substituted DDDs (given in Table 1) obtained by monitoring the UV-Vis absorbance at 260 nm with varying temperature (1st replicate)

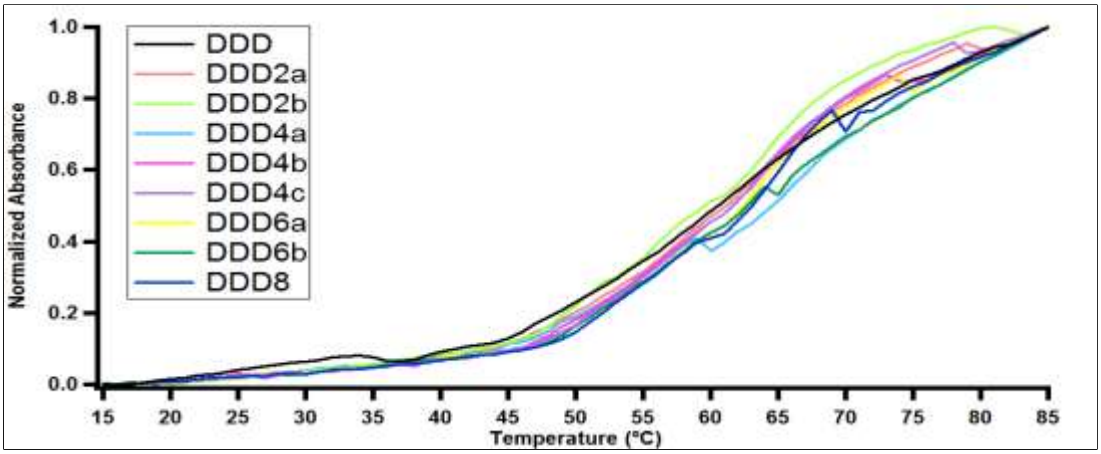

Figure B2. Normalized thermal denaturation curves of DDD and d5mC substituted DDDs (given in Table 1) obtained by monitoring the UV-Vis absorbance at 260 nm with varying temperature (2nd replicate)

C. Normalized Heating Traces of DDD and DDD8 in the Absence and Presence of Small Molecules

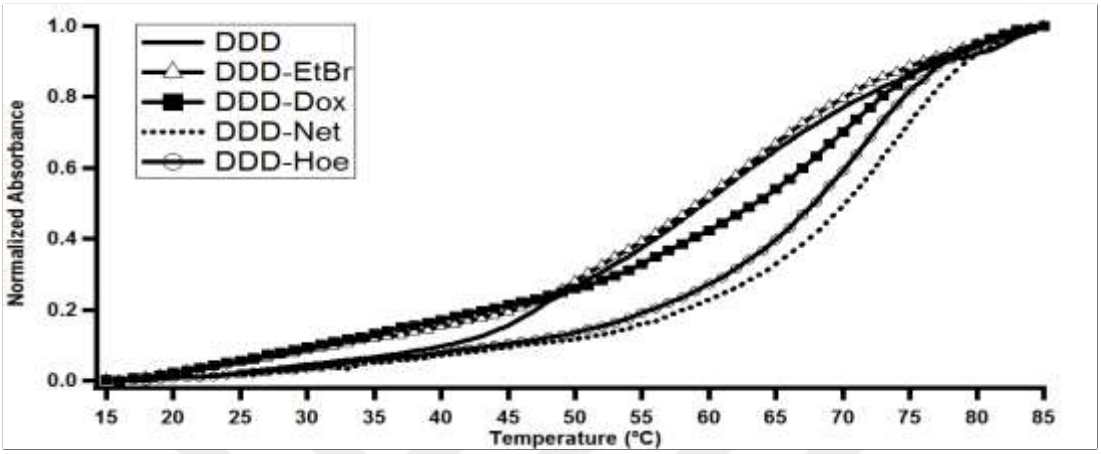

Figure C1. Normalized heating traces of DDD in the absence and presence of small molecules obtained by observing the UV-Vis absorbance changes at 260 nm with increasing temperature (1st replicate)

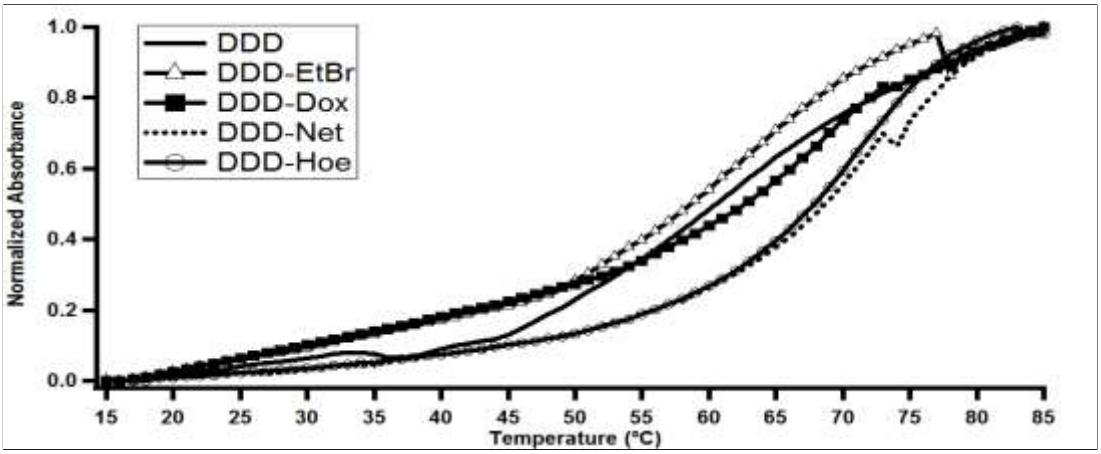

Figure C2. Normalized heating traces of DDD in the absence and presence of small molecules obtained by observing the UV-Vis absorbance changes at 260 nm with increasing temperature (2nd replicate)

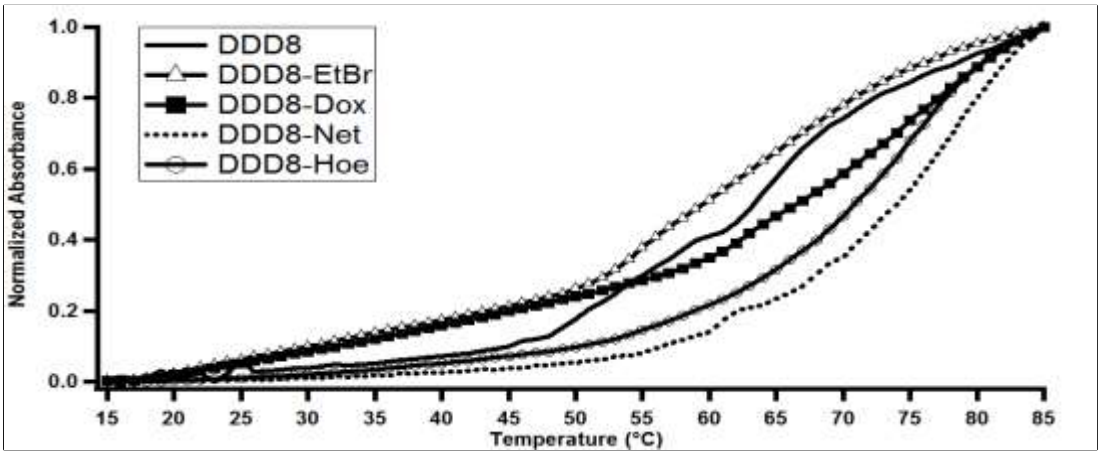

Figure C3. Normalized heating traces of DDD8 in the absence and presence of small molecules obtained by observing the UV-Vis absorbance changes at 260 nm with increasing temperature (1st replicate)

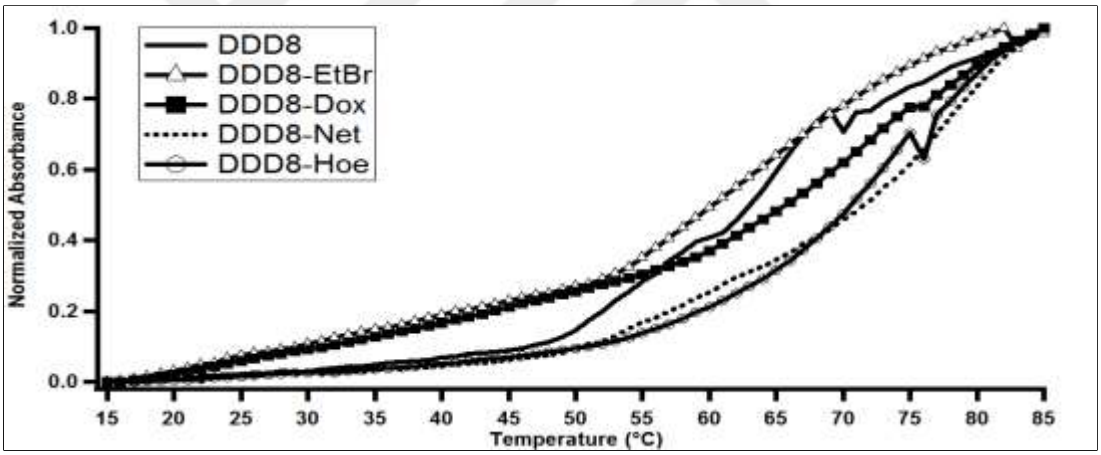

Figure C4. Normalized heating traces of DDD8 in the absence and presence of small molecules obtained by observing the UV-Vis absorbance changes at 260 nm with increasing temperature (2nd replicate)